

IL NUOVO CIMENTO

1959

IL NUOVO CIMENTO

PERIODICO ITALIANO DI FISICA

fondato a PISA nel 1855 da C. MATTEUCCI e R. PIRIA

dal 1897 Organo della Società Italiana di Fisica

è pubblicato

sotto gli auspici del Consiglio Nazionale delle Ricerche

a cura del Direttore

GIOVANNI POLVANI

Presidente della Società

e

dei Vicedirettori

M. CONVERSI e N. DALLAPORTA

con la collaborazione di un Comitato di redazione

costituito dai professori

G. BERNARDINI, G. BOLLA, A. BORSELLINO, E. CAIANIELLO, P. CALDIROLA,

G. CARERI, M. CINI, R. DEAGLIO, B. FINZI, S. FRANCHETTI,

F. FUMI, A. GIACOMINI, L. GIULOTTO, D. GRAFFI, G. OCCHIALINI,

E. PERUCCA, L. A. RADICATI, C. SALVETTI, G. SALVINI, M. SIMONETTA,

G. TORALDO DI FRANCIA, M. VERDE, G. WATAGHIN.

Segretario di Redazione

R. CORBI

Redazione

Bologna, Via Irnerio n. 46

presso l'Istituto di Fisica dell'Università

Direzione

Milano, Via Saldini n. 50

presso l'Istituto di Fisica dell'Università

IL NUOVO CIMENTO

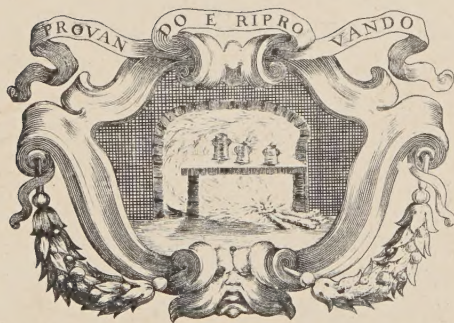
ORGANO DELLA SOCIETÀ ITALIANA DI FISICA
SOTTO GLI AUSPICI DEL CONSIGLIO NAZIONALE DELLE RICERCHE

VOLUME XI

Serie decima

Anno centesimoquinto


1959



PRINTED IN ITALY

NICOLA ZANICHELLI EDITORE
BOLOGNA

Alfredo Lucero 1959



Digitized by the Internet Archive
in 2024

IL NUOVO CIMENTO

ORGANO DELLA SOCIETÀ ITALIANA DI FISICA

SOTTO GLI AUSPICI DEL CONSIGLIO NAZIONALE DELLE RICERCHE

VOL. XI, N. 1

Serie decima

1° Gennaio 1959

On the Mechanism of the $(n, 2n)$ Reaction at 14 MeV Neutron Energy - II.

K. WINTER (*), B. TORKI and E. REMY (+)

Laboratoire de Physique Atomique et Moléculaire du Collège de France - Paris

(ricevuto il 28 Agosto 1958)

Summary. — The correlation of the respective directions of emission of the two neutrons in the ${}^9\text{Be}(n, 2n){}^8\text{Be}$ reaction has been investigated by using coincidence detection of the outgoing neutrons. In an azimuthal plane, separation angles ranging from 45° to 90° are predominant; a maximum correlation of $(20 \pm 3)\%$ is obtained at 60° . This angular correlation is attributed to simultaneous emission of two neutrons. Angular distribution measurements on the same reaction proved, by using time-of-flight techniques, that second neutrons are emitted by a compound nucleus, whereas first neutrons are emitted both directly and by a compound nucleus.

1. - Introduction.

Investigations of the mechanism of three-particle reactions, such as the $(n, 2n)$ reaction, are important for the interpretation of anomalies in medium-energy nuclear reactions: the nature of the compound systems formed in the course of three-particle reactions and the manner of their disintegration can be studied separately; whereas, in a two-particle reaction, such as the inelastic scattering of neutrons, effects of these two stages could not be distinguished.

In a previous paper ⁽¹⁾ (referred to as I) we have reported on measurements

(*) Now at CERN, SC-Group, Geneva 15.

(+) Now at Max-Planck-Institut für Physik, München.

(1) E. REMY and K. WINTER: *Nuovo Cimento* **10**, 664 (1958).

of the distribution in energy of neutrons emitted in $(n, 2n)$ reactions from the interaction of 14 MeV neutrons with various elements. By using time-of-flight techniques, continua of the first neutrons were separated from low energy groups due to the subsequent emission of a second neutron in $(n, 2n)$ reactions. It is concluded (see I) that the principal mechanism of the $(n, 2n)$ reaction in medium weight and heavy nuclei is successive emission of the two neutrons. The compound systems emitting the second neutrons have lifetimes which are long compared with the transit time of nucleons over nuclear dimensions: *i.e.* there is a well-defined quantum state, a compound nucleus, between the emissions of the first and the second neutron.

Fig. 1 shows a competition diagram for different mechanisms of the $(n, 2n)$ reaction. A time sequence has been assumed in the formation of the first compound system by 14 MeV neutrons incident on the target nucleus. In the

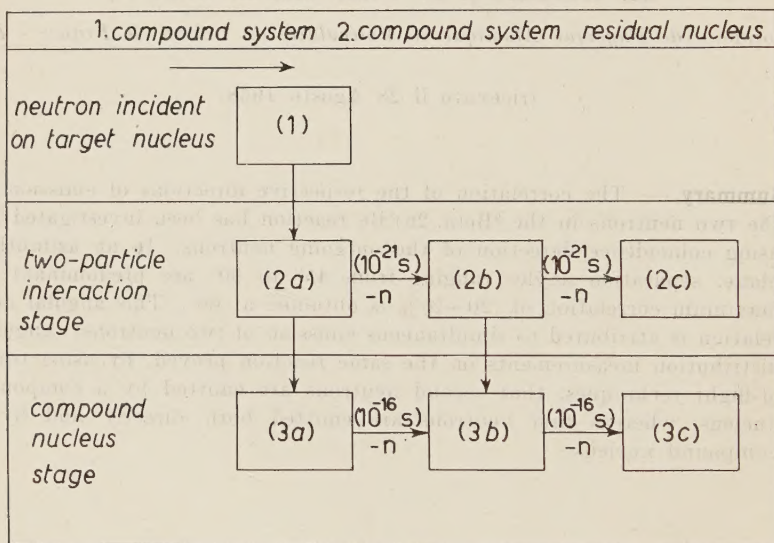


Fig. 1.

first approximation (1), the incident wave is considered as a wave scattered by the real part of the complex potential of the target nucleus. In the second approximation (2a), the wave inside the potential is modified by the interaction of the incident neutron with a single nucleon of the target nucleus, and finally by the interaction with others, until a compound nucleus is formed (3a). However, the two-particle interaction stage (2a), having a lifetime of the order of the transit time of nucleons over nuclear dimensions (10^{-21} s), can disintegrate, in competition with the final formation of a compound nucleus, by direct emission of a nucleon, *e.g.* a neutron, leading to a second compound system (2b). Again, there is a possibility of competition

between final formation of a compound nucleus (3b) and disintegration by direct emission, if energetically possible, of a second neutron to the residual nucleus (2c).

A sequence of the $(n, 2n)$ reaction in the two-particle interaction stage, leading from (2a) to (2b) and (2c), (see Fig. 1), should be considered as simultaneous emission of the two neutrons; whereas, once a compound nucleus has been formed, either (3b) or (3a), the emission of the two neutrons will be successive, leading to a distribution in energy which shows two separate groups, due to the first and the second neutrons (see I).

Evidently, there are two different possible courses of the $(n, 2n)$ reaction leading to successive emission and to such a distribution in energy: either the first neutron is emitted directly by the two-particle interaction stage (2a) with subsequent formation of a compound nucleus (3b) via (2b); or it is emitted by the compound nucleus (3a). Both possibilities lead to successive emission of the two neutrons; they cannot be distinguished by a measurement of the energy spectrum.

This paper will be concerned with the investigation of this alternative.

As a direct test for the emission of neutrons by the two-particle interaction stage (2a, 2b), we investigated the respective directions of emission of the two neutrons in the 14 MeV neutron induced ${}^9\text{Be}(n, 2n){}^8\text{Be}$ reaction. To decide the above mentioned alternative we investigated separately the angular distributions of the first and the second neutron.

2. - Angular correlation measurements.

Two neutrons, forming a virtual singlet state in the two-particle interaction stage, may be emitted simultaneously (see Fig. 1). In the center of mass system of the virtual neutron-neutron state, the two neutrons will be emitted at 180° with respect to each other. In the laboratory system, the respective directions of emission will be correlated at angles smaller than or equal to 90° . Consequently, a contribution of this pick-up mechanism in $(n, 2n)$ reactions can be identified by its angular correlation.

ANSEROVA *et al.* ⁽²⁾ investigated the respective directions of emission of the neutrons emitted in ${}^9\text{Be}(n, 2n){}^8\text{Be}$ reactions, by using Be-loaded photographic emulsions (see I). After examination of 84 events they concluded that the two neutrons are not emitted in the same direction and with the same energy, but in different directions and with different energies. This investigation has been repeated recently ⁽³⁾, also with negative result.

⁽²⁾ N. S. ANSEKOVA, IOU. A. NEMÍLOV and B. L. FOUNCHTEÏN: *Rec. Trav. Inst. Rad. V. G. Chlopin*, **7**, 114 (1956).

⁽³⁾ R. CHASTEL and CAO-XUAN: private communication.

However, no experiments on the angular correlation of neutrons emitted in $(n, 2n)$ reactions have been reported using coincidence detection of the outgoing neutrons.

2.1. Experimental method. — A conical beam of 14 MeV neutrons, yielded by the $T(d, n)^4\text{He}$ reaction, has been obtained by using a combined paraffin-lead collimator (Fig. 2). The ratio of the neutron fluxes inside and outside the collimated beam has been measured to be of the order of 10^2 .

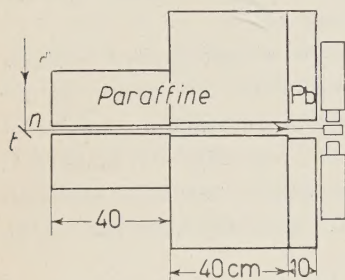


Fig. 2.

Within this cone, at 108 cm of the neutron source, a beryllium scatterer, 5 cm long and 3 cm in diameter, was placed. It was faced, in an azimuthal plane, *i.e.* perpendicular to the incident neutron beam, by two neutron detectors containing plastic scintillators, 5 cm long and 5 cm in diameter. The two neutrons emitted in the ${}^9\text{Be}(n, 2n){}^8\text{Be}$ reaction have been detected in coincidence: signals supplied by the neutron detectors are

fed into a fast-slow coincidence circuit connected with a time-to-pulse-height converter. The total time resolution was 5 μs . A complete description of the electronic circuits has been given elsewhere ⁽⁴⁾. Discriminators in the slow lines are adjusted in such a way that the slow coincidence output signal gates open the amplitude analyser following the time-sorter only for signals analysed in the fast circuit which satisfied the required cut-off pulse height. The discriminators thus established a minimum neutron energy accepted for coincidence detection; this minimum energy has been measured to be 500 keV (see I).

In this way, a time spectrum was measured corresponding to the differences in flight times of the two neutrons emitted in the ${}^9\text{Be}(n, 2n){}^8\text{Be}$ reaction. The full width at half height of this difference time spectrum was 5 μs ; the peak of the spectrum was shifted, by the help of delay lines, to the center of the amplitude analyser. The superposed, uniformly shaped, spectrum of random coincidences was simply subtracted. The contribution of $(n-\gamma)$ coincidences has been proved to be negligible by inserting absorbers between one of the neutron detectors and the beryllium scatterer. The quantity of γ -rays accepted for coincidence detection has been found to be of the order of 1%, by measuring the time-of-flight spectrum (see Fig. 6). The integral of the time-spectrum, after subtraction of random coincidences, supplied the number of

⁽⁴⁾ E. REMY and K. WINTER: *Journ. Phys. Rad.*, **18**, 112A (1957).

coincidences for a given flux of incident neutrons. The neutron flux has been monitored by counting α -particles associated with 14 MeV neutrons in the $T(d, n)^4\text{He}$ reaction.

2.2. Results and discussion. — One of the neutron detectors, kept in a fixed position, established the direction of emission of one of the two neutrons. By varying, with the help of the other detector, the respective directions of emission of the two neutrons, the number of coincidences for a given flux of incident neutrons was measured at angles of separation of 45° , 67° , 90° , 135° and 180° . The number of coincidences as a function of the separating angle of the respective directions of emission is shown in Fig. 3.

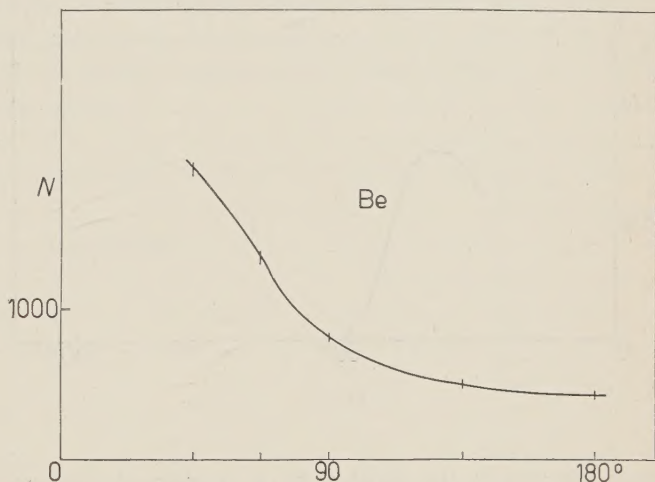


Fig. 3.

In addition to the investigated effect of angular correlation, crystal-to-crystal scattering of single neutrons varies as a function of the angle. Some contribution of this effect on the coincidence rate was proved by the shape of the time spectrum which changed with the angle. The coincidence detection of crystal-to-crystal scat-

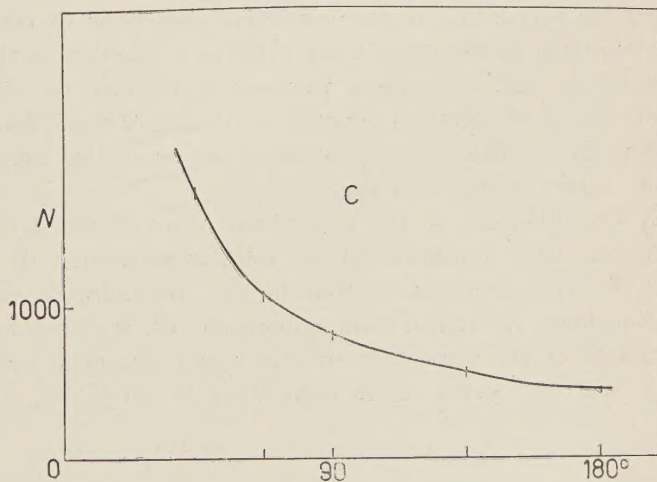


Fig. 4.

tering of single neutrons requires a minimum energy loss of 500 keV in each of the scintillators. Since the energy loss by elastic neutron scattering

in plastic scintillators depends on the angle of scattering, this background angular correlation is a function of the distribution in energy of neutrons emitted in the ${}^9\text{Be}(n, 2n){}^8\text{Be}$ reaction. Therefore we were searching for an element

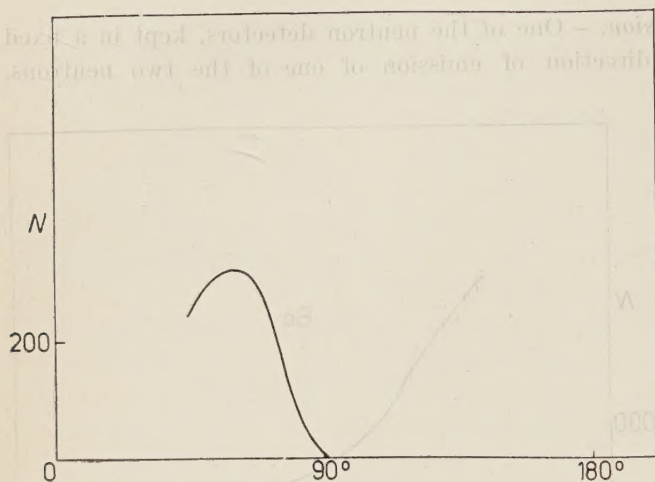


Fig. 5.

since the γ -rays are emitted by a compound nucleus. The time between the emissions of the neutron and of the subsequent γ -ray is long compared with the transit time of nucleons over nuclear dimensions, *i.e.* there will be no angular correlation in the respective directions of emission. Consequently, a comparison of the coincidence rates as a function of the separation angle, for beryllium and for carbon, provides a method to eliminate the background correlation of crystal-to-crystal scattering of single neutrons. The rate of background coincidences as a function of the separation angle, obtained with a carbon target is shown in Fig. 4.

The difference of the coincidence rates obtained with beryllium and with carbon, after normalization at 180° , is attributed to the angular correlation of the two neutrons emitted in the ${}^9\text{Be}(n, 2n){}^8\text{Be}$ reaction. The difference coincidence rate, read from smooth curves, is shown in Fig. 5, indicating correlation of the respective directions of emission at separation angles between 45° and 90° ; a maximum correlation of $(20 \pm 3)\%$ is obtained at 60° .

(⁵) J. GARG and B. TORKI: private communication.

(⁶) For the neutron spectrum of ${}^9\text{Be}(n, 2n){}^8\text{Be}$ see I.

3. - Angular distributions of the first and the second neutron.

Since subsequent emission of the second neutron in $(n, 2n)$ reactions leads to separate groups in the energy spectra, due to the first and the second neutron, angular distributions of the first and the second neutron can be measured separately. Such a type of spectra has been obtained with medium weight and heavy nuclei (see I). Angular distribution measurements, reported recently ⁽⁷⁾, are indicating that both courses of the $(n, 2n)$ reaction leading to subsequent emission of the second neutron (see I, Introduction) occur with medium weight and heavy nuclei.

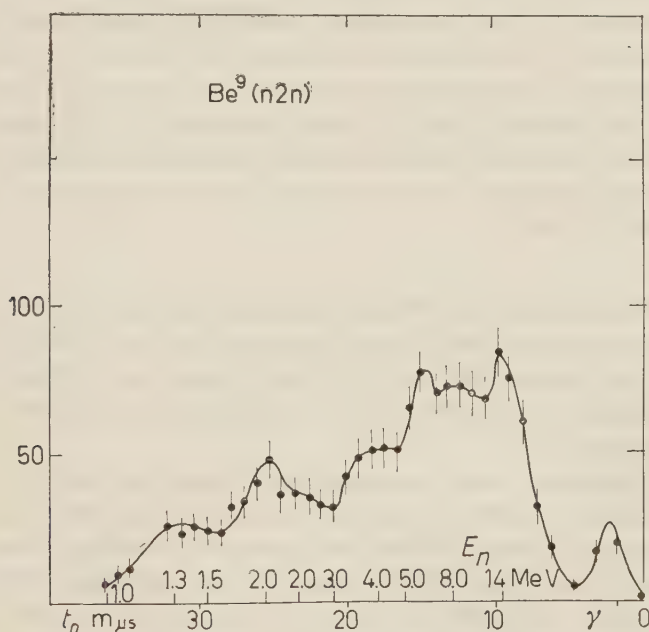


Fig. 6.

In the energy spectrum observed with ${}^9\text{Be}$, under the bombardment with 14 MeV neutrons, neutron groups at 1.3 MeV and at 2 MeV are resolved (see I), agreeing with calculated transition energies to levels of ${}^9\text{Be}$. Neutron energies between 5 and 12 MeV (see Fig. 6) are not resolved, containing either a great number of successive transitions of first neutrons or the maximum intensity for simultaneous emission or a mixture of both. In the spectrum observed there

⁽⁷⁾ B. TORKI: *Proc. of the Int. Congress on Nucl. Phys.* (Paris, 1958).

is no indication of the transition to the 11.3 MeV level in ${}^9\text{Be}$ which would yield 2.7 MeV neutrons. We could not decide (see I) whether this level does not exist or whether this transition does not occur because the time between the emission of the first and the second neutron at this excitation energy is short, *i.e.* of the order of the transit time of nucleons over nuclear dimensions, so that there is no defined excited quantum state between the two emissions. A contribution of simultaneous emissions by the two-particle interaction stage (see Fig. 1) has been identified by its angular correlation.

In addition, we investigated the angular distribution of neutrons emitted in the ${}^9\text{Be}(n, 2n){}^8\text{Be}$ reaction, to decide whether, in successive emissions, the first neutron is emitted directly by the two-particle interaction stage (2a) or whether it is emitted by a compound nucleus (3a) (see Fig. 1).

Direct emission by the two-particle interaction stage would give rise to anisotropic angular distributions, peaked at small angles (*); whereas, emission by a compound nucleus would result in angular distributions which are symmetrical with respect to 90° , or even isotropic (*), if the level density of a highly excited compound nucleus would be proportional to $(2j+1)$, where j designates the level spin; but this additional hypothesis has not been proved to be valid in all cases.

3.1. Experimental method. — The distribution in energy of neutrons emitted in 14 MeV neutron induced ${}^9\text{Be}(n, 2n){}^8\text{Be}$ reactions has been measured at seven angles contained between 30° and 120° , by using time-of-flight techniques. Two measurements were made on the neutrons to establish the zero as well as the arrival time.

A 100 keV deuteron beam bombarded a tritium-titan target. The reaction $\text{T}(d, n){}^4\text{He}$ yields a 14 MeV neutron associated with a 3 MeV recoil α -particle emitted at 180° with respect to the direction of the neutron. Signals supplied by an α -particle detector established a time zero for associated 14 MeV neutrons in a conical beam, the width of which was defined by the solid angle of the α -particle detector. Within this cone, at 25 cm of the neutron source, a beryllium scatterer, 5 cm long and 3 cm in diameter, was placed. It was faced by a neutron detector containing a plastic scintillator, 5 cm long and 5 cm in diameter, placed outside the time-correlated neutron beam at a distance of 30 cm of the scatterer, this distance representing the flight distance before detection of neutrons emitted by the scatterer. The neutron signal thus supplied the arrival time. The time interval defined by the zero and the arrival

(*) N. AUSTERN, S. T. BUTLER and H. McMANUS: *Phys. Rev.*, **92**, 350 (1953).

(*) W. HAUSER and H. FESHBACH: *Phys. Rev.*, **87**, 366 (1952); L. WOLFENSTEIN: *Phys. Rev.*, **82**, 690 (1951).

time was measured by using a time-to-pulse-height converter. A complete description of the electronic circuits and of their performance has been given elsewhere (^{4,10}). By inserting a combined lead-uranium shield between the neutron source and neutron detector, random coincidences were attenuated by a factor of 10, varying from 10% at 90° to 40% at 30° and to 35% at 120° of the real coincidence rate.

3.2. Results and discussion. — Time-of-flight spectra have been measured at 7 angles ranging from $(30 \pm 7)^\circ$ to $(120 \pm 7)^\circ$, each for an integrated flux of 10^7 α -particles or 10^9 neutrons in 4π . A neutron spectrum obtained with ^9Be at 90° is shown in Fig. 6; the time scale is linear, the corresponding neutron energies are indicated.

Angular distributions have been deduced by dividing the measured spectra

into three regions, ranging from 1 to 2 MeV, from 2 to 4 MeV and from 4 to 10 MeV, and by taking integrals of these regions as functions of the angle of emission. The first two regions, ranging from 1 to 4 MeV contain exclusively

second neutrons emitted in the $^9\text{Be}(n, 2n)^8\text{Be}$ reaction (see I), the latter contains first neutrons; a small contribution of subsequently emitted second neutrons at 5.1 MeV and 6.2 MeV can be neglected; but there is a contribution of neutrons emitted simultaneously.

Angular distributions deduced

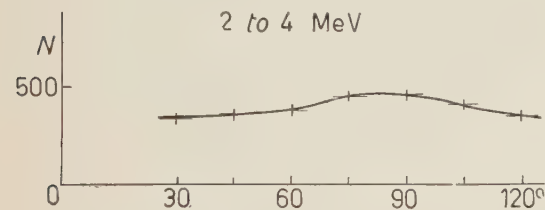


Fig. 8.

for these three energy regions are shown in Figs. 7-9.

Symmetry with respect to 90° has been found for neutron energies ranging from 1 to 2 MeV (Fig. 7) and from 2 to 4 MeV (Fig. 8), indicating the subsequent emission of second neutrons by a compound nucleus, in agreement with our previous results (see I). However, in the energy region from 4 to 10 MeV (Fig. 9), there is a strong anisotropic contribution peaked at small angles as well as another contribution showing symmetry with respect to 90°.

(¹⁰) E. REMY and K. WINTER: *Nuovo Cimento*, **10**, 664 (1958).

The latter one, showing symmetry at 90° , is attributed to first neutrons emitted by a compound nucleus ((3a) in Fig. 1), but the possible area under this contribution does not account for the total number of subsequently emitted second neutrons found in the energy region from 1 to 4 MeV. Consequently, first neutrons leading to subsequent emission of second neutrons must also be contained in the contribution which

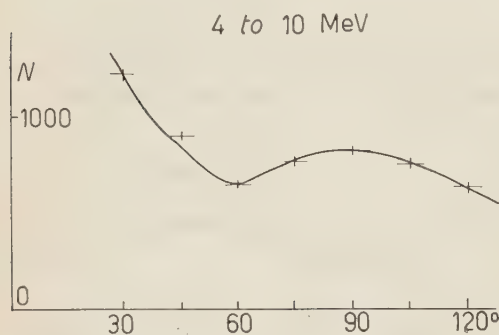


Fig. 9.

is peaked at small angles, indicating direct emission of first neutrons by the two-particle interaction stage with subsequent formation of a compound nucleus emitting the second neutron.

The remaining portion of the anisotropic contribution, which is peaked at small angles, accounts for neutrons emitted simultaneously and with almost equal energies.

4. - Conclusions.

The principal mechanism of 14 MeV neutrons induced $(n, 2n)$ reactions in medium weight and heavy nuclei is the successive emission of the two neutrons. The second compound system (see Fig. 1) has a lifetime which is long compared with the transit time of nucleons over nuclear dimensions: *i.e.* a defined quantum state, a compound nucleus, is formed between the emissions of the first and the second neutron. This result, previously deduced from measurements of energy spectra (see I), has been confirmed by recent angular distribution measurements (⁷).

On the other hand, the first neutron in a $(n, 2n)$ reaction leading to subsequent emission of the second neutron is emitted both, directly by the two-particle interaction stage and by a compound nucleus (⁷).

In 14 MeV neutron induced $(n, 2n)$ reactions with light nuclei, *e.g.* ${}^9\text{Be}(n, 2n){}^8\text{Be}$, these alternative courses of successive neutron emission have been proved by the angular distribution measurement.

A third possible mechanism, simultaneous emission of two neutrons in the ${}^9\text{Be}(n, 2n){}^8\text{Be}$ reaction, has been proved by the angular correlation measurements. This contribution is emitted mainly at small angles with respect to the direction of incident 14 MeV neutrons, the two neutrons having almost equal energies (see Figs. 6 and 9).

A possible contribution of simultaneous emission of two neutrons in $(n, 2n)$ reactions with medium weight and heavy nuclei cannot be proved since the

(n- γ) coincidence rate is very important. But there is some positive evidence for simultaneous emission in the $^{58}\text{Ni}(p, 2p)$ reaction ⁽¹¹⁾.

* * *

We would like to express our gratitude to Professor FRANCIS PERRIN for his hospitality and for his continued and stimulating encouragement.

We wish to acknowledge gratefully fellowships of the « Commissariat à l'Energie Atomique » (K.W.) of the C.N.R.S. (B.T.) and of the « Stifterverband für die Deutsche Wissenschaft » (E.R.).

⁽¹¹⁾ B. L. COHEN: *Phys. Rev.*, **108**, 768 (1957).

RIASSUNTO (*)

Si è studiata la correlazione fra le rispettive direzioni di emissione dei due neutroni nella reazione $^9\text{Be}(n, 2n)^8\text{Be}$ servendosi della rivelazione per coincidenza dei neutroni uscenti. Nel piano azimutale predominano angoli di separazione da 45° a 90° ; si ha un massimo di correlazione di $(20 \pm 3)\%$ a 60° . Si attribuisce questa correlazione angolare all'emissione simultanea di due neutroni. Misure della distribuzione angolare nella stessa reazione hanno provato, con l'ausilio di tecniche di tempo di volo, che i secondi neutroni sono emessi da nuclei composti, mentre i primi neutroni sono emessi sia direttamente, sia da un nucleo composto.

(*) Traduzione a cura della Redazione.

Zur Interpretation von Jets mit dem Modell der angeregten Nukleonen.

J. BURMEISTER, K. LANIUS und H. W. MEIER

*Deutsche Akademie der Wissenschaften zu Berlin
Kernphysikalisches Institut Zeuthen - Berlin*

(ricevuto il 4 Settembre 1958)

Summary. — A method for the determination of γ_c in nucleon-nucleon collisions of very high energy based on the model of excited nucleons is presented. Isotropic angular distribution of the secondary particles in the centre of mass systems of the emitting nucleons is assumed. The energy of all secondaries is assumed to be the same in both systems. Relations for γ_c and the Lorentz factor γ' of the nucleon after the collisions in the centre of gravity frame of reference are given. The γ_c values computed for a great number of high energy jets are compared with the values following from the statistical method of Castagnoli *et al.* A comparison is made with the data given by Koba for the multiplicity in the two centre model. The relations recently presented by TSCHERNAWSKI for the Heisenberg case of π -N-collisions are in good agreement with our assumptions.

Einleitung.

Die experimentellen Ergebnisse über die Vielfacherzeugung von Sekundärteilchen bei Wechselwirkung von hochenergetischen Teilchen mit Materie wurden in den meisten Untersuchungen mit den Voraussagen der Modelle von Heisenberg ⁽¹⁾, Fermi ⁽²⁾ und Landau ⁽³⁾ verglichen. Allen drei Modellen ist gemeinsam, daß ein und nur ein Raumgebiet hoher Energiedichte entsteht, das dann die Ursache für die Vielfacherzeugung ist.

⁽¹⁾ W. HEISENBERG: *Zeits. Phys.*, **133**, 65 (1952).

⁽²⁾ E. FERMI: *Phys. Rev.*, **81**, 683 (1951).

⁽³⁾ S. S. BELEN'KIJ und L. D. LANDAU: *Fortschr. Phys. Wiss.*, **56**, 309 (1955).

In jüngster Zeit wurden insbesondere durch die Untersuchungen an Jets in Kernemulsionen von CIOK u.a. ^(4,5) Hinweise darauf gefunden, daß die Abstrahlung der Anregungsenergie unabhängig voneinander aus zwei Zentren erfolgt, die nach dem Stoß im Schwerpunktsystem in entgegengesetzten Richtungen auseinanderfliegen (*). Theoretische Arbeiten, die auf dieser Modellvorstellung beruhen, wurden schon vor einiger Zeit publiziert (TAKAGI ⁽⁷⁾, KRAUSHAAR und MARKS ⁽⁸⁾, Koba ⁽⁹⁾).

In der vorliegenden Arbeit versuchen wir, eine größere Anzahl hochenergetischer Jets mit dem Zwei-Zentren-Modell zu interpretieren. Dabei nehmen wir an, daß die nach dem Stoß im Schwerpunktsystem auseinanderfliegenden Zentren angeregte Nukleonen sind.

Das in der Arbeit verwandte experimentelle Material wurde zum Teil in unserem Laboratorium gewonnen, zu einem anderen Teil entstammt es der Literatur ⁽¹⁰⁻¹⁴⁾ und privaten Mitteilungen ⁽⁺⁾.

1. – Berechnung von γ_c nach dem Zwei-Zentren-Modell.

Den untenstehenden Beziehungen liegt im Schwerpunktsystem (S-System) das folgende Modell zugrunde (Abb. 1): Vor dem Stoß bewegen sich beide Nukleonen mit gleicher Geschwindigkeit aufeinander zu. Infolge der Wechsel-

⁽⁴⁾ P. CIOK, T. COGHEN, J. GIERULA, R. HOŁYŃSKI, A. JURAK, M. MIĘSOWICZ, T. SANIEWSKA, O. STANISZ und J. PERNEGR: *Nuovo Cimento*, **8**, 166 (1958).

⁽⁵⁾ P. CIOK, T. COGHEN, J. GIERULA, R. HOŁYŃSKI, A. JURAK, M. MIĘSOWICZ, T. SANIEWSKA und J. PERNEGR: *Nuovo Cimento* (im Druck).

(*) Zur gleichen Deutung kam auch COCCONI ⁽⁶⁾ bei der Analyse einiger hochenergetischer Jets.

⁽⁶⁾ G. COCCONI: Vorabdruck.

⁽⁷⁾ S. TAKAGI: *Progr. Theor. Phys.*, **7**, 123 (1952).

⁽⁸⁾ W. L. KRAUSHAAR und L. J. MARKS: *Phys. Rev.*, **93**, 326 (1954).

⁽⁹⁾ Z. Koba: *Progr. Theor. Phys.*, **7**, 123 (1952).

⁽¹⁰⁾ P. CIOK, M. DANYSZ, J. GIERULA, A. JURAK, M. MIĘSOWICZ, J. PERNEGR, J. VRANA und W. WOLTER: *Nuovo Cimento*, **6**, 1409 (1957).

⁽¹¹⁾ A. DEBENEDETTI, C. M. GARELLI, L. TALLONE und M. VIGONE: *Nuovo Cimento*, **4**, 1142 (1956).

⁽¹²⁾ B. EDWARDS, J. LOSTY, D. W. PERKINS, K. PINKAU und J. REYNOLDS: *Phil. Mag.*, **3**, 237 (1958).

⁽¹³⁾ R. G. GLASSER, D. M. HASKIN und M. SCHEIN: *Phys. Rev.*, **99**, 1555 (1955).

⁽¹⁴⁾ E. G. BOOS, A. CH. WINIZKI, J. S. TAKABAJEW und I. J. TSCHASNIKOW: *Journ. Exp. Theor. Phys.*, **34**, 622 (1958).

(+) Wir möchten an dieser Stelle Herrn Prof. Dr. M. MIĘSOWICZ, Krakau, Dr. J. GIERULA, Warschau, Dr. J. PERNEGR, Prag, sowie Dr. G. ŽDANOW, FIAN, Moskau, und ihren Mitarbeitern für die Überlassung der Winkelverteilungen der Jets ihrer Laborenatorien unseren Dank aussprechen.

wirkung findet eine Umwandlung von kinetischer Energie in Anregungsenergie der Nukleonen statt. Es wird angenommen, daß beide Stoßpartner gleich stark angeregt werden und demzufolge nach dem Stoß gleiche Geschwindigkeiten besitzen.

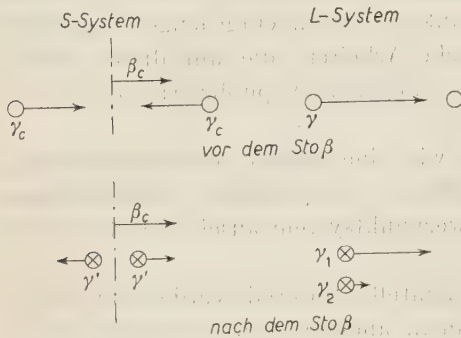


Abb. 1. - Schematische Darstellung des Stoßes mit den entsprechenden Lorentzfaktoren der Nukleonen ($\gamma = (1 - \beta^2)^{-\frac{1}{2}}$).

Die Abstrahlung der Anregungsenergie erfolgt als Emission von Sekundärteilchen und geschieht für beide Nukleonen unabhängig voneinander. Die Winkelverteilung der abgestrahlten Teilchen wird in den entsprechenden Ruhssystemen der strahlenden Nukleonen als isotrop vorausgesetzt. Die Energie pro Sekundärteilchen betrage in den Ruhssystemen $E'' = 0.5 \text{ GeV}$ (*).

Ausgehend vom Energiesatz im Laborsystem (L-System) erhalten wir unter Berücksichtigung der Anregungsenergien die Gleichung (+)

$$(1) \quad \gamma_{cII} = \frac{1}{\sqrt{2}} \left[\gamma_1 + \gamma_2 + \frac{3}{2} \frac{E''}{mc^2} (n_1 \gamma_1 + n_2 \gamma_2) \right]^{\frac{1}{2}}.$$

Hierbei ist m die Nukleonenmasse und $n_s = n_1 + n_2$ die Zahl der (von den beiden Nukleonen) beim Stoß erzeugten geladenen Mesonen, γ_1, γ_2 bedeuten die Lorentzfaktoren der Nukleonen nach dem Stoß gegenüber dem L-System. Mit $n_1 \approx n_2 \approx n_s/2$ folgt

$$(1a) \quad \gamma_{cII} \approx \frac{1}{\sqrt{2}} \left[(\gamma_1 + \gamma_2) \left(1 + \frac{3}{4} \frac{E''}{mc^2} n_s \right) \right]^{\frac{1}{2}}.$$

Für den Lorentzfaktor der Nukleonen nach dem Stoß im S-System liefert der Energiesatz im S-System die Beziehung

$$(2) \quad \gamma' = \gamma_{cII} \left/ \left(1 + \frac{3}{4} \frac{E''}{mc^2} n_s \right) \right.$$

(*) Siehe hierzu die Untersuchungen über die Transversalimpulse der Sekundärteilchen von Jets ^(12,15).

⁽¹⁵⁾ O. MINAKAWA, Y. NISHIMURA, M. TZUZUKI, H. YAMANOUCHI, H. AIZU, H. HASEGAWA, Y. YSHII, S. TOKUNAGA, Y. FUJIMOTO, S. HASEGAWA, J. NISHIMURA, K. NIU, K. YISHIKAWA, K. IMAEDA und M. KAZUNO: *INSJ-7* preprint, Tokyo, March (1958).

(+) Die Indizes I und II beziehen sich auf das Ein- bzw. Zwei-Zentren-Modell.

Der Inelastizitätskoeffizient K_{II} ergibt sich zu

$$(3) \quad K_{II} = \frac{\gamma_{c_{II}}}{\gamma_{c_{II}} - 1} \frac{1}{\frac{4}{3}(mc^2/E'')(1/n_s) + 1}.$$

2. – Vergleich der Energiebestimmungen mit Hilfe der beiden Modelle.

Da sich weder die Gleichung (1) noch (1a) direkt mit den Beziehungen von CASTAGNOLI u.a. ⁽¹⁶⁾ für γ_{c_I} vergleichen lassen, wurde ein Vergleich der experimentellen Daten durchgeführt. Hierzu wurde γ_{c_I} in erster und zweiter Näherung (s. Anhang) sowie $\gamma_{c_{II}}$ nach der Gleichung (1) für alle verfügbaren Jets mit Energien $> 10^{11}$ eV und $N_h \leq 5$ berechnet.

Zur Berechnung von $\gamma_{c_{II}}$ wurden die Spuren auf die Kegel so aufgeteilt, daß bei einer deutlichen Trennung der beiden Kegel die entsprechenden Spurenzahlen genommen wurden. War keine klare Unterscheidung möglich, so wurden die Spuren im Verhältnis 1:1 getrennt. In einigen Fällen wurde über die Ergebnisse verschiedener Aufteilungen gemittelt.

Die Aussonderung der Nukleon-Kern-Stöße erfolgte näherungsweise dadurch, daß nur Ereignisse als N-N-Stöße aufgefaßt wurden, bei denen l mit der Beziehung

$$(4) \quad l = \frac{2n_s - 1}{2.4 \gamma_{c_I}^{\frac{1}{2}} + 1}$$

berechnete Zahl der getroffenen Nukleonen l kleiner als 2 war (*).

In den Abb. 2 und 3 ist $\gamma_{c_{II}}$ in Abhängigkeit von $\gamma_{c_I}^{(1)}$ bzw. $\gamma_{c_I}^{(2)}$ dargestellt. Wie aus der Abb. 3 hervorgeht, stimmen die mit dem Modell der angeregten

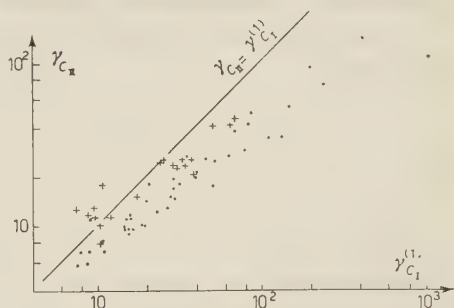


Abb. 2. – Vergleich der nach dem Modell der angeregten Nukleonen berechneten Lorentzfaktoren $\gamma_{c_{II}}$ mit den Werten, die sich nach CASTAGNOLI u.a. ⁽¹⁶⁾ in erster Näherung ergeben; (•) $l < 2$; (+) $l \geq 2$ (l berechnet mit Hilfe von (4)).

⁽¹⁶⁾ C. CASTAGNOLI, G. CORTINI, C. FRANZINETTI, A. MANFREDINI und D. MORENO: *Nuovo Cimento*, **10**, 1539 (1953).

(*) Vorläufige Rechnungen hatten gezeigt, daß auch für das Modell der angeregten Nukleonen kleine l -Werte auftreten, wenn der nach (4) berechnete Wert klein ist.

Nukleonen erhaltenen γ_c -Werte gut mit den Daten überein, die man bei

Berücksichtigung der Winkel- und Energieverteilung nach ⁽¹⁶⁾ erhält.

Die Betrachtungen der folgenden Abschnitte wurden mit den nach Gleichung (1) berechneten Werten für γ_c durchgeführt.

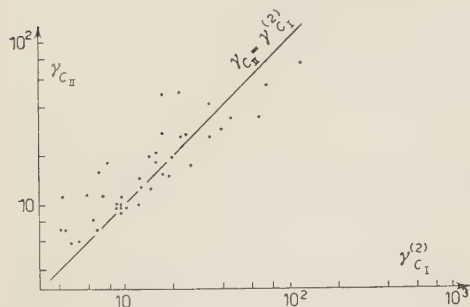


Abb. 3. – Vergleich von γ_{cII} mit den Werten $\gamma_{cI}^{(2)}$ in zweiter Näherung.

3. Vergleich der Multiplizitäten mit den Aussagen der Theorien des Zwei-Zentren-Modells.

Im folgenden seien die experimentellen Multiplizitäten mit den von KOBA ⁽⁹⁾ geforderten Teilchenzahlen verglichen.

KOBA gibt für die Zahl der erzeugten Teilchen n_s den folgenden Ausdruck an:

$$(5) \quad n_s \sim \begin{cases} \gamma_c^3 & \text{für } K_{II} = 1, \\ [K_{II}/(1 - K_{II})]^3 & \text{für } K_{II} < 0,8. \end{cases}$$

In der Abb. 4 ist $\lg n_s^*$ in Abhängigkeit von $\lg \gamma_{cII}$ aufgetragen (*), wobei die einzelnen Gruppen durch verschiedene nach der Gleichung (3) berechnete K_{II} -Werte charakterisiert sind.

Durch die Meßpunkte der verschiedenen Gruppen der Abb. 4 wurden mit Hilfe der Ausgleichsrechnung Geraden $\lg \gamma_{cII} = a_K \lg n_s^* + b_K$ gelegt, und die Größen a_K , b_K auf die Größen $m(K_{II})$, $C(K_{II})$ der Relation $n_s^* = C(K_{II})\gamma_c^{(m(K_{II}))}$ umgerechnet. Den Verlauf von m mit K_{II} gibt die Abb. 5

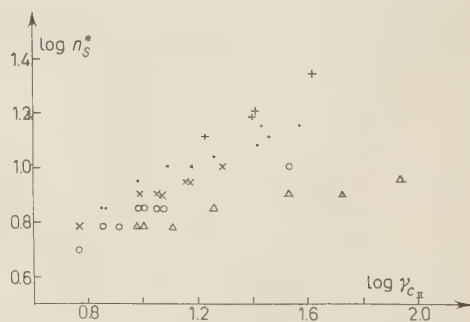


Abb. 4. – Der Zusammenhang zwischen der Multiplizität und γ_{cII} für verschiedene Inelastizitätskoeffizienten; \triangle) $K_{II} = 0,76 \div 0,80$; \circ) $0,81 \div 0,82$; \times) $0,83 \div 0,85$; \bullet) $0,86 \div 0,88$; $+$) $0,89 \div 0,92$.

(*) Hierbei ist $n_s^* = \begin{cases} n_s - 1, & \text{falls das Primärteilchen ein n oder p ist,} \\ n_s - 2, & \text{falls das Primärteilchen ein } \alpha\text{-Teilchen ist.} \end{cases}$

wieder. Wie hieraus hervorgeht, scheint n_s für $K_{II} < 0,8$ von K_{II} nahezu unabhängig zu sein, während für wachsende K_{II} -Werte ein Anstieg zu verzeichnen ist. Weiterhin hat $O(K_{II})$ die gleiche Größenordnung wie der Proportionalitätsfaktor der Relation (5).

Kürzlich erhielten wir Kenntnis von einer neuen theoretischen Arbeit von TSCHERNAWSKI ⁽¹⁷⁾ über die Vielfacherzeugung von Mesonen. Hierin behandelt er in dem Abschnitt über die peripheren Stöße das Modell der angeregten Nukleonen und untersucht verschiedene Versionen der Wechselwirkung. Beim Vergleich mit dem Experiment findet er, daß die von der Fermi-Landauschen Theorie der π -N-Wechselwirkung geforderten Multiplizitäten gegenüber den anderen Versionen die beste Übereinstimmung mit dem empirischen Material aufweisen. Die Winkelverteilungen der erzeugten Teilchen in den Ruhssystemen der Nukleonen nach dem Stoß sollten gemäß dieser Theorie stark anisotrop sein. Dies steht jedoch in krassem Widerspruch zu dem experimentellen Befund, wonach nahezu isotrope Verteilungen vorliegen ⁽⁵⁾.

Der durchgeführte Vergleich der Multiplizitäten scheint uns nicht zulässig zu sein, da sich die dabei verwendeten Werte für γ' auf ein Zwei-Zentren-Modell ^(1,5) beziehen, das sich wesentlich von dem Modell der angeregten Nukleonen unterscheidet. Wir vergleichen nunmehr die Beziehungen der Arbeit ⁽¹⁷⁾ mit den von uns verwendeten Relationen.

Löst man die Gleichung (2) der vorliegenden Arbeit nach n_c auf, so erhält man (mit $\gamma_{cII} = \gamma_c$)

$$(6) \quad n_s = \frac{4}{3} \frac{mc^2}{E''} \left(\frac{\gamma_c}{\gamma'} - 1 \right) \quad (*) .$$

Unter allen von TSCHERNAWSKI behandelten Versionen zeigt die für den Heisenbergischen Fall der π -N-Wechselwirkung gültige Beziehung

$$(7) \quad n_s = \frac{4}{3} \frac{mc^2}{E''} \frac{\gamma_c}{\gamma'}$$

⁽¹⁷⁾ D. TSCHERNAWSKI: Vorabdruck.

(*) Die Gleichung (6) gilt im Gegensatz zu (7) auch für kleine Werte γ_c/γ' . Im Grenzfall des elastischen Stoßes ist $\gamma_c/\gamma' = 1$ und somit $n_s = 0$, d.h. es werden keine Sekundärteilchen erzeugt.

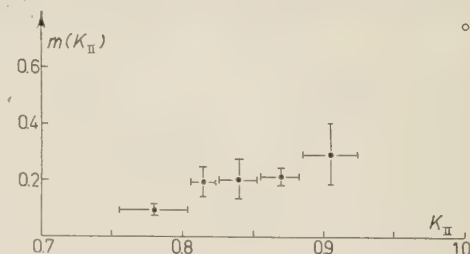


Abb. 5. — Variation von m mit K_{II} ; \circ der von Koba ⁽⁹⁾ geforderte theoretische Wert von 0,75 für $K_{II} = 1$.

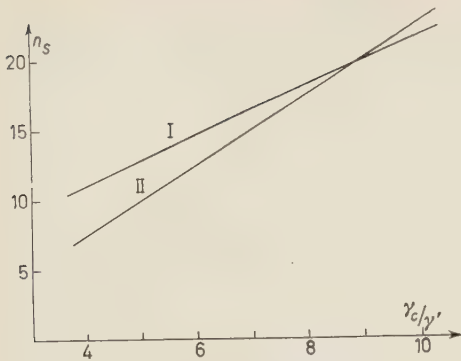


Abb. 6. – Vergleich der Relationen für die Multiplizitäten; I) Gleichung (7) von Tschernawski ⁽¹⁷⁾, II) Gleichung (6), verwendet in der vorliegenden Arbeit.

die beste numerische Übereinstimmung mit (6), wobei gilt:

$$(8) \quad E'' = m_\pi c^2 \ln \left(\frac{m \gamma_c}{m_\pi \gamma'} \right).$$

Der wesentliche Unterschied besteht darin, daß wir in unserer Beziehung (die als Bestimmungsgleichung für γ' diente) $E'' = \text{const} = 0.5 \text{ GeV}$ setzten.

Die Abb. 6 zeigt den Verlauf der beiden Beziehungen (6) und (7) in dem Energiegebiet der von uns verwendeten Jets.

In der Abb. 7 ist weiter der Zusammenhang zwischen dem Trans-

versalimpuls und der Größe γ_c/γ' dargestellt.

Es muß schließlich bemerkt werden, daß die Heisenbergsche Version der π -N-Wechselwirkung auch hinsichtlich der Winkelverteilung der erzeugten Teilchen in den Ruhssystemen der Nukleonen nach dem Stoß Übereinstimmung mit dem Experiment ⁽⁵⁾ zeigt, da diese Theorie eine nahezu isotrope Verteilung fordert ⁽¹⁷⁾.

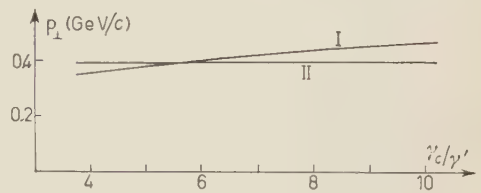


Abb. 7. – Vergleich der Relationen für die Transversalimpulse; I) Gleichung (8) von Tschernawski ⁽¹⁷⁾, II) $p_\perp = \text{const}$, verwendet in der vorliegenden Arbeit.

4. – Die Inelastizität.

In der Abb. 8 sind die auf Grund des Modells der angeregten Nukleonen ermittelten Werte des Inelastizitätskoeffizienten K_{II} (Gleichung (3)) in Abhängigkeit von γ_{cII} aufgetragen. Die Abb. 9 zeigt K_{II} als Funktion von n_s .

Wie aus beiden Abbildungen hervorgeht, liefert das Modell der angeregten Nukleonen relativ hohe K -Werte. Dies steht in Widerspruch zu den Ergebnissen anderer Untersuchungen, in denen niedrigere K -Werte ermittelt wurden. Bei der Beurteilung dieses Resultats muß man jedoch beachten, daß die Verwendung des Inelastizitätskoeffizienten zur Interpretation von Jets sehr pro-

blematisch ist. TSCHERNAWSKI kommt in der Arbeit⁽¹⁷⁾ zu der Schlußfolgerung, daß sich sowohl vom experimentellen als auch theoretischen Standpunkt aus keine eindeutigen Kriterien zur Unterscheidung der Sekundär- und Primärteilchen angeben lassen.

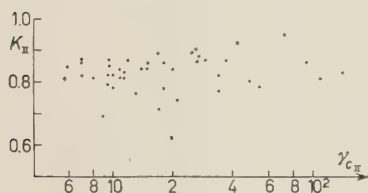


Abb. 8. — Variation des Inelastizitätskoeffizienten mit γ_{cII} .

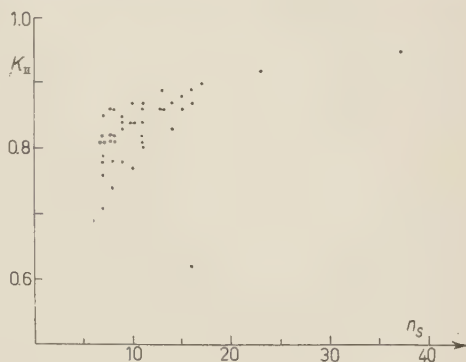


Abb. 9. — Variation des Inelastizitätskoeffizienten mit n_s .

* * *

Abschließend möchten wir Herrn Prof. Dr. M. MIESOWICZ, Dr. J. GIERULA, Dr. I. GRAMENITZKI, Dr. J. PERNEGR und Dr. G. ŽDANOV sowie Herrn T. COGHEN für die wertvollen Diskussionsbemerkungen auf der Tagung in Liblice bei Prag unseren Dank aussprechen.

AN H A N G

Die Bestimmung von $\gamma_{cI}^{(1)}$ (der obere Index weist auf die erste Näherung hin) erfolgte mit Hilfe der Beziehung⁽¹⁶⁾

$$\lg \gamma_{cI}^{(1)} = -\frac{1}{n_s} \sum_{i=1}^{n_s} \lg \operatorname{tg} \vartheta_i.$$

Bei einigen Jets wurden Spuren beobachtet, die innerhalb der Meßgenauigkeit in der Richtung des Primärteilchens lagen. Auf Grund der Symmetriebedingung im S -System wurde in diesen Fällen bei der Berechnung von γ zugleich mit dieser inneren Spur die Spur mit dem größten Winkel fortgelassen.

In zweiter Näherung gilt⁽¹⁶⁾

$$\ln \gamma_{cI}^{(2)} = \ln \gamma_{cI}^{(1)} + A_k E.$$

Hierbei berücksichtigt A_k die Abweichung der experimentellen von der isotropen Winkelverteilung im S-System und F die Form des Energiespektrums.

Geht man von der Verteilung

$$dF \sim \cos^{2k} \vartheta' d \cos \vartheta'$$

aus, so gilt

$$\lg \left| \frac{n_s - 2n(\leq \vartheta)}{n_s} \right| = (2k + 1) \lg \left| \frac{1 - \alpha^2}{1 + \alpha^2} \right|, \quad \alpha = \gamma_{cI}^{(1)} \operatorname{tg} \vartheta.$$

Den so gefundenen Werten von k wurden die in ⁽¹⁶⁾ angegebenen Größen A_k zugeordnet.

Der Berechnung von F lag das Heisenberg-Spektrum zugrunde ⁽¹²⁾. Dabei wurde die «Abschneideenergie» für alle γ_c -Werte zu $\varepsilon_0 = 1.2$ angenommen. Wie aus der Abb. 3 hervorgeht, läßt sich bei geeigneter Variation von ε_0 mit γ_{cI} eine bessere Übereinstimmung mit der Geraden $\gamma_{cII} = \gamma_{cI}^{(2)}$ erreichen.

RIASSUNTO (*)

Si presenta un metodo per la determinazione di γ_c nelle collisioni nucleone-nucleone di energia molto alta basato sul modello dei nucleoni eccitati. Si assume la distribuzione angolare isotropica delle particelle secondarie nel sistema del centro di massa dei nucleoni emittenti. L'energia di tutti i secondari si assume uguale nei due sistemi. Si danno relazioni per γ_c e per il fattore di Lorentz γ' del nucleone dopo le collisioni nel sistema del centro di massa. Si confrontano i valori di γ_c calcolati per un gran numero di jet di alta energia coi valori ottenuti seguendo il metodo statistico di Castagnoli *et al.* Si fa un confronto coi dati di Koba per la molteplicità nel modello a due centri. Le relazioni recentemente presentate da TSCHERNAWSKI per il caso di Heisenberg delle collisioni π -N sono in buon accordo con le nostre assunzioni.

(*) Traduzione a cura della Redazione.

Investigation of Nuclear Interactions of Energies between 10 and 100 GeV.

E. FENYVES, E. GOMBOSI and P. SURÁNYI

Central Research Institute of Physics - Budapest

(ricevuto il 9 Settembre 1958)

Summary. — The angular and energy distribution of shower particles of seven nuclear interactions, mostly complex collisions, were measured. The Lorentz factor γ_{cm} of the center of mass system (CMS) was determined from the energy of secondaries and the Lorentz factor γ_{sym} of the symmetry system was obtained from the angular distribution. It was found that $\gamma_{\text{sym}}/\gamma_{\text{cm}} = 0.92 \pm 0.15$, which corresponds to a symmetrical emission of shower particles in the CMS. Energy distribution in the CMS as well as transversal momentum distribution of shower particles were also determined.

1. — Introduction.

We have measured the angular distribution of shower particles generated in nuclear interactions of cosmic ray particles in emulsion. The nuclear interactions were found by surface scanning in plates of the I stack irradiated in the Po-Valley Expedition, 1955. The only requirement in selecting the events was that the energy of almost all shower particles should be determinable without respect to the nature of the primary particle and the number of gray and black prongs. Thus the majority of these events corresponds to nucleon-nucleus or nucleus-nucleus collisions. Our aim was to investigate *a)* the symmetry of the emission of shower particles in the forward and backward cone in the CMS, *b)* the energy distribution in the CMS, and *c)* the transversal momentum distribution of shower particles.

2. - Symmetry of the angular distribution in the CMS.

The velocity of the CMS relative to the laboratory system (LS) was determined in the usual way ⁽¹⁾ from

$$V = \frac{\sum_i p_i \cos \vartheta_i}{\sum_i E_i},$$

where p_i , E_i and ϑ_i are momentum, energy and angle of emission, respectively, of shower particles in the LS (*). From V the Lorentz factor of the CMS can be calculated:

$$\gamma_{\text{cm}} = \frac{1}{\sqrt{1 - V^2}}.$$

As usual, all particles with $I \leq 1.5I_{\text{min}}$ were considered as shower particles and their energies and momenta determined at lower energies by simple scattering and at higher energies by relative scattering measurements.

We have found seven nuclear interactions in which the energy of almost all shower particles could be measured. However, owing to the great statistical error in the values of the γ_{cm} determined, the deviation from the forward-backward symmetry of the angular distribution indicated large fluctuations in individual cases. Therefore, the value of γ_{sym} which best transforms the angular distribution as measured in the LS into a symmetrical one in the CMS was estimated for each event and the ratio $\gamma_{\text{sym}}/\gamma_{\text{cm}}$ was built for each interaction (Table I). γ_{sym} was determined according to the method of CASTA-

TABLE I.

Symbol of jet	γ_{cm}	γ_{sym}	$\gamma_{\text{sym}}/\gamma_{\text{cm}}$
17 + 17 α	4.6 \pm 1.3	3.6 \pm 0.8	0.78 \pm 0.27
6 + 11 α	5.2 \pm 1.6	6.5 \pm 1.8	1.25 \pm 0.52
5 + 10 α	7.8 \pm 2.7	6.9 \pm 2.2	0.88 \pm 0.41
14 + 13n	5.9 \pm 2.1	7.7 \pm 1.9	1.30 \pm 0.57
17 + 10n	4.3 \pm 1.5	3.9 \pm 1.1	0.89 \pm 0.40
26 + 18z	5.5 \pm 1.6	4.7 \pm 1.0	0.85 \pm 0.32
1 + 8p	23.2 \pm 10.5	25.4 \pm 8.1	1.09 \pm 0.61

(*) The above relation holds only if we assume that the conservation of momentum is valid for charged particles independently of uncharged particles being emitted; this assumption can be made only if the number of shower particles is high.

(1) R. G. GLASSER, D. M. HASKIN and M. SCHEIN: *Phys. Rev.*, **99**, 1555 (1955).

GNOLI *et al.* ⁽²⁾ from

$$\ln \gamma_{\text{sym}} = -\frac{1}{n_s} \sum_i \ln \text{tg } \vartheta_i,$$

where n_s is the number of shower particles.

It can be seen from Table I that the weighted mean of the values of $\gamma_{\text{sym}}/\gamma_{\text{cm}}$ is

$$\frac{\gamma_{\text{sym}}}{\gamma_{\text{cm}}} = 0.92 \pm 0.15,$$

and the fluctuation of individual values around this mean value is not significantly higher than normal.

Thus we can conclude that the angular distribution of shower particles generated in such nuclear interactions which are mostly complex collisions and involving energies between 10 and 1000 GeV, is symmetrical in the forward and backward direction within the limits of error given above. This result is in good agreement with the hydrodynamical meson production theory of Landau ⁽³⁾ which predicts symmetrical emission of shower particles in the forward-backward direction in the CMS also for complex collisions.

Applying the same procedure as above to the jet data published in the literature ^(1,4-8) we obtain for these jets

$$\frac{\gamma_{\text{sym}}}{\gamma_{\text{cm}}} = 1.03 \pm 0.14.$$

which is in good agreement with our result. We must emphasize, however, that the data published in the literature are strongly biased, because the authors have expressly searched for jets of nucleon-nucleon collision character.

Our result shows at the same time that symmetry of the angular distribution of the collisions in the CMS cannot be used as an argument proving the collisions to be nucleon-nucleon collisions, as was done earlier.

⁽²⁾ C. CASTAGNOLI, G. CORTINI, G. FRANZINETTI, A. MANFREDINI and A. MORENO: *Nuovo Cimento*, **10**, 1539 (1953).

⁽³⁾ S. Z. BELEN'KIJ and L. D. LANDAU: *Usp. Fiz. Nauk.*, **56**, 309 (1955).

⁽⁴⁾ E. FRIEDLÄNDER: *Studii di Cercetari de Fizika* (in press).

⁽⁵⁾ E. G. BOOS, A. H. VINICKIJ, J. S. TAKIBAEV and I. A. ČASNIKOV: *Žu. Èksper. Teor. Fiz.*, **34**, 621 (1958).

⁽⁶⁾ V. D. HOPPER, S. BISWAS and J. F. DARBY: *Phys. Rev.*, **84**, 457 (1951).

⁽⁷⁾ M. DEMEUR, C. DILWORTH and M. SCHÖNBERG: *Nuovo Cimento*, **9**, 92 (1952).

⁽⁸⁾ A. DEBENEDETTI, C. M. GARELLI, L. TALLONE and V. VIGONE: *Nuovo Cimento*, **4**, 1142 (1956).

It is also worth while by note that in the paper of EDWARDS *et al.* ⁽⁹⁾ symmetry in complex collisions in the CMS is a basic assumption used in the discussion of results on elasticity. Although the energy of their jets is much higher than the energy of the jets investigated by us, the symmetry found in the present work may support the validity of the basic assumption made by EDWARDS *et al.*

3. - Energy and transversal momentum distribution of shower particles.

Assuming that all particles are mesons we have calculated from the energies of the shower particles as measured in the LS and from the values obtained for γ_{cm} the energy distribution in the CMS and the transversal momentum distribution for all particles of the seven interactions (Fig. 1 and 2). The energy distribution has a maximum at an energy somewhat higher than $m_{\pi}c^2$ which was predicted by the Heisenberg theory of multiple meson production ⁽¹⁰⁾.

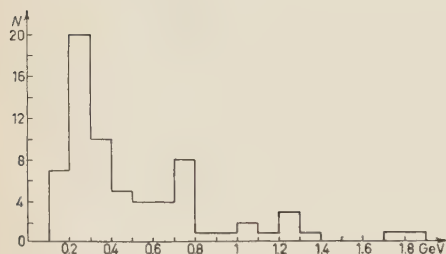


Fig. 1. - Transversal momentum distribution.

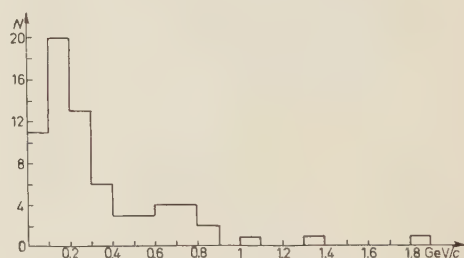


Fig. 2. - Energy distribution in the C.M. system.

The transversal momenta have a mean value of about 0.3 GeV/c which is in rough agreement with values found by other authors. At such relatively low primary energies, however, the energies of secondary particles are also low and the fact that we have measured only shower particles with $I \leq 1.5 I_{\min}$ affects the form of the energy and transversal momentum distributions.

Thus the above distributions are strongly biased by the mode of selection of the shower particles. Furthermore, owing to the large spread of the primary

⁽⁹⁾ E. EDWARDS, I. LOSTY, D. A. PERKINS, K. PINKAU and I. REYNOLDS: *Phil. Mag.*, **3**, 237 (1958).

⁽¹⁰⁾ W. HEISENBERG: *Vorträge über kosmische Strahlung* (Berlin-Göttingen-Heidelberg 1953).

energies of the individual interactions the building of a composite energy and momentum distribution is not justified and thus no definite conclusion can be drawn from the distributions found here as to the validity of multiple meson production theories.

RIASSUNTO (*)

È stata misurata la distribuzione angolare ed energetica delle particelle di uno sciame di sette interazioni nucleari, prevalentemente collisioni complesse. Il fattore di Lorentz γ_{cm} del sistema del centro di massa (CMS) è stato determinato dall'energia dei secondari e il fattore di Lorentz del sistema di simmetria γ_{sym} è stato ottenuto dalla distribuzione angolare. Si è trovato che $\gamma_{\text{sym}}/\gamma_{\text{cm}} = 0.92 \pm 0.15$ corrispondente all'emissione simmetrica delle particelle dello sciame nel CMS. Sono anche state determinate la distribuzione energetica nel CMS, nonché la distribuzione dell'impulso trasversale delle particelle dello sciame.

(*) Traduzione a cura della Redazione.

On the Interpretation of Cosmic Ray Jets: The "Funnel" Model.

T. GOZANI and K. SITTE

Department of Physics, Technion, Israel Institute of Technology - Haifa

(ricevuto l'11 Settembre 1958)

Summary. — Arguments are presented in favour of the interpretation of cosmic ray jets as composite collisions, in a single act, of the primary with a compound of target nucleons. In particular, it is pointed out that the identity of « successive » collisions is lost at high energies, because the expanding meson cloud enwraps the compound before ejecting the bulk of the secondaries. According to this view, the primary energies assigned to the jets by the customary procedures are too low in many cases, and especially for events with large numbers N_h of heavy prongs. The resulting difference in the true primary energies of the jets with, say, $N_h \leq 3$ and $N_h > 3$ accounts for the apparently excessive frequency of the events of low N_h . But if one wishes to retain the model of the nucleus as an aggregate of corpuscles, the cross section of the avalanche of interacting nucleons will increase with penetration, and the usual picture of the interaction volume shaped like a cylindrical tunnel must be replaced by that of an inverted funnel. This « funnel model » predicts a stronger dependence of the multiplicities on the atomic weight of the target nucleus, and seems to fit the—rather scanty—experimental data somewhat better. It is then shown that according to this model, the larger part of the observed multiplicity spread is not due to the « fundamental fluctuations » in the emission of secondaries in a nucleon-nucleon collision, but to the randomness in the number of particles involved. For nucleon-nucleon interactions at about $5 \cdot 10^{12}$ eV, the « fundamental fluctuations » can be approximated by a Gaussian with a width $\sigma = 6.5$.

1. — Although so far no completely satisfactory theory of meson production in high-energy nuclear collisions has been developed, wide agreement has now been reached about a number of general features which must be adopted by any such theory. In particular, it is now evident that Fermi's original assumption ⁽¹⁾ defining as « collision volume » the overlapping part of the col-

⁽¹⁾ E. FERMI: *Progr. Theor. Phys.*, **5**, 570 (1950); *Phys. Rev.*, **81**, 683 (1950).

liding meson fields, cannot be maintained and must be replaced by a model in which collision and ejection of meson secondaries are considered as two essentially separate acts. The first only provides the energy necessary to «heat» the field, and the second takes place only after this field has expanded to a much larger volume. This picture forms the basis of both Heisenberg's ⁽²⁾ and Landau's ⁽³⁾ theories, and of their various modifications proposed to meet the experimental criteria.

However, a comparison with the experiment is further complicated by the fact that empirical data are available only from the analysis of jets in emulsions or from air showers: both referring not to pure nucleon-nucleon encounters but to the more complex phenomenon of the traversal of a nucleus by an energetic particle. Cascade theories describing this process have been worked out by HEITLER and TERREAUX ⁽⁴⁾, and by McCUSKER and ROESSLER ⁽⁵⁾. A more general approach has been used by COCCONI ⁽⁶⁾, and by BELEN'KIJ and MILEKHIN ⁽⁷⁾. In all these cases, the phenomenon is treated as the collision of the incident nucleon with all the particles contained in the «tunnel» or «tube» which its passage cuts through the nucleus; COCCONI viewed the problem as a simultaneous interaction of the primary with n nucleons and applied the Fermi model to this «composite collision», while BELEN'KIJ and MILEKHIN based their work on Landau's theory.

More recently, PERKINS and his collaborators ⁽⁸⁾ have cast doubt on the applicability of this model of composite collisions, claiming from their analysis of high-energy jets that the majority of these events should be interpreted as nucleon-nucleon collisions. In the present paper, the description of a nucleon-nucleus encounter as a single interaction between two unequal partners will again be adopted, and used in conjunction with the picture of the expanding meson cloud. Accordingly, we shall begin with showing by a very simple argument that if the latter view is taken, the former assumption—the composite-collision model—must necessarily be accepted.

Let $\langle p_s \rangle_c$ be the average momentum of the secondaries, in the center-of-mass system of the collision of a nucleon with a compound of n nucleons, and

(2) W. HEISENBERG: *Zeits. Phys.*, **113**, 61 (1939); *Zeits. Phys.*, **126**, 569 (1949); *Suppl. Nuovo Cimento*, **6**, 493 (1949).

(3) L. LANDAU: *Izv. Akad. Nauk SSSR*, 51 (1953); S. Z. BELEN'KIJ and L. LANDAU: *Suppl. Nuovo Cimento*, **3**, 15 (1956).

(4) W. HEITLER and C. TERREAUX: *Proc. Phys. Soc.*, A **66**, 929 (1953); C. TERREAUX: *Helv. Phys. Acta.*, **24**, 551 (1951).

(5) F. C. ROESSLER and C. B. A. McCUSKER: *Nuovo Cimento*, **10**, 127 (1953).

(6) G. COCCONI: *Phys. Rev.*, **93**, 1107 (1954).

(7) S. Z. BELEN'KIJ and G. A. MILEKHIN: *Žurn. Éksp. Teor. Fiz. USSR*, **29**, 20 (1955).

(8) B. EDWARDS, J. LUSTY, D. H. PERKINS, K. PINKAU and J. REYNOLDS: *Phil. Mag.*, **3**, 237 (1958).

$\langle \gamma_s \rangle_c \approx c \cdot \langle p_s \rangle_c$ their average energy, all expressed in units of nucleon rest mass. Meson emission from the heated cloud will then take place only when the cloud's linear extensions have reached a dimension of about $\hbar / \langle p_s \rangle_c$. On the other hand, the width of the target nucleus, in the C-system, will be of the order $R_0 \cdot A^{1/3} / (\gamma_n)_c$, where $(\gamma_n)_c$ stands for the energy of the n -particle compound in the C-system, measured in nucleon rest masses:

$$(1) \quad (\gamma_n)_c = (\gamma + n) / (2\gamma n + n^2 + 1)^{1/2}.$$

γ is the energy of the incident nucleon in the laboratory (L-) system. Evidently, for sufficiently large primary energies γ the meson cloud will encompass the entire nucleus before emission takes place, and then the concept of a sequence of interactions with individual nucleons, or of an intranuclear cascade, becomes meaningless since no distinction can be made between successive collisions. One can easily verify that in the region of jet energies ($\gamma \gtrsim 500$), this is true for all emulsion nuclei.

Another simple argument against the model of an intranuclear cascade as a succession of interactions, and for the idea of a «delayed» meson emission from the expanding cloud—though not necessarily for the composite-collision picture—, follows from the experimental evidence that the interaction mean free path *in the emulsion* of jet secondaries has been found to be very nearly geometrical. Hence it is difficult to see why only nucleons, and not all shower particles, should participate in the intranuclear cascade. But if this were the case, the number of meson-producing encounters would increase very rapidly with increasing nuclear dimensions, and their contribution to the total multiplicity of the collision would be very appreciable in spite of the comparatively lower energy of the π -meson secondaries. The first collision of a 10^{13} eV primary, for instance, would produce about 40 nucleon-active secondaries (neutral particles must be included in considerations of the intranuclear cascade), and even if for the secondaries of the forward cone Heitler's assumption of «plural» collisions⁽⁴⁾ offers some reduction, the second-generation collisions of the mesonic secondaries would add a high multiple of this number: a most unsatisfactory prediction.

If, on the other hand, the model of meson emission from the expanding cloud is accepted, the only real difference between nucleon-nucleon encounters and nucleon-nucleus, or composite, collisions lies in the amount of energy transferred to the cloud, and hence available for secondary production. In other words, one might say that even in a nucleon-nucleon collision the π -mesons originated in the interaction contribute to the secondary production—in the «cloud stage»—just as in a nucleon-nucleus collision. For example, if in accordance with an intranuclear-cascade model distinctions can be made between π -meson-nucleon interaction and nucleon-nucleon encounters—pos-

sibly in a distinctive composition of the shower—, events originating in light nuclei might differ from those initiated in heavy nuclei where the contribution of the π -mesons would be stronger. No such difference can exist according to the expanding-cloud picture.

The following discussion will, therefore, be based on the two assumptions of composite collisions and of secondary emission from the expanded meson cloud. Together with the general kinematical relations, these two elements already determine all the essential features of the method. In particular, the dependence of the numbers n_s of secondaries produced in a collision with a compound of n nucleons on this number n of participants is now fixed, without specific assumptions concerning the details of the underlying theory of meson production. For it is logical to conclude from our general assumptions that the average energy $\langle\gamma_s\rangle$ of the secondaries should only depend on the energy available per nucleon in the C-system, but not on the way in which this energy became available. One may also regard this assertion as a plausible extension of the conclusion of KAMEKO and OKAZAKI⁽⁹⁾ to processes other than nucleon-nucleon collisions. If we write $\langle\gamma_s\rangle_c = \varphi(\gamma/n)$, it follows from the well-known definition of the energy available in the C-system, W_c ,

$$(2) \quad W_c = (2n\gamma)^{\frac{1}{2}} \quad (\gamma \gg n)$$

that

$$(3) \quad n_s = (2n\gamma)^{\frac{1}{2}} / \varphi(\gamma/n).$$

Since the energy dependence of n_s can be approximated by a power law, $\langle\gamma_s\rangle_c$, will, in a similar approximation, also be represented by a relation

$$(4) \quad \langle\gamma_s\rangle_c = A \cdot (\gamma/n)^m,$$

from which one has

$$(5) \quad n_s = B \cdot n^{\frac{1}{2}+m} \cdot \gamma^{\frac{1}{2}-m}.$$

The empirical $\gamma^{\frac{1}{2}}$ -law for the multiplicity thus demands a $n^{\frac{1}{2}}$ -dependence of the multiplicity on the number of participants.

However, this latter statement requires some clarification before it is applied to a discussion of the experimental material. It must be pointed out that the argument is valid only if the primary energy is properly determined, *i.e.* under the assumption of a composite collision. All the customary methods of energy measurement, though, are based on the kinematics of a nucleon-nucleon collision. Take, for instance, the simplest case, applicable when the

⁽⁹⁾ SH. KAMEKO and M. OKAZAKI: *Nuovo Cimento*, **8**, 1 (1958).

relation $\beta_{\pi}/\beta_c = 1$ of the velocities β_{π} and β_c of secondaries and C-system holds: symmetry of emission in the C-system then demands that the angle $\theta_{\frac{1}{2}}$ containing one-half of all jet particles in the L-system obeys the relation

$$(6) \quad \operatorname{tg} \theta_{\frac{1}{2}} = 1/\gamma_c = (2/\gamma)^{\frac{1}{2}}.$$

Under the conditions of a composite collision, and owing to the new relation between the energies γ_c and γ in C- and L-system (always in extreme relativistic approximation),

$$(7) \quad \gamma_c = (\gamma/2n)^{\frac{1}{2}}$$

the symmetry condition imposes on $\theta_{\frac{1}{2}}$ the demand

$$(8) \quad \operatorname{tg} \theta_{\frac{1}{2}} = (2n/\gamma)^{\frac{1}{2}}.$$

The true primary energy γ is, therefore, larger by a factor n than the energy γ_N computed under the assumption of a nucleon-nucleon collision. This, together with equ. (5), defines the relation between the multiplicity n_s , the number n of participants, and the apparent primary energy γ_N :

$$(9) \quad n_s = B \cdot n \cdot \gamma_N^{\frac{1}{2}-m}.$$

We shall now present a purely statistical argument in favour of this view. It is derived from an analysis of the energy spectrum of 88 high-energy jets induced by nucleonic primaries: McCUSKER and ROESSLER⁽¹⁰⁾, BRISBOUT *et al.*⁽¹¹⁾, EDWARDS *et al.*⁽⁸⁾, TAKIBAEV *et al.*⁽¹²⁾, ALPERS *et al.*⁽¹³⁾, GUREVICH *et al.*⁽¹⁴⁾, divided into two groups according to the number N_h of heavy prongs: $N_h \leq 3$, and $N_h > 3$. It has become customary to consider the first group as representing essentially only the nucleon-nucleon collisions among the jets, and the second as consisting of the more complex interactions.

⁽¹⁰⁾ C. B. A. McCUSKER and F. C. ROESSLER: *Nuovo Cimento*, **5**, 1136 (1957).

⁽¹¹⁾ F. A. BRISBOUT, C. DAHANAYAKE, A. ENGLER, Y. FUJIMOTO and D. H. PERKINS: *Phil. Mag.*, **1**, 605 (1956).

⁽¹²⁾ Z. S. TAKIBAEV, P. A. USIK and M. G. ANTONOVA: *Dokl. Akad. Nauk USSR*, **111**, 341 (1956).

⁽¹³⁾ V. V. ALPERS, I. I. GUREVICH, V. M. KUTUKOVA, A. B. MIŠAKOVA, B. A. NIKOLSKI and L. V. SUROVA: *Dokl. Akad. Nauk USSR*, **112**, 33 (1957).

⁽¹⁴⁾ I. I. GUREVICH, A. P. MIŠAKOVA, B. A. NIKOLSKY and L. V. SURKAVA: *Žurn. Éksp. Teor. Fiz.*, **34**, 267 (1958).

The results are shown in Fig. 1. It is seen that the spectrum for the two groups is practically the same, and it may be noted for reference later on that the energy distribution of the events listed differs significantly from the primary spectrum of cosmic radiation at these energies: its initial slope corresponds to a power law with an exponent ~ 0.5 , and only at the highest energies—where unfortunately the statistical uncertainties become quite large—it appears to approach the exponent of the primary spectrum, ~ 1.5 . Since in this energy region the collision cross-section is undoubtedly constant, the deviation must result from a strong scanning bias in favour of events of high multiplicity, *i.e.* in the average of high primary energies.

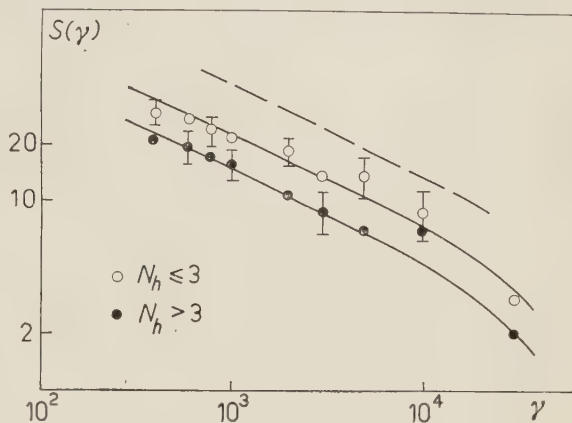


Fig. 1. — Integral energy spectrum of the 88 jets. Empty circles: $N_h \leq 3$; full circles: $N_h > 3$. The dashed line represents the spectrum of the group $N_h < 3$, shifted so as to increase the relative frequency of this group to about 60%.

However, at this stage we are concerned with another point: the apparent predominance of the «nucleon-nucleon» group $N_h \leq 3$ over the «nucleon-nucleus» group $N_h > 3$. About 60% of all the jets quoted in the literature belong to the first class, and only about 40% to the second. This is contrary to expectations: given the value of the «fundamental» cross-section σ_0 for nucleon-nucleon interactions, it is easy to compute from purely geometrical arguments the fraction of all jets involving only one target nucleon. All collision with the hydrogen of the emulsion belong into this group, and all those peripheral collisions with other nuclei in which the length of the «tunnel» is too small to permit in the average more than one interaction. A similar estimate for showers of lower primary energy has been made previously in an attempt to evaluate the effect of second-generation collisions⁽¹⁵⁾: for the present study, the method had to be slightly modified since the target nucleon is itself capable of further secondary production. Details about the method of calculation will be given in the last section; here it may suffice to state that its result is a probability of (35 ÷ 40)% for interactions of the nucleon-nucleon type. Moreover, it is interesting to note that this result is very insensitive

⁽¹⁵⁾ J. G. ASKOWITH and K. SITTE: *Phys. Rev.*, **97**, 159 (1955).

to the choice of the parameter σ_0 , as long as no unreasonably small value is adopted (less than about $\frac{1}{2}$ the geometrical value, or 30 mb). It is clear why this should be so: large σ_0 « shorten » the path but extend the total collision area, and small σ_0 permit a longer path, while cutting down the total collision area. Over a considerable range of values for the « fundamental cross-section », the two effects very nearly cancel each other.

Admittedly, the relative frequency of jets in the two groups alone would not constitute a safe basis for an attempt to re-interpret nucleon-nucleus collisions. Surely there is no precisely defined N_h which distinguishes nucleon-nucleon and more complex collisions. But on the one hand, over one-half of the events in the first group has $N_h = 0$, and all of them seem to agree so well in their typical properties with the features expected of nucleon-nucleon interactions, that it is difficult to ascribe to the group a large admixture of complicated collisions. On the other hand, this statistical argument is used only as a further support bearing out the conclusions already reached, and not as the sole foundation of the composite-collision model.

The explanation suggested for this strange frequency ratio is the following: according to equ. (7) and (8), a jet originated in a collision of a primary of energy γ with n nucleons, will have in the L-system symmetry properties equal to those of a nucleon-nucleon interaction at primary energy (γ/n) . Since in the determination of jet energies the simpler interaction model was generally assumed, the data given underestimate the true primary energies by a factor n . Correspondingly, in our graph of Fig. 1 the points belonging to the group $N_h > 3$ should be moved towards the right, to energies higher than those given by this factor n representing the average number of participating nucleons. One might even be tempted to turn the argument around, and to ask by which factor the primary energies must be raised, or the energy spectrum shifted, in order to give the « right » frequency ratio. The close similarity of the spectra of the two groups permits an answer, although of course its semi-quantitative nature as a very crude approximation is self-evident. The choice $n \approx 8$ would reduce the frequency ratio of the two groups to the expected one between 2:3 and 1:2. This must be considered as an order-of-magnitude estimate, and quantitatively of not more value than a comparison of the multiplicities of the two groups. According to equ. (5) and (9), the second group should, at the same primary energy, have a multiplicity larger by a factor n . Actually, the ratio of the two multiplicities is about 2. It seems fair to say that the result thus lends support in a qualitative way to the composite-collision picture, while demonstrating the quantitative insufficiency of data and classification.

2. — Having advocated in general terms the case for the composite-collision model, we shall now proceed to criticize its customary formulations. Both in McCusker's cascade theory ⁽⁵⁾, and in Cocconi's summary presentation ⁽⁶⁾, we

find the peculiar picture of a nucleus perforated, as it were, by the traversing nucleon. But surely this model can be adequate only if the «nuclear matter» has the properties of a fluid, divisible without discontinuity or at least built up of constituents much smaller than the projectile. If, however, we regard the nucleus as a compound of corpuscles of the same kind as the incident particle, then we run into troubles with the model of the cylindrical tunnel. We cannot have the primary slice off parts of the target nucleons lying inside the tunnel, and we cannot have non-integer «numbers of collisions»; but neither can we expect the nucleons to line up obediently along the tunnel so as to provide head-on collisions with all the particles in the collision volume.

It must be noted that this difficulty is found not only in a model which aims at a description of the process as a step-by-step cascade. The simplified treatment in terms of composite collisions equally cannot ignore encounters with particles not entirely inside the cylindrical tunnel. But once such a particle is hit and starts moving alongside the primary, the collision cross-section is increased—«the tunnel is widened», we may say—and further collisions will occur with an enhanced frequency. Again most of the target nucleons will lie near the periphery of the (non-cylindrical) tunnel, and thus after the encounter in their turn add to the effective avalanche cross-section. In other words, if we take seriously the corpuscular constitution of the nucleus, we must discard the idea of a tunnel-shaped collision volume, and replace it by one resembling an inverted funnel.

In order to estimate the quantitative difference between the «tunnel» and the «funnel» model, we have used a crude approximation which offers the advantage of great simplicity. First of all, we shall restrict the considerations to primary energies for which the trajectory of the target nucleons after the collision remains in a good approximation parallel to that of the primary. The widening of the «funnel» is thus a consequence of the randomness of the impact parameter only, and not of the divergence of the avalanche of nuclear matter. Secondly, although more precisely the funnel should be pictured as a multiple-tube aggregate, we shall approximate its cross-section by a circular one of equal area (Fig. 2). Using as definition for the «mean free path in nuclear matter» λ

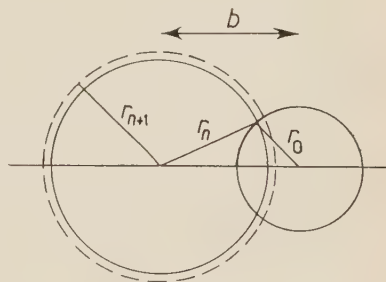


Fig. 2. — Schematic diagram of the true collision area of an avalanche of radius r_n with a nucleon (r_0), and of the approximation used (circle of radius r_{n+1}).

$$(10) \quad \sigma \lambda = 4\pi R_0^3/3 = V_0,$$

where σ is the—variable—funnel cross-section and R_0 the nucleon radius, we can compute the *average* development of the funnel, *i.e.*, the value of σ and λ as a function of the path length s in the nuclear matter, on the assumption of average impact parameters $\langle b \rangle = 2(r+r_0)/3$. It turns out that for funnel lengths not exceeding $6R_0$, a linear approximation may be used:

$$(11) \quad r = r_0[1 + \alpha(s/\lambda_0)],$$

r is the funnel radius, r_0 the radius connected with the fundamental cross-section σ_0 by $\pi r_0^2 = \sigma_0$, and λ_0 the corresponding mean free path according to (10). For $\sigma_0 = 2/3 \cdot \sigma_{\text{geom}} \approx 40$ mb, the best value for the constant is $\alpha = 0.38$. The deviations of the correct average radii from (11) are nowhere larger than about 10%.

With these radii, we can now compute the funnel volume V , and hence the number of participating nucleons $n = V/V_0$. Except for near-central and for peripheral collisions, we take as funnel volume that of a cut-off cone of a height equal to the length of the primary path. For an impact parameter b with respect to the nucleus, one has

$$(12) \quad n = V/V_0 = \frac{1}{3} \alpha \cdot \{ [1 + 2\alpha(R_0/\lambda_0) \cdot \sqrt{A^{\frac{2}{3}} - (b/R)^2}]^3 - 1 \}.$$

In the case of central or peripheral collisions, this approximation becomes poor and has to be replaced by a somewhat improved calculation.

Results for a number of nuclei, and for $\sigma_0 = 60, 40$ and 30 mb, are shown in Fig. 3a-3d. Attention is drawn to the dependence on the atomic weight A of the target nucleus which is much stronger than in the case of the tunnel model. This fact is more clearly demonstrated in Fig. 4 where the values of $n(A)$, obtained at average impact parameters $\langle b \rangle$ according to tunnel and funnel model, are compared.

Thus, a check on the dependence of the multiplicities n_s in a jet—which, according to (5) and (9) reflects the complexity of the collision—should offer the simplest test for the relative merits of tunnel and funnel model. Unfortunately, owing to the paucity of the empirical material available, this test remains inconclusive at this time. The only relevant data are those obtained in the emulsion chamber work of KAPLON *et al.* (16); and even of those, only the analysis of jets originated in copper yields statistically significant results. But unfortunately, copper is one of the elements least suitable for a statistical

(16) M. F. KAPLON, D. M. RITSON and W. D. WALKER: *Phys. Rev.*, **97**, 716 (1953); M. F. KAPLON and D. M. RITSON: *Phys. Rev.*, **88**, 386 (1952).

comparison with emulsion material whose mean atomic weight, properly averaged, is very close to the 64 of Cu. Moreover, the usual practice of assigning

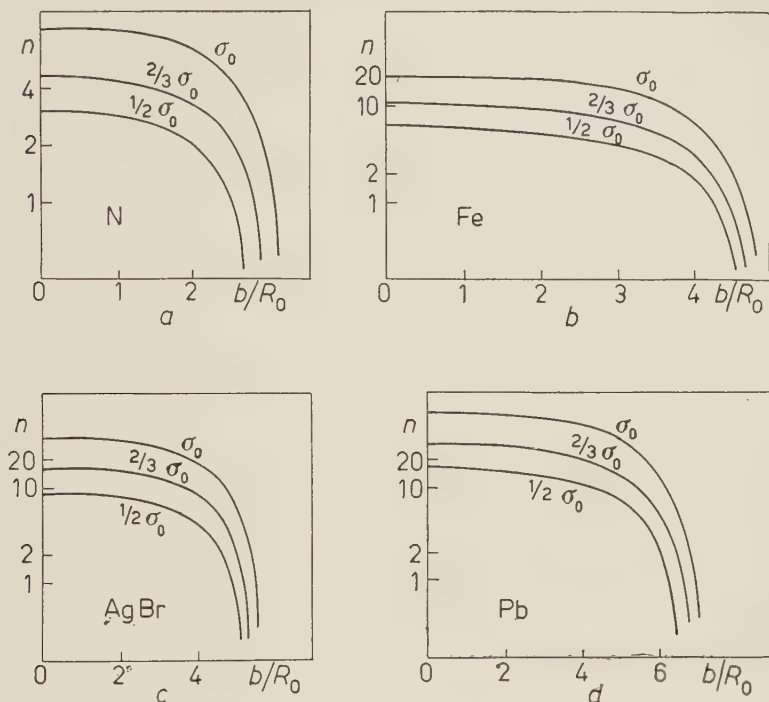
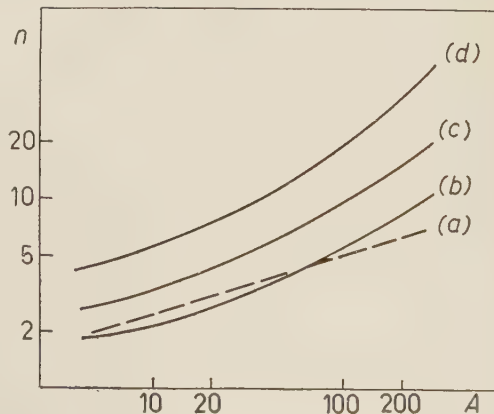


Fig. 3. — Number of nucleons participating in a composite collision, as a function of the impact parameter b and for three values of σ_0 , in four elements: a) N; b) Fe; c) AgBr ($A = 96$); d) Pb.

the jets of $N_h > 3$ to heavy target nuclei, and the others to light nuclei, evidently fails in this case since the group $N_h \leq 3$ includes peripheral collisions in Ag and Br as well.

It follows that while it is probably correct to regard jets with many heavy prongs as originated in a heavy nucleus, these events

Fig. 4. — Dependence on the atomic weight A of the average number of nucleons participating in a collision, for: a) tunnel model ($A^{1/2}$ -law); b) funnel model, $\sigma = 30$ mb; c) funnel model, $\sigma_0 = 40$ mb; d) funnel model, $\sigma_0 = 60$ mb.



do not represent the sum total of collisions with Ag or Br nuclei but only those with comparatively small impact parameters. To compare them with an unbiased sample of interactions in Cu nuclei is, therefore, misleading.

Yet a rough estimate can be made if we exclude peripheral collisions by comparing events occurring with an average impact parameter $\langle b \rangle_{\text{AgBr}} = (R_{\text{AgBr}} + r_0)/3$ in the heavy emulsion nuclei, with the unbiased average $\langle b \rangle_{\text{Cu}} = 2(R_{\text{Cu}} + r_0)/3$ in copper. In order to do this, the values of $B \cdot n = n_s/\gamma_N^{\frac{1}{2}}$ have been computed for the all showers, using the empirical $\gamma^{\frac{1}{2}}$ -law for the multiplicities. The results are:

Emulsions, all N_h :	$\langle B \cdot n \rangle = 2.2$
Emulsions, $N_h \leq 3$:	$\langle B \cdot n \rangle = 1.4$
Emulsions, $N_h > 3$:	$\langle B \cdot n \rangle = 3.5_5$
Copper:	$\langle B \cdot n \rangle = 1.9_7$

The ratio of the $N_h > 3$ group to the copper data may be compared with the values computed according to the tunnel model, and according to the funnel model with three values of σ_0 , listed in Table I. While it should be emphasized that owing to the arbitrariness of the assumption for $\langle b \rangle$ no undue weight must be given to the calculated values, the much better agreement of the funnel data with the observations is indicative if not convincing. More emulsion chamber data would be highly desirable.

TABLE I. — Ratios $n_{\text{Em}}/n_{\text{Cu}}$ of the number of nucleons involved in a collision in heavy emulsion nuclei, at $b = (R_{\text{Em}} + r_0)/3$, and in copper at $b = 2(R_{\text{Cu}} + r_0)/3$ according to tunnel and funnel model.

	$n_{\text{Em}}/n_{\text{Cu}}$
tunnel ($A^{\frac{1}{3}}$ — law)	1.45
funnel $\sigma_0 = 60$ mb	2.25
» $\sigma_0 = 40$ mb	2.0
» $\sigma_0 = 30$ mb	1.8
Experimental	1.8

Another test for the choice of tunnel or funnel model could, in principle, be based on Occonci's suggestion⁽⁶⁾ to determine the « apparent » n from multiplicity and half-angle. But without a much more accurate knowledge concerning the probabilities of multiplicity fluctuations, no safe conclusions can be drawn from such an analysis. The problem of fluctuations will be discussed in the next section; here it may suffice to state that with the present material, and in particular in view of the scanning bias, no definite answer could be given.

Two more general consequences of the composite-collision model may still

be pointed out. Firstly, it follows from the assertion made that the primary energies were, in many cases, underestimated by a large factor, that the inelasticities determined for such events are too high by the same factor. No, or no appreciable, correction need be made for nucleon-nucleon collisions, i.e. essentially for the group $N_h \leq 3$; but for the others, the estimates reported should on the average be reduced in the same ratio as their multiplicity exceeds that of the first group. As it is seen from the summary above, for the jets originating in emulsion nuclei this ratio of the mean multiplicities is $3.55/1.4 \approx \approx 2.5$. The question of a possible relation between the inelasticity and the number of heavy prongs N_h is apparently not yet clearly answered by the emulsion experiments so far reported; more recent studies have cast some doubt on the validity of the affirmative conclusion of BERTOLINO⁽¹⁷⁾ and of HOANG⁽¹⁸⁾.

Secondly, we wish to emphasize that the funnel model of composite collisions is by no means incompatible with a two-centers model of the kind suggested by TAKAGI⁽¹⁹⁾, KRAUSHAAR and MARKS⁽²⁰⁾, and ZACEPIN⁽²¹⁾. Strong evidence favouring such a model has quite recently been published by the Polish-Czech co-operative emulsion group⁽²²⁾. In fact, the asymmetries resulting from this model are one of the most useful criteria guiding the analysis of individual events on the basis of the composite-collision model. A more detailed report concerning this point will be submitted later.

3. — The occurrence of very large multiplicity fluctuations at equal half-angle, and hence presumably equal primary energy, has often been commented upon, and has sometimes been quoted as an argument in favour of a purely «statistical» theory of meson production. It is evident that if the composite-collision viewpoint is adopted, the argument for a wide spread in a nucleon-nucleon collision at fixed primary energy loses strength. In this model, there are four reasons for fluctuations in the number n_s of shower particles in a jet:

i) The differences in the path length of the primary, defined by the impact parameter b with respect to the nucleus, and described by the probability $p_s(b)db$ of a collision within the impact parameter interval (b, db) .

ii) The randomness of the collision process along this path s (or the «density fluctuations» of the nuclear matter on s), expressed by the proba-

⁽¹⁷⁾ G. BERTOLINO: *Nuovo Cimento*, **2**, 1130 (1955); **3**, 141 (1956).

⁽¹⁸⁾ T. E. HOANG: *Journ. de Phys.*, **15**, 337 (1954).

⁽¹⁹⁾ S. TAKAGI: *Prog. Theor. Phys.*, **7**, 123 (1952).

⁽²⁰⁾ W. L. KRAUSHAAR and L. J. MARKS: *Phys. Rev.*, **93**, 326 (1954).

⁽²¹⁾ V. I. ZACEPIN: *Suppl. Nuovo Cimento*, **8**, 585 (1958).

⁽²²⁾ P. CIOK, T. COGHAN, J. GIERULA, R. HOLYŃSKI, A. JURAK, M. MIĘSOWICZ, T. SANIEWSKA, O. STANISZ and J. PERNEGR: *Nuovo Cimento*, **8**, 166 (1958); **10**, 741 (1958).

bility $p_n(s)$ that while traversing the nucleus, the primary will collide with exactly n target nucleons.

iii) The «fundamental fluctuations» in the emission process, *i.e.* the probabilities $p_N(n, \gamma)$ that in a collision of a primary of energy γ with n nucleons, exactly N secondaries are ejected.

iv) The deviations from the mean charged-to-neutral ratio, characterized by the probability $p_{n_s}(N)$ that exactly n_s out of the N secondaries are charged particles.

It then follows for the probability distribution $P_0(n_s, \gamma)$ of the jet multiplicities at energy γ :

$$(13) \quad P_0(n_s, \gamma) = \int_0^{b_{\max}} \sum_{n=1}^{b_{\max}} \sum_{N=n_s}^{\infty} P_s(b) \cdot p_n(s) \cdot p_N(n) \cdot p_{n_s}(N) db.$$

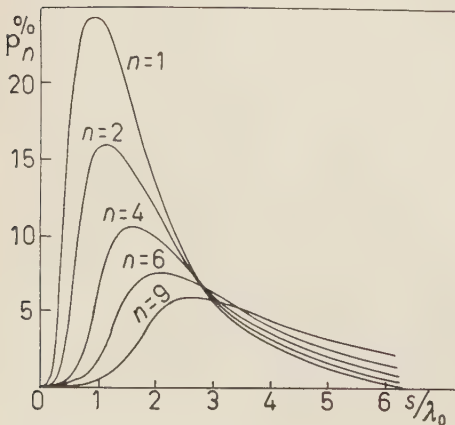
Three of the four probabilities are readily determined:

a) The «geometrical» probability p_s is given by

$$(14) \quad P_s(b) db = 2\pi b db / \pi(R_0 A^{\frac{1}{3}} + r_0)^2.$$

b) $p_n(s)$ can be evaluated, at least approximately, on the basis of the determination of the mean free path λ_n for the n -th successive «generation» of collisions described above. Straightforward application of the elementary calculations gives, first,

$$(15) \quad P_n(s) = \int_0^s \exp[-y_1/\lambda_1] dy_1/\lambda_1 \int_0^{s-y_1} \exp[-y_2/\lambda_2] dy_2/\lambda_2 \dots \\ \dots \int_0^{s-(y_1+\dots+y_{n-1})} \exp[-y_n/\lambda_n] dy_n/\lambda_n \cdot \exp[-(s-y_1-\dots-y_n)/\lambda_{n+1}].$$



The integration gives after some transformations

$$(16) \quad p_n(s) = \lambda_{n+1} \sum_{i=1}^{n+1} \lambda_i^{n-1} \cdot \exp[-s/\lambda_i] / \prod_{k \neq i}^{n+1} (\lambda_i - \lambda_k).$$

Fig. 5 shows some of the p_n as a function of s .

Fig. 5. — Probabilities p_n of collisions with exactly n target nucleons, as a function of the path length s/λ_0 .

c) The last factor $p_{n_s}(N)$ is the well-known binomial function

$$(17) \quad p_{n_s}(N) = N! q^{n_s} (1 - q)^{N - n_s} / n_s! (N - n_s)! ,$$

where q is the mean value of the charged-to-neutral ratio, for which the fraction $\frac{2}{3}$ may be used.

Hence it is possible, at least in principle, to determine the unknown « fundamental fluctuations » $p_N(n)$ if the multiplicity distributions $P_0(n_s, \gamma)$ are given. Practically, however, we meet a formidable obstacle: the effect of the scanning bias.

It has been pointed out above that already the deviation of the jet spectrum from the energy distribution of the primaries renders proof of a significant scanning bias in favour of events of high multiplicity. Consequently, the observed multiplicity distributions $P(n_s, \gamma)$ will differ from our theoretical P_0 : large multiplicities will appear enhanced and low multiplicities diminished. Moreover, the empirically determined averages n_s will be higher than the true mean multiplicities $\langle n_s \rangle$, and the error thus made will itself depend on $\langle n_s \rangle$, i.e. on the primary energy. Only for large γ 's it appears from the spectrum of Fig. 1 that the bias is small. It may here be noted that not even the empirical γ^1 -law for the average multiplicities can be retained if the bias is indeed appreciable. The true energy dependence would be steeper than the one derived from the present material.

Since the scanning bias can be assumed to depend on the number of shower particles n_s only, it is of course theoretically possible to eliminate, or to determine, the « bias function » $b(n_s)$. For if $\pi(\gamma)d\gamma$ is the differential primary spectrum, and $s(\gamma)d\gamma$ the observed jet distribution, then we have, owing to the fact that the primary interaction cross-section is not energy-dependent,

$$(18) \quad s(\gamma) d\gamma = \sum_{n_s} \pi(\gamma) \cdot P_0(n_s, \gamma) \cdot b(n_s) d\gamma ,$$

or for the observed multiplicity distribution

$$(19) \quad P(n_s, \gamma) = P_0(n_s, \gamma) \cdot b(n_s) .$$

In practice, the experimental material is by far insufficient for such a detailed test of the assumptions, and it was not deemed worth while to carry out the necessary cumbersome calculations. Instead, an attempt was made to estimate the effect of the « fundamental fluctuations » by another, less accurate but better documented, method.

One notes, first of all, that for nucleon-nucleon collisions only the third and fourth of the fluctuation-inducing effects can occur. This simplifies the calculation, but leaves the bias problem still unsolved. But since we are then

dealing with events of the lowest multiplicities, one may hope that although just there the bias is absolutely at its largest, its effect will not vary too much over the—reduced—range of multiplicities involved. In a first approximation, we may therefore assume a *constant* bias, and hence for the purpose of estimating the influence of the «fundamental fluctuations» on the multiplicity distribution, identify the observed $P(n_s, \gamma)$ with the theoretical $P_0(n_s, \gamma)$.

A glance at the experimental data supports this view, and suggests one further measure. In order to be as sure as possible of the character of the interactions, only events with $N_h = 0$ were selected for this study. The influence of the energy dependence of the multiplicities was minimized by computing the values of $n_s(\bar{\gamma}/\gamma)^{\frac{1}{2}}$, where $\bar{\gamma}$ is the average energy of the 20 jets of this subgroup. The results are shown in the histogram of Fig. 6a, and they reveal an interesting feature: it appears that they consist of two separate groups, the larger one of 17 jets centering at an \bar{n}_s between 10 and 15, and a smaller one at $\bar{n}_s \sim 30$. It is most suggestive to consider the smaller group as resulting from a collision of a primary with two target nucleons, giving twice the number of secondaries. These events will, therefore, be excluded from the further analysis which is thus restricted to 17 jets with $\bar{n}_s = 9.5$ at $\bar{\gamma} = 5290$. Its multiplicity spread is no longer very large: the values of $n_s(\bar{\gamma}/\gamma)^{\frac{1}{2}}$ range from 4.3 to 17.5. The error which derives from neglecting the scanning bias is, therefore, unlikely to be very serious.

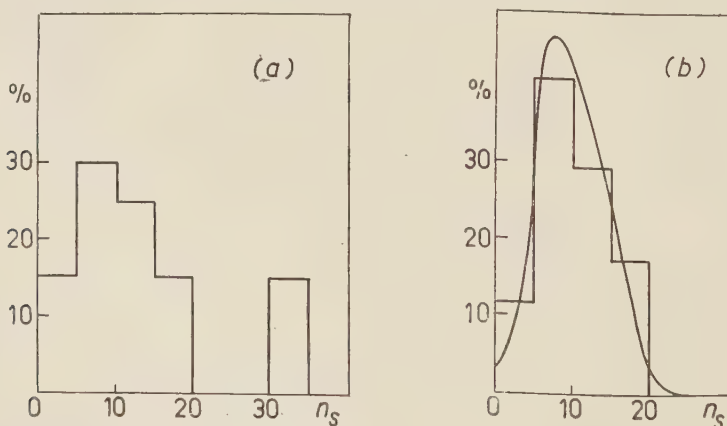


Fig. 6. — a) Histogram of $n_s(\bar{\gamma}/\gamma)^{\frac{1}{2}}$ for all jets with $N_h = 0$. b) The same histogram after elimination of the events with the highest multiplicity, and the distribution calculated with $\sigma = 6.5$.

An attempt was then made to fit the experimental data by assuming a Gaussian for the «fundamental fluctuations»:

$$(20) \quad P_N = (1/\sigma\sqrt{2\pi}) \cdot \exp [-(N - \bar{N})^2/2\sigma^2].$$

Together with (17), this leads to a probability $P(n_s)$ to find n_s charged jet secondaries

$$(21) \quad P(n_s) = (q^{n_s}/n_s! \sigma \sqrt{2\pi}) \cdot \int_0^\infty \frac{N!}{(N-n)!} (1-q)^{N-n_s} \exp[-(N-\bar{N})^2/2\sigma^2] dN,$$

where for our sample, $\bar{N} = 15$. The experimental histogram, and the best-fitting calculated curve ($\sigma = 6.5$), are shown in Fig. 6b. The marked deviation of the curve from a simple Gaussian illustrates the effect of charge fluctuations.

If one assumes that the same Gaussian (20), with \bar{N} a known function of γ , represents the «fundamental fluctuations» for all energies *per nucleon*, it is possible to work out the complete multiplicity distribution $P_0(n_s, \gamma)$ according to (13). However, neglecting the bias function over this wide range, —indicated in the histogram of Fig. 7b—we can certainly, at best, hope for

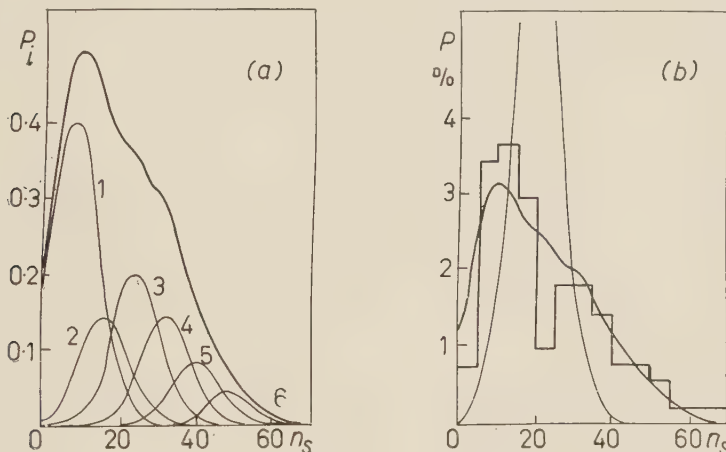


Fig. 7. — a) Contribution to the various n_s of collisions with n nucleons, and resulting distribution. b) Histogram of the observed distribution of $n_s(\gamma/\gamma)^{1/2}$ for all jets, compared with the calculated resulting distribution, and with a Gaussian of width $\sigma = 6.5$.

a crude approximation and the calculations are extremely lengthy and tedious. The exact calculation was, therefore, not carried through at this time. Instead, the two decisive points we wish to emphasize will be demonstrated in an oversimplifying model calculation: first, that the «fundamental fluctuations» account for only a small part of the multiplicity spread observed in jets, and second, that a composite-collision model with a moderate «fundamental fluctuation» can explain the wide multiplicity distribution.

To prove the first point, a Gaussian with $\sigma = 6.5$ and $\bar{N} = 20$, corresponding to the average of the complete sample, is plotted as a thin line in the histogram

of Fig. 7b. Clearly, the disagreement is too marked to be attributed to the neglected fluctuations in the neutral-to-charged ratio; at those large multiplicities, their effect is rather small. Next, we have chosen a « typical » frequency distribution of n , the number of nucleons participating in the composite collisions averaged over all emulsion elements. For simplicity of the calculation, the—infrequent—large n corresponding to central collisions in heavy elements have been omitted. The following values were chosen for the frequencies F_i of an interaction with i nucleons: $F_1 = 0.40$; $F_2 = 0.14$; $F_3 = 0.20$; $F_4 = 0.14$; $F_5 = 0.08$; $F_6 = 0.04$. With this assumption the average multiplicity $\langle n_s \rangle$ in a nucleon-nucleon collision at the energies of our sample is determined: it is related to the observed average \bar{n}_s by

$$(22) \quad \bar{n}_s = \sum_i F_i \cdot i \langle n_s \rangle.$$

For our sample, one has $\langle n_s \rangle \approx 8$. Again disregarding charge fluctuations, the approximate multiplicity distribution is then given by

$$(23) \quad P^*(n_s) = (1/\sigma \sqrt{2\pi}) \cdot \sum_i F_i \cdot \exp[-(n_s - i \langle n_s \rangle)^2 / 2\sigma^2].$$

Fig. 7a shows, as an illustration, the relative contributions of the collisions with different complexity (thin lines) to the resulting distribution (thick line). In Fig. 7b, this resulting distribution is plotted together with the experimental histogram. It is seen that the characteristic shape of the experimental curve is very well reproduced, and that is all that can be reasonably expected at this stage.

In conclusion, it may therefore be said that the composite-collision model of cosmic ray jets seems to give a satisfactory explanation of all the features observed, including the multiplicity distribution. It is not necessary to postulate the occurrence of very large « fundamental fluctuations » in a nucleon-nucleon interaction; they account for only a fraction of the total spread.

RIASSUNTO (*)

Si presentano argomenti a favore dell'interpretazione dei getti di raggi cosmici come collisioni composite del primario con un nucleone bersaglio composto che avvengono in un singolo atto. Si rileva in particolare che l'identità di collisioni « successive »

(*) Traduzione a cura della Redazione.

va perduta alle alte energie perchè la nube mesonica che si espande avvolge il composto prima di emettere la massa dei secondari. Secondo questa concezione le energie primarie attribuite ai getti dai procedimenti usuali sono in molti casi troppo basse, specialmente per eventi con grande numero N_h di rami pesanti. La differenza risultante per energie primarie vere dei getti con *p.e.* $N_h \leq 3$ e $N_h > 3$ spiega la frequenza apparentemente eccessiva degli eventi con basso N_h . Ma se si desidera di conservare il modello del nucleo costituito da un aggregato di corpuscoli, la sezione d'urto della valanga dei nucleoni interagenti aumenterà con la penetrazione ed il quadro usuale del volume d'interazione a forma di tunnel cilindrico deve essere sostituito da quello di un imbuto rovesciato. Tale «modello a imbuto» fa prevedere una maggior dipendenza delle molteplicità dal peso atomico del nucleo bersaglio e sembra meglio adatto ad accordarsi coi dati sperimentali «alquanto scarsi». Si dimostra poi che secondo questo modello la maggior parte dello sparpagliamento della molteplicità osservato non è dovuta alle «fluttuazioni fondamentali» nell'emissione dei secondari in una collisione nucleone-nucleone, bensì alla casualità del numero di particelle coinvolte. Per interazioni nucleone-nucleone a circa $5 \cdot 10^{12}$ eV le «fluttuazioni fondamentali» si possono approssimare con una gaussiana di ampiezza $\sigma = 6.5$.

Spurious Scattering of 6.2 GeV Protons in Nuclear Emulsions (*).

F. W. FISCHER

Boeing Airplane Company, Seattle - Wash.

J. J. LORD

Department of Physics, University of Washington, Seattle - Wash.

(ricevuto il 24 Settembre 1958)

Summary. — Multiple scattering measurements of 6.2 GeV proton tracks in emulsion have been carried out for cell lengths up to 10000 microns. It was found that the spurious scattering contribution remained constant for cell lengths greater than about 3000 microns. Measurements on a group of parallel tracks showed that the region of the microscopic dislocations responsible for spurious scattering had dimensions on the order of 1 mm to 2 mm.

1. — Introduction.

In considering the multiple scattering of particles in their passage through nuclear emulsions, errors are introduced by apparent scattering from a number of sources. Corrections for these errors must be applied to measured tracks. One major source of this error, usually called spurious scattering, is suggested by BISWAS, PETERS, and RAMA ⁽¹⁾ to be due to microscopic dislocations within the emulsion. This spurious scattering has been confirmed and studied by FAY ⁽²⁾, LOHRMANN and TEUCHER ⁽³⁾, BRISBOUT *et al.* ⁽⁴⁾, and APOSTOLAKIS

(*) Assisted by the Joint Program of the ONR and AEC and a grant from the National Science Foundation.

⁽¹⁾ S. BISWAS, B. PETERS and H. RAMA: *Proc. Ind. Acad. Sc.*, A **41**, 154 (1955).

⁽²⁾ H. FAY: *Zeits. f. Naturfor.*, **10a**, 572 (1955).

⁽³⁾ E. LOHRMANN and M. TEUCHER: *Nuovo Cimento*, **3**, 59 (1956).

⁽⁴⁾ F. A. BRISBOUT, C. DAHANAYAKE, A. ENGLER, P. H. FOWLER and P. B. JONES: *Nuovo Cimento*, **3**, 1400 (1956).

et al. ⁽⁵⁾. While it is probably true that the dislocations originate during the processing of the emulsions it has been surprising that, with but few exceptions ^(4,5) all workers obtain about the same magnitude for the scattering.

The present work was undertaken to extend these measurements ⁽¹⁻⁵⁾ to larger cell lengths and also to learn something of the character of the emulsion dislocations. For this purpose Ilford type G-5 glass backed emulsions 2 in. \times 4 in. in area and 600 μ m in thickness were exposed to one pulse of the 6.2 GeV internal proton beam of the Berkeley Bevatron. The particles entered the emulsion parallel to the surface so that the average track length was about 6 cm.

The spurious scattering measurements made of these tracks are in general agreement with those of other investigators up to the largest cell lengths reported ⁽¹⁻⁵⁾, 4 000 μ m. The results herein reported show that, while the spurious scattering increases rapidly to cell lengths of about 3 000 μ m, it appears to remain constant to the longest cell lengths used in this experiment, 10 000 μ m.

2. - The measurements.

The multiple scattering measurements were carried out with a standard medical type Tiyoda microscope that was attached to a heavy cast iron precision stage of local construction. The positions of the track under observation were then measured with a filar micrometer eyepiece.

The multiple scattering of the 6.21 GeV proton tracks in this experiment was measured by the method of FOWLER ⁽⁶⁾ in terms of second differences. As shown in Table I the mean of the absolute values of the second differences,

TABLE I. - *Multiple scattering second difference as a function of cell length.*

Cell length (μ m)	No. of over-lapping cells	Observed second differences D_0	Noise second differences D_{RGS}	Theoret. second diff. D_T	Spurious scattering second diff. D_{si}
250	917	.146 \pm .004	.096 \pm .01	.024	.107 \pm .010
500	502	.202 \pm .008	.091 \pm .01	.068	.167 \pm .011
750	288	.318 \pm .019	.111 \pm .01	.131	.278 \pm .022
1 000	670	.414 \pm .016	.117 \pm .01	.205	.344 \pm .020
2 000	319	1.008 \pm .056	.110 \pm .01	.601	.800 \pm .070
5 000	51	2.63 \pm .37	.11 \pm .01	2.47	.842 \pm .4
10 000	30	7.25 \pm 1.32	.11 \pm .01	7.24	.3 \pm 1.5

⁽⁵⁾ A. J. APOSTOLAKIS, J. O. CLARKE and J. V. MAJOR: *Nuovo Cimento*, **5**, 337 (1957).

⁽⁶⁾ P. H. FOWLER: *Phil. Mag.*, **41**, 169 (1950).

D_0 , was determined for cell lengths from 250 to 10 000 μm . As is standard practice, individual second differences greater than \pm times the mean were not included in either the measured or theoretical mean values.

Contributions to the second differences due to errors from thermal expansion of the microscope, reading error, grain noise, and stage noise were determined by the method given by PETERS (¹). Thermal errors were eliminated by shielding and the contribution to D_0 , the measured second difference, by the latter three sources of error is designated by D_{RGS} in Table I. In all cases D_{RGS} is quite small compared to D_0 : The corresponding theoretical value of the multiple scattering second difference, D_T , was calculated from the Molière (⁷) theory.

The spurious scattering second differences in this experiment were shown to have a normal distribution (¹), therefore the mean of their absolute values is closely given by:

$$D_{ss}^2 = D_0^2 - D_T^2 - D_{RGS}^2.$$

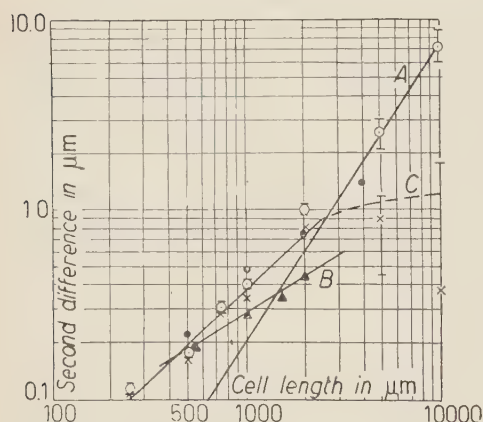


Fig. 1. — Multiple Coulomb scattering as a function of cell length. Curve A from Molière theory. \odot measured second differences. Spurious scattering second differences: \times present work, \bullet Lohrmann and Teucher, \blacktriangle Bristol group.

wherein the D_{ss} remains constant for cell lengths greater than about 2 mm to 5 mm.

The calculated values of D_{ss} are given in Table I. These values and those of other workers have been plotted in Fig. 1. Curve C of this figure shows that spurious scattering errors become negligible for second differences greater than 1 μm .

To explore the idea that spurious scattering is due to microscopic emulsion dislocations, measurements were taken of 6 parallel tracks located within a circle of 70 μm diameter. It was then possible to map out the local dislocations that give rise to spurious scattering. The results indicated that the regions of local dislocations were of the order of 1 mm to 2 mm in diameter. This is consistent with curve C of Fig. 1

(⁷) G. MOLIÈRE: *Zeits. f. Naturforsch.*, **3a**, 78 (1948).

* * *

We wish to thank Professors Y. B. KIM and S. H. NEDDERMEYER for helpful discussions. The assistance of J. F. KIRKBRIDE and B. F. RUFFNER is gratefully acknowledged. The exposure of the emulsions was made possible by Dr. E. J. LOFGREN and the Staff of the Berkeley Bevatron.

RIASSUNTO (*)

Sono state eseguite misure di scattering multiplo su tracce in emulsione di protoni di 6.2 GeV adottando celle fino a 10 000 μm . Si è trovato che il contributo dello scattering spurio resta costante per lunghezze di celle superiori a circa 3 000 μm . Misure eseguite su un gruppo di tracce parallele mostrano che la regione delle dislocazioni microscopiche che causano lo scattering spurio ha dimensioni dell'ordine di $(1 \div 2)$ mm.

(*) Traduzione a cura della Redazione.

Possible Explanation of the Radiation Observed by Van Allen at High Altitudes in Satellites.

P. J. KELLOGG

University of Minnesota - Minneapolis, Minn.

(ricevuto il 24 Settembre 1958)

Summary. — We consider the possibility, suggested by P. ROTHWELL and T. GOLD in conversation with the author, that the radiation observed by VAN ALLEN and co-workers at high altitudes is due to the decay electrons and protons from neutrons produced in the earth's atmosphere by cosmic rays and stored in the earth's magnetic field. Order of magnitude estimates for the densities to be expected are presented. Only scattering loss is considered. Using a lifetime of $3 \cdot 10^9$ s for loss through scattering, an upper limit of 10^{-2} electrons/cm³ near the earth and $.05(R_E/r_0)^3$ electrons/cm³ at large distances r_0 in the equatorial plane is obtained. The proton density at large distances is $.03(R_E/r_0)^2$ cm⁻³, for a lifetime of 10^{12} s. If plasma accelerations are not important, then the spectrum of electrons will be that of neutron β -decay. The protons are produced by fast neutrons coming directly from nuclear stars and their spectrum will be approximately that of the protons from stars. The electron density is sufficient to give a counting rate a few times larger than is observed, while the proton density is sufficient to give a counting rate 10^4 times higher than the observed lower limit. The lifetimes of stored particles are therefore probably much less than those given by scattering. There should be a strong latitude effect which is roughly estimated as proportional to $\cos^6 \lambda$. Reasons are given for believing that collective effects will reduce the density below this near the poles.

1. — Introduction.

An experiment by VAN ALLEN and co-workers ⁽¹⁾ in the American satellite, Explorer III, has demonstrated the existence of an intense zone of radiation

⁽¹⁾ J. A. VAN ALLEN, G. H. LUDWIG, E. C. RAY and C. E. MCILWAIN: *IGY Satellite Report, it Series no. 3*, National Academy of Sciences-National Research Council, Washington 25, D.C.

at altitudes above 1000 km above the earth's surface. The radiation detector, a Geiger counter inside the satellite, does not permit a direct observation of the nature of the radiation; however, the sharp lower boundary of the radiation zone makes it very unlikely that the primary radiation is X-rays and strongly suggests charged particles. The high intensity of the radiation and its relative constancy in time suggests that particles are being stored in the earth's magnetic field.

We review briefly the results of the perturbation theory of the motion of charged particles in a magnetic field. A detailed discussion may be found in the books of ALFVÉN and SPITZER ^(2,3). We consider the motion of a charged particle in a region of space containing a magnetic field where the radius of curvature of the particle in the magnetic field is very small compared to the distances over which the magnetic field varies. We shall want to consider only fields which are constant in time, so the velocity of the particle is constant. If the magnetic field were uniform, the orbit of the particle would be a spiral around the lines of force, and the pitch angle ψ which the orbit makes with the lines of force would be constant. If the magnetic field is not uniform, the magnetic moment

$$(1) \quad \frac{1}{2} \frac{mv^2 \sin^2 \psi}{\sqrt{1-\beta^2}} \frac{1}{B}$$

of the particle due to its circular motion is constant. Here $v \cos \psi$ is the component of velocity parallel to the magnetic field, so particles are reflected from regions where

$$(2) \quad \frac{1}{B} = \frac{\sin^2 \psi_0}{B_0}.$$

If the magnetic field is not uniform around the particle orbit, then the particle will be bent more strongly at one side of its orbit than the other and will precess in a direction perpendicular to the magnetic field and to the gradient of field. The velocity of the guiding center due to this precession is given by:

$$(3) \quad \frac{mc}{eB\sqrt{1-\beta^2}} v^2 \cos^2 \psi \frac{1}{2B} |\nabla_{\perp} B|.$$

For the rest of this paper we will approximate the magnetic field of the earth by a field of a dipole. This is sometimes not a very good approximation,

(2) H. ALFVÉN: *Cosmical Electrodynamics* (Oxford, 1950).

(3) L. SPITZER: *Physics of Fully Ionized Gases* (1956).

particularly when we compute derivatives of the magnetic field. Inclusion of higher moments of the earth's field would be necessary to an accurate treatment of the shape of the radiation zone and its distortion of the earth's magnetic field, but these are beyond the scope of this paper. In spherical co-ordinates, the components of magnetic field are given by

$$(4) \quad B_r = \frac{2\mu \cos \theta}{r^3}, \quad B_\theta = \frac{\mu \sin \theta}{r^3},$$

where μ is the earth's magnetic moment. The equation for a line of magnetic field is

$$(5) \quad r = r_0 \sin^2 \theta,$$

where r_0 is the radius of the line at the magnetic equator. The intensity of the magnetic field at any point is given by

$$(6) \quad B = \frac{\mu}{r^3} \sqrt{4 - 3 \sin^2 \theta}$$

and the intensity of magnetic field along a line can be expressed in terms of either co-ordinate by

$$(7) \quad B = \frac{\mu \sqrt{4 - 3 \sin^2 \theta}}{r^3 \sin^6 \theta} = \frac{\mu}{r^3} \sqrt{4 - 3 \frac{r}{r_0}}.$$

Along a line of force the magnetic field is weakest at the equator and increases toward the poles; therefore, particles whose pitch angle at the equator is not too small will be reflected from regions of stronger magnetic field as they proceed toward the poles of the earth and will be in trapped orbits. We would now like an estimate of the time a particle would be expected to remain in such a trapped orbit. The only process we will consider for removal of particles from trapped orbits will be the scattering of particles in close collisions. This process is certain to occur and will set an upper limit to the lifetime. Well above the earth's atmosphere it is believed that space is filled with ionized hydrogen with a density of about 1000 particles/cm³. In such a medium the lifetime for scattering through an angle comparable to 90° is given by ⁽¹⁾

$$(8) \quad t = \frac{1}{8\pi N v (e^2/2E)^2 \ln(2E/e^2 N^{\frac{1}{2}})},$$

⁽¹⁾ L. SPITZER: *Physics of Fully Ionized Gases* (1956), eq. (5.13).

where N is the number of scattering centers per cm^3 and E , v are the energy and velocity of the particle. Table I gives some lifetimes of particles.

TABLE I.

		t
Protons	0.1 keV	$3 \cdot 10^5$ s
	1.0 keV	$1 \cdot 10^7$ s
	10.0 keV	$2.5 \cdot 10^8$ s
	1.0 MeV	$2 \cdot 10^{11}$ s
Electrons	10.0 keV	$6 \cdot 10^6$ s
	100.0 keV	$2 \cdot 10^8$ s
	5 MeV	$3 \cdot 10^9$ s
	1.0 MeV	$1 \cdot 10^{10}$ s

In Table II, we present certain characteristics of trapped orbits. r_0 is defined above, R_E is the radius of earth and atmosphere, λ is the latitude at which the line through r_0 reaches the atmosphere and ψ_m is the minimum pitch angle at the equator for trapped orbits. From Table II we see that the particles of quite large pitch angles can be stored so that the scattering through 90° is a reasonable value to take to give the lifetime.

TABLE II.

r_0/R_E	λ	ψ_m
1.05	12.6°	64.0°
1.1	17.6°	55.0°
1.2	24.1°	43.4°
1.5	35.4°	27.2°
3.0	54.8°	12.3°
7.0	68.0°	2.3°

The lifetime of a 1 MeV electron against synchrotron radiation in a field a $\frac{1}{2}$ gauss is comparable to, but not much less than, the value in Table I.

The storage times in Table I are quite long; therefore, it seems likely that other scattering processes may be of importance and, in particular, if any plasma oscillations are set up they will be much more effective in throwing particles out of the storage region than close scatterings. Thorough consideration of such plasma oscillations, however, is beyond the scope of this paper since we wish merely to demonstrate that Van Allen's zone of radiation represents a place where theories of plasma oscillations can be tested.

We note, however, that the lower boundary of the zone is stable against flute instability since the dominant force is the centrifugal force caused by the particle's precession around the earth and motion along the curved line of force and this force is into the plasma ⁽⁵⁾.

We must now consider how particles get into trapped orbits. The fact that the lifetimes are very long means that it is very difficult for charged particles to diffuse into this region as well as to diffuse out of it. If the region is to be filled by charged particles diffusing from outside, the flux of particles in this region can only be time average of the flux incident on the outside of the region, and we shall have lost any advantage of storage. Therefore, it seems necessary to consider some other means of trapping particles in this region. It may be that clouds of particles from the sun can penetrate into the Earth's field and then break up, leaving large numbers of particles in trapped orbits. Such a mechanism does probably contribute some particles, but it will not be considered in this paper.

Another mechanism for trapping charged particles evolved in conversation between the author and P. ROTHWELL and T. GOLD, and was put in final form by GOLD. Cosmic rays produce large numbers of neutrons in the earth's atmosphere. Some of these neutrons will diffuse out of the earth's atmosphere and proceed away from the earth unaffected by further collisions or by the earth's magnetic field. When these neutrons decay the resulting proton (~ 1 keV) and electron (~ 1 MeV) have, according to Table II, a good chance of being trapped. In the next section we estimate the flux of neutrons upward from the earth due to cosmic rays.

2. - Estimate of neutron flux.

We review briefly the history of a neutron in the atmosphere ⁽⁶⁾. Many neutrons are emitted as evaporation particles from air nuclei struck by primary cosmic rays or their energetic secondaries and have energies between a few and 30 MeV. These energetic neutrons lose energy rapidly through inelastic collisions with air nuclei until they drop below the first excited state in nitrogen at 2.3 MeV. After this they lose energy by elastic scattering, losing a fraction of their energy, $-2(m/M)$, per collision on the average, where m is the neutron mass, M is the mass of an air nucleus. When their energy has dropped approximately to thermal energy, they are absorbed by the nitrogen of the air in the reaction $^{14}\text{N} + n \rightarrow ^{14}\text{C} + p$. Some other reactions are important, but this dominates. Deep within the atmosphere the number of

⁽⁵⁾ M. ROSENBLUTH and C. L. LONGMIRE: *Ann. of Phys.*, **1**, 120 (1957).

⁽⁶⁾ H. A. BETHE, S. A. KORFF and G. G. PLACZEK: *Phys. Rev.*, **57**, 573 (1940).

neutrons between E and dE is equal to the rate of production of neutrons times the time a neutron takes to lose energy dE and is therefore approximately proportional to

$$(9) \quad \frac{dE}{(\text{energy loss per collision})} (\text{collision time}) = - \frac{dE}{2(m/M)E} \frac{l}{v},$$

where l is the mean free path for the neutrons. Near the top of the atmosphere neutrons have a chance of escaping before being slowed down and the spectrum is somewhat distorted in that there are more high energy neutrons. To make an estimate of the flux of neutrons leaving the atmosphere, we use the formula of Bethe, Korff and Placzek ⁽⁶⁾ for the number of neutrons having velocity between v and $v+dv$ at a depth x in the atmosphere

$$(10) \quad N(v, x) dv = \frac{m}{M} l \frac{dv}{v^2} \frac{1}{\sqrt{\pi} L} \int \left\{ \exp \left[-\frac{(x-x_0)^2}{2L^2} \right] - \exp \left[-\frac{(x+x_0+(2/\sqrt{3}))^2}{2L^2} \right] \right\} q(x_0) dx_0.$$

Here q is the rate of production of neutrons at a depth x_0 and L , given by

$$(11) \quad L^2 = L^2(E) = \frac{1}{3} \frac{M}{m} \int_{E_0}^E l^2 \frac{dE}{E},$$

is the mean distance which a neutron of energy E has diffused in slowing down from energy E_0 , which we take to be ~ 2 MeV.

The integral can be evaluated approximately as follows. At energies well above 1 keV, l is constant and several ($4 \div 10$) times larger than at energies well below 1 keV ⁽⁷⁾. Hence in equation (10) we may take

$$(12) \quad \frac{L^2}{l^2} \approx \begin{cases} \frac{1}{3} \frac{M}{m} \ln \frac{E_0}{E} & \text{for } E > 1 \text{ keV,} \\ \frac{1}{3} \frac{M}{m} \ln \frac{E_0}{1 \text{ keV}} \approx (4.2)^2 & \text{for } E < 1 \text{ keV.} \end{cases}$$

It will prove more convenient if we modify equation (9) to take into account capture of neutrons by air nuclei. The fraction of neutrons captured per collision is given by $\sigma(\text{capt})/\sigma(\text{total}) = \sigma_c/\sigma_t$ and so we may write

$$(13) \quad \frac{dN}{dE} = \frac{M}{2mE\sigma_t} \sigma_c N,$$

(7) D. J. HUGHES and J. A. HARVEY: *Neutron Cross Sections* (New York, 1955).

$\sigma(\text{capt})$ is proportional to $1/\sqrt{E}$ and so we multiply Bethe, Korff and Plazcek's neutron distribution by a factor

$$(14) \quad \exp \left[+ \int_{E_0}^E \frac{M}{2mE} \frac{\sigma_c}{\sigma_t} dE \right] = \exp \left[- \sqrt{\frac{\alpha}{E}} \right],$$

where $\alpha = .05 \text{ eV}$ and we have used ⁽⁷⁾ $\sigma_c = (.34/\sqrt{E})_{\frac{4}{5}}^{\frac{4}{5}} \text{ barns}$ and $\sigma_t = \frac{4}{5}(10) + \frac{1}{5}(3.7) \text{ barns}$.

Not much is known about the function q . At large depths in the atmosphere the slow neutrons in the atmosphere should be in equilibrium with production which indicates that q falls off with an absorption length of about 200 g/cm^2 , *i.e.* about ten times longer than a neutron mean free path. Near the top of the atmosphere it may be expected to decrease more slowly or even to increase with atmospheric depth, because of the greater number of secondaries produced. In view of our ignorance concerning q and its probable slow variation we shall neglect its variation with x_0 . According to diffusion theory, the flux of neutrons leaving the top of the atmosphere is given by

$$(15) \quad I = -\frac{1}{3}lv \frac{\partial N}{\partial x}.$$

Then we may evaluate the integral in equation (15) at the top of the atmosphere to give:

$$(16) \quad I = \frac{1}{3}lv \left(\frac{M}{m} ql \right) \frac{1}{\sqrt{2\pi}L} \frac{dv}{v^2} \left(1 + \exp \left[-\frac{2}{3} \left(\frac{l}{L} \right)^2 \right] \exp \left[-\sqrt{\frac{\alpha}{E}} \right] = \right. \\ \left. = \frac{2}{3} \left(\frac{M}{m} ql \right) \frac{dv}{v} \frac{1}{\sqrt{2\pi}} \frac{l}{L} \exp \left[-\sqrt{\frac{\alpha}{E}} \right], \right.$$

since $l/L \ll 1$ for most of the range of interest.

The constant factor $(M/m)ql$ may be evaluated using the results of SOBERMAN ⁽⁸⁾ who measured the counting rate in BF_3 proportional counters near the top of the atmosphere; that is to say, measured

$$(17) \quad c(x) = \int_0^{v_{\max}} N(x, v) \sigma_B v N_B V dv,$$

where $\sigma_B \approx 650/\sqrt{E} \text{ barns}$ is the capture cross-section of ^{10}B , N_B is the number

⁽⁸⁾ R. K. SOBERMAN: *Phys. Rev.*, **102**, 1399 (1956).

of ^{10}B nuclei per cm^3 , and V is the volume of the counter. In order to put this into a form which is as independent of q as possible we compute:

$$(18) \quad \left. \frac{dc}{dx} \right|_{x=0} = \frac{Mg}{\sigma} \left. \frac{dc}{dp} \right|_{p=0} = (\sigma_B v N_B V) (60) \left(\frac{M}{m} ql \right) \frac{1}{\sqrt{2\pi}} \frac{l}{L} \frac{1}{\sqrt{\alpha}},$$

since l/L is constant over the region where σ_B is large. We evaluate dc/dp by drawing a straight line between the point $c=0$, pressure $=0$ and an average of Soberman's highest measurements. The results are $dc/dp = 0.4$ counts/min-millibar at the equator; 2.1 counts/min-millibar at St. Paul, Minnesota ($\sim 55^\circ$ geomagnetic); 4 counts/min-millibar near the pole. All of these measurements were made in the period 1952-54, so represent values when the solar activity is low or minimum. This gives for $(M/m)ql$, .014 neutrons/ $\text{cm}^2 \text{ s}$ at the equator, .07 at St. Paul and .14 at the pole.

The total number of neutrons leaving the top of the atmosphere/ $\text{cm}^2 \text{ s}$ is given for comparison by

$$(19) \quad I = \frac{2}{3} \frac{M}{m} ql \int \frac{1}{2} \frac{dE}{E} \frac{1}{\sqrt{2\pi}} \frac{l}{L} \exp \left[- \left| \sqrt{\frac{\alpha}{E}} \right| \right] \approx .76 \frac{M}{m} ql,$$

where the integral is taken from 0 to 2 MeV. We split the integral (19) also at $E=1$ keV and put $\exp[-\sqrt{\alpha/E}]=1$ for energies above 1 keV. Then the integrals can be done easily using equation (11). The number of neutrons leaving the atmosphere is smaller than one might guess for the observed cosmic ray flux of one particle/ $\text{cm}^2 \text{ s}$ incident on the atmosphere. The reason seems to be the decrease of mean free path at low energies, as discussed in connection with eq. (11), which allows the neutrons to penetrate deeply, then prevents them from leaving after they have been slowed down. We ought, therefore, also to consider neutrons which are produced in stars and which leave the atmosphere directly without another collision. We review briefly the production of particles in stars. These results have been taken from the work of R. McKEAGUE⁽⁹⁾, who measured the stars produced in light elements in nuclear emulsion by 1 GeV protons. We assume that the production of neutrons is the same as that of protons. In its first collision with an air nucleus, a primary proton will produce about .5 neutrons in the backward direction with energies in the range $(0 \div 30)$ MeV (black tracks), the maximum number being produced at $(4 \div 6)$ MeV. The mean free path for these neutrons is about $\frac{1}{5}$ that of the cosmic rays, so about $\frac{1}{6}$ will escape. The upward flux is therefore about .1 per $\text{cm}^2 \text{ s}$ near the poles, and about $\frac{1}{7}$ of this near the equator, when we take into account the variation of primary flux with geomagnetic

(9) R. McKEAGUE: *Proc. Roy. Soc., A* **236**, 104 (1956).

latitude. In addition, about .1 neutrons are produced in the backward direction in the energy range $(30 \div 400)$ MeV. The mean free path of these neutrons is about the same as that of the cosmic rays, so $\frac{1}{2}$ will escape, giving a flux of .05 per $\text{cm}^2 \text{ s}$ near the poles, and $\frac{1}{4}$ of this near the equator. Clearly these estimates are not as accurate as those for the diffusing neutrons. These fluxes are therefore of the same order as the flux of diffusing neutrons. Fewer will decay in a given volume because of their greater velocity, but on the other hand, the lifetime of the resulting proton will be much longer because of its higher energy. The decay electron will have about the same energy as an electron from a neutron at rest over most of the energy range, so we do not have to consider these electrons further.

3. - Estimate of particle densities.

We now consider the decay of the neutrons after they have left the atmosphere. As an approximation we take the neutrons to be travelling straight upwards and consider the diffusing neutrons first.

$$I_0 \exp \left[- \sqrt{\frac{\alpha}{E}} \right] \frac{l}{L} \frac{dv}{v},$$

is the flux of neutrons leaving the earth with velocity between v and $v+dv$ the number which decay between the distance Z and $Z+dZ$ is given by

$$(20) \quad dN = I_0 \int \exp \left[- \sqrt{\frac{\alpha}{E}} \right] \frac{l}{L} \exp \left[- \frac{Z}{\lambda v} \right] \frac{dZ}{\lambda v} \frac{dv}{v} \text{ per second,}$$

where λ is the neutron lifetime of 12 min.

If we neglect the variation of L with energy, the maximum of the integrand in eq. (20) occurs at

$$(21) \quad \sqrt{E} = \frac{1}{3} \left[\sqrt{\alpha} + \frac{Z}{\lambda} \sqrt{\frac{m}{2}} \right].$$

From previous discussion we know that l/L is very slowly varying for $E \ll 2$ MeV so we will not make much error if we put l/L equal to its value at the maximum. The integral in eq. (20) may then be evaluated to give

$$(22) \quad \frac{dN}{dt} = I_0 \left(\frac{l}{L} \right)_{\max} \left(Z + \frac{1}{(\sqrt{2\alpha/m})\lambda} \right),$$

for the number of neutrons decaying per second between Z and $Z+dZ$.

For $\alpha = .05$ eV, we have $\sqrt{(2\alpha/m)}\lambda = 2160$ km. To get the rate of decay per cm^3 we must multiply by R_E^2/r^2 , where R_E is the radius of the earth's atmosphere.

The expression for the flux which we have used is based on slowing down by elastic collisions and, therefore, fails when the energy of the neutrons is greater than about 2 MeV. 2 MeV neutrons travel a mean distance of $4 \cdot 10^{-12}$ cm before decaying. It will be shown later that this limitation is not important, but that other considerations probably limit the density of particles at somewhat smaller distances than this.

The neutrons which do not begin the diffusion process, but escape directly have a velocity high enough so that we may neglect the exponential factor coming from the decay of the neutron, therefore we have:

$$(23) \quad \frac{dN}{dt} = I_{1,2} \frac{dZ}{\lambda v},$$

where I_1, I_2 are the fluxes estimated above.

We now estimate the density of electrons stored in the radiation zone. In the lower part of the zone where the density of air atoms determines the lifetime of the electrons against scattering, we may expect that the density of electrons is inversely proportional to the atmospheric density, and will therefore increase exponentially with height. This correspondence will be only approximate because the electrons will change altitude somewhat in their rapid precession in the earth's actual field. If this effect proves to be calculable, then the electron density will be a very sensitive method of determining the atmospheric density and scale height at very great altitudes. At present, the highest direct measurements of atmospheric density have been made so far below 1000 km that any value of atmospheric density could appear reasonable, so it is possible to calculate lifetimes only in the region above the atmosphere, where the lifetimes in Table I are valid. Close to the earth, the density of electrons will be given approximately by the product of rate of formation, lifetime, and an average fraction of electrons which go into trapped orbits. From Table II we see that even for electrons with $r_0/R_E = 1.05$, $\cos 64^\circ = .43$ of isotropically emitted electrons go into trapped orbits, so we may take something like $\frac{1}{2}$ for an average for this fraction. For the rate of formation we use eq. (22) neglecting z in the denominator and, using a lifetime of $3 \cdot 10^9$ s, we obtain:

$$\frac{1}{2} I_0 \left(\frac{l}{L} \right) \frac{1}{(\sqrt{2\alpha/m})\lambda} 3 \cdot 10^9 \approx 6 \cdot 10^{-3} \text{ electrons/cm}^3,$$

for the density of electrons, where we have used the equatorial value of neutron flux.

Van Allen measures a counting rate in excess of 15 000 counts/s and estimates that the dead time correction would give a counting rate of more than 35 000 counts/s in the counter of 20 cm² cross-section. We may estimate roughly that electrons from neutron decays, therefore approximately .5 MeV electrons, will produce about .02 photons per electron in the 1 g/cm² steel shell of the satellite. Inside the satellite the X-ray flux ought to be fairly uniform and equal to twice the flux of X-rays *out* of an element of the surface. Using the efficiency of .3% which VAN ALLEN gives for the counter in this X-rays range, we obtain a flux of

$$\frac{35\,000}{20} \cdot \frac{1}{.003} \frac{\text{photons}}{\text{cm}^2 \text{ s}} \cdot \frac{1}{.02} \frac{\text{electrons}}{\text{photon}} \cdot \frac{1}{2} = 1.5 \cdot 10^7 \text{ electrons/cm}^2 \text{ s},$$

corresponding to an electron density of $1.5 \cdot 10^7/c = 5 \cdot 10^{-4}/\text{cm}^3$ or greater. We conclude that such neutrons are capable of supplying a sufficient number of electrons.

We now make a rough estimate of the density of electrons far from the earth. These electrons will follow paths reaching far out at the equator and coming near the earth at the poles, so we must take the variation of dN/dt with position into account. On the other hand, particles with small pitch angles will still be trapped so we assume all emitted particles are trapped. Electrons with guiding centers which cross the equator between r_0 and $r_0 + dr_0$ will be those emitted into a volume of revolution generated by the lines of B passing through r_0 and $r_0 + dr_0$. An element of this volume may be written $2\pi r \sin \theta D dl$, where $dl = r d\theta (B/B_0) = dr (B/B_r)$ is an element of length along the line of magnetic field, and D is the perpendicular distance between lines. The flux between lines is constant so we may write

$$(24) \quad 2\pi r \sin \theta DB = 2\pi r_0 dr_0 B_0.$$

The total volume is therefore:

$$(25) \quad 2 \int_{R_E}^{r_0} 2\pi r_0 dr_0 \frac{B_0}{B_r} dr = 2\pi \frac{dr_0}{r_0^2} \int_{R_E}^{r_0} \frac{r^3}{\sqrt{1 - r/r_0}} dr.$$

We now compute the number of electrons emitted into this volume. We multiply dN/dt from equation (22) by $(R_E/r)^2$ to get the volume source density for electrons. Neglecting \sqrt{x} in the denominator of eq. (22) and multiplying

by the lifetime to get the density of electrons, we obtain

$$\begin{aligned}
 (26) \quad n &= \frac{I_0 R_E^2 (l/L) t \int_{R_E}^{r_0} dr / \sqrt{1-(r/r_0)}}{\int_{R_E}^{r_0} r^3 dr / \sqrt{1-(r/r_0)}} = \\
 &= \frac{I_0 R_E^2 (l/L) t}{r_0^3} \cdot \frac{1}{(R_E/r_0) + \frac{3}{5} \cdot 1 - (R_E/r_0)^2 - \frac{1}{7} (1 - (R_E/r_0))^3} \approx \\
 &\approx .05 \left(\frac{R_E}{r_0} \right)^3 \text{ electrons/cm}^3 \quad \text{for } \frac{R_E}{r_0} \ll 1,
 \end{aligned}$$

where we have used the neutron flux measured at St. Paul as representing an average figure for the earth.

This equation refers to the density everywhere along a line of B crossing the equatorial plane at r_0 . Hence above the atmosphere at a constant height we should expect the electron density to show a strong latitude dependence. Writing $r = r_0 \sin^2 \theta$ we have, away from the equator

$$(27) \quad \varrho \sim .05 \frac{R_E^3 \sin^6 \theta}{r^3}.$$

This equation is of doubtful accuracy and we shall show later that there are probably even fewer particles near the poles. Nevertheless, it is clear that the number of stored particles must be very small near the poles.

We estimate the density of protons from fast neutrons in the same way. In this case (eq. (23)) the production rate varies only as r^{-2} so we obtain

$$(28) \quad \varrho = \frac{I_1 R_E^2}{\lambda v} t \frac{\int r dr / \sqrt{1-(r/r_0)}}{\int r^3 dr / \sqrt{1-(r/r_0)}}.$$

The lifetimes for these particles will not be given by eq. (8) because nuclear scattering dominates the Coulomb scattering for protons of these energies. Over the important part of the energy range under discussion, the cross-section is approximately $3/E$ barns, where E is in MeV. This leads to lifetimes of $5 \cdot 10^{11}$ s for 5 MeV protons and $2 \cdot 10^{12}$ s for 50 MeV protons, which energies we take as representative of the two groups. Then eq. (28) becomes, for $(R_E/r_0) \ll 1$

$$(28a) \quad \varrho = \begin{cases} .04 (R_E/r_0)^2 & \text{for 5 MeV protons,} \\ .02 (R_E/r_0)^2 & \text{for 50 MeV protons.} \end{cases}$$

The actual energy spectrum, of course, will be the same as that from stars, but slightly distorted by the dependence of lifetime on energy. The density of particles at low altitudes near the equator may be estimated as before and the results are collected in Table III.

TABLE III.

	Electrons	« 5 MeV » Protons	« 50 MeV » Protons	Total
Particle density	$6 \cdot 10^{-3} \text{ cm}^3$	$2 \cdot 10^{-3}$	$1 \cdot 10^{-3}$	—
Particle flux	$2 \cdot 10^8 \text{ cm}^2 \text{ s}$	$6 \cdot 10^6$	10^7	—
Energy flux	100 $\text{erg/cm}^2 \text{ s}$	50	800	10^3

We have already seen that the electron density is sufficient to give a counting rate a few times higher than is observed. The « 5 MeV » protons will not have sufficient energy to penetrate the walls of the Geiger counter and satellite, but most of the « 50 MeV » protons can do so, and would therefore give a counting rate about 5000 times higher than what is observed. The observations give a lower limit only, of course, but one would guess that collective processes are important in removing particles from storage, so that the lifetimes which we have used are too long.

4. — Certain collective effects.

We would now like to show that eqs. (26) and (28) are not likely to be valid for very large radii, even if the lifetimes we have used turn out to be correct, due to plasma instability. In spiralling around the lines of magnetic force, the plasma particles have magnetic moments which tend to reduce the field in the interiors of their orbits; therefore, the plasma has a tendency to be diamagnetic. This tendency is often counteracted by the behaviour near the edges of the plasma. Nevertheless, we shall consider only the diamagnetic effects here. Then, inside the plasma, an expression like:

$$(29) \quad B = B_0 - 4\pi M = B_0 - 2\pi\varrho \frac{m\bar{v}_p^2}{\sqrt{1-\beta^2}} \frac{1}{B}.$$

will hold where M is the magnetic moment density, B_0 is the applied field, \bar{v}_p^2 is the average square of the velocity component parallel to the field, and ϱ is the density of particles.

Solving for B , we obtain

$$(30) \quad B = \frac{1}{2} \left| B_0 \pm \sqrt{B_0^2 - 4 \left(2\pi \varrho \frac{m \bar{v}_p^2}{\sqrt{1 - \beta^2}} \right)} \right|,$$

so that we see that we have no solution when the energy density of the plasma is greater than one-half of the energy density of the applied magnetic field. If we consider a plot of B versus ϱ , we see that near the limit

$$(31) \quad \varrho = \frac{B_0^2}{16\pi} \left[\frac{m \bar{v}_p^2}{\sqrt{1 - \beta^2}} \right]^{-1},$$

the addition of a few particles causes a very great change in the magnetic field and we may expect that somehow instabilities develop which prevent the limit, eq. (31), being exceeded by throwing particles out of the region. This argument is perhaps not completely convincing, because we neglected the effects at the edge of the plasma but what we are saying is merely that a plasma probably cannot be confined by a magnetic field whose energy density is smaller than that of the plasma.

The limit (eq. (31)) is exceeded at about 8 earth radii. Beyond 8 earth radii, then, we may expect that the energy density falls off at least as fast as $1/r^6$. We should also expect rather complicated and interesting effects in this region. We note that the line of B which crosses the equator at 8 earth radii reaches the earth at a geomagnetic latitude which is rather close to the auroral zone. It may be that the aurora is a manifestation of the instability which we expect in this region, and that the observed correlation with solar phenomena is due to some triggering process.

In this section we give a more accurate treatment of the density of stored particles. Let $n(r_0, \psi_0, \mu) \sin \psi_0 d\psi_0 r_0 dr_0 d\mu$ be the number of particles with guiding centers which cross the equatorial plane between r_0 and $r_0 + dr_0$ and at the equator have pitch angle between ψ_0 and $\psi_0 + d\psi_0$ and have magnetic moment μ . We write the rate of change of n as

$$(32) \quad \frac{dn}{dt} = \left(\frac{dn}{dt} \right)_{\text{source}} - \left(\frac{dn}{dt} \right)_{\text{scat}},$$

where dn/dt_{source} is the rate of increase of n due to decays of neutrons and dn/dt_{scat} is the rate of decrease of n due to scattering of the particles. If the density of collision centers were uniform we should write

$$(33) \quad \left(\frac{dn}{dt} \right)_{\text{capt}} = n \sigma v N_a,$$

where N_a is the number of collision centers per cm^3 . We expect that the number of collision centers will be a function of r , so we need to average in the following way, where the integral is taken over the orbit of the particles in question from the equator to the turning point

$$(34) \quad \left(\frac{dn}{dt}\right)_{\text{capt}} = n\sigma v \frac{\int N_a(r)(dr/v_r)}{\int dr/v_r},$$

where v_r is the radial velocity of the guiding center; $v_r = v \cos \psi (B_r/B) (dn/dt)_{\text{source}}$ is somewhat more complicated. Let (dN/dT) be the number of particles produced per cm^3/s by neutron decays. It may be a function of r and θ . We assume these particles are produced isotropically, so $(dN/dT) \sin \psi d\psi r_0 dr \sin \theta d\theta$ is the number of particles produced with pitch angle between ψ and $\psi + d\psi$ in the volume element $r^2 dr \sin \theta d\theta$. Particles with equatorial co-ordinates r_0 to $r_0 + dr_0$ and ψ_0 to $\psi_0 + d\psi_0$ are those emitted in a volume bounded by the lines of B through r_0 and $r_0 + dr_0$, and the turning points corresponding to ψ_0 , r_0 .

We may express the pitch angle in terms of the pitch angle at the equator by means of equation (1),

$$(35) \quad \sin \psi d\psi = \frac{(B/B_0) \sin \psi_0 \cos \psi_0 d\psi_0}{\sqrt{1 - (B/B_0) \sin^2 \psi_0}}.$$

Let D be the perpendicular distance between two lines of B which cross the equator at r_0 and $r_0 + dr_0$, so $D = dr (B/B_0)$. Then, using eq. (24), we have

$$(36) \quad 2\pi r_0 dr_0 B_0 = 2\pi r \sin \theta DB = 2\pi r \sin \theta dr B_\theta.$$

We have, finally, for the rate of creation of particles

$$(37) \quad \left(\frac{dn}{dt}\right)_{\text{source}} r_0 dr_0 \sin \psi_0 d\psi_0 = \int \frac{dN}{dT} \left(\frac{\sin \psi_0 \cos \psi_0 d\psi_0}{\sqrt{1 - (B/B_0) \sin^2 \psi_0}} \right) \left(\frac{B}{B_0} \right) r d\theta r_0 dr_0.$$

In this integral we should express r in terms of θ by $r = r_0 \sin^2 \theta$

$$(38) \quad \frac{B}{B_0} = \frac{\sqrt{4 - 3 \sin^2 \theta}}{\sin \theta} \quad \text{and} \quad \frac{B}{B_0} = \frac{\sqrt{4 - 3 \sin^2 \theta}}{\sin^3 \theta}$$

and the integral is to be taken from along the fluxline between the turning points corresponding to r_0 , ψ_0 .

At equilibrium we have $dn/dt = 0$ so that we may solve eqs. (34) and (37) for n to obtain

$$(39) \quad n = \frac{\int dr/v_r}{\int N_a \sigma v(dr/v_r)} \int dt \frac{dN}{B_0} r \left(\frac{\cos \psi_0}{\sqrt{1 - (B/B_0) \sin^2 \psi_0}} \right) d\theta.$$

$n(\psi_0 r_0) r_0 dr_0$ is the number of particles of equatorial pitch angle ψ_0 which cross the equator between r_0 and dr_0 . To obtain the number of particles in an element of volume we must multiply by $dq/2\pi$ and by $dl/r \cos \psi T$ where $dl = r d\theta (B/B_0)$ is an element of length along a line of force, $v \cos \psi$ is the velocity parallel to a line of force and T is the half-period, the time to travel from one turning point to another. We express $r_0 dr_0$ in terms of r by eq. (24) and obtain

$$(40) \quad \varrho(r, \theta, \psi_0) r^2 \sin \theta dr d\theta d\varphi = \frac{1}{T(r_0, \psi_0)} n \frac{B}{B_0} \frac{r^2 \sin \theta dr d\theta d\varphi}{2\pi v \cos \psi},$$

for the number of particles having equatorial pitch angle ψ_0 in the volume element $r^2 \sin \theta dr d\theta d\varphi$. To get the density of particles of all pitch angles, we multiply by

$$(41) \quad \sin \psi d\psi = \frac{B}{B_0} \frac{\sin \psi_0 \cos \psi_0 d\psi_0}{\sqrt{1 - (B/B_0) \sin^2 \psi_0}},$$

and integrate over pitch angle from zero to $\psi_{0\min}$ where $\psi_{0\min}$ is the smallest pitch angle for which particles reach the volume element in question before being reflected.

The half-period T is given by

$$(42) \quad T = \int \frac{dr}{v_r} = \int \frac{B}{B_r} \frac{1}{v \cos \psi} dr = \frac{1}{v} \int_{r_1}^{r_0} \frac{\sqrt{4 - 3r/r_0}}{l \sqrt{1 - r/r_0}} \left| \frac{1}{1 - \frac{\sqrt{4 - 3r/r_0}}{(r/r_0)^3} \sin^2 \psi_0} \right| dr \\ = \frac{r_0}{v} \int_{x_1}^1 \frac{\sqrt{4 - 3x}}{\sqrt{1 - x}} \left| \frac{dx}{1 - \frac{\sqrt{4 - 3x}}{x^3} \sin^2 \psi_0} \right|.$$

The integral has the value $(\pi/3)\sqrt{2} \approx 1.48$ for $\psi_0 \approx \pi/2$ and 2.74 for $\psi_0 \approx 0$ so is not a strong function of ψ_0 .

We now attempt a more accurate treatment of the storage problem using these equations. We consider only particles with $r_0 \gg R_E$, so these considerations do not apply close to the earth near the equator. We take the earth's atmos-

phere to be a perfect absorber with a sharp upper boundary so that

$$(43) \quad \int N_a \sigma v \frac{dr}{v_r} \int \frac{d\psi}{v_r} = \begin{cases} 1/t & \text{for } \psi_0 > \psi_{\text{cmax}} \\ \infty & \text{for } \psi_0 < \psi_{\text{cmax}} \end{cases}$$

where t is given in Table I and $\psi_{0\text{max}}$ is the largest pitch angle which allows particles to enter the atmosphere.

We evaluate approximately the integral in equation (39) in the extreme cases of large and small ψ_0 . For $\psi_0 \approx \pi/2$, θ will also not be much different from $\pi/2$. In the integrand $dN/dt \approx dN/dt(r_0)$ so we have

$$(44) \quad \frac{dn}{dt} = \cos \psi_0 v T \frac{dN}{dt}(r_0),$$

where T is given by eq. (42).

For small ψ_0 we write

$$(45) \quad \left(\frac{dn}{dt} \right) = \int_{r_1}^{r_0} \frac{dN}{dt}(R_E) \frac{R_E^3}{r^3} \left[\frac{\cos \psi_0}{1 - \frac{\sqrt{4 - 3r/r_0}}{r^3} \sin^2 \psi_0} \right] \frac{B}{B_r} dr,$$

where we have changed eq. (37) to make r the variable of integration.

r_1 is the value which makes the square root vanish, and we are interested in the case $r_1 \ll r_0$. Then the principal contribution comes from $r \approx r_1$. We therefore neglect terms of order r_1/r_0 and put $B/B_r = 1$ and $\sqrt{4 - r/r_0} \approx 2$, obtaining

$$(46) \quad \frac{dN}{dt}(R_E) R_E^3 \cos \psi_0 \int_{r_1}^{r_0} \frac{dr}{r^3 \sqrt{1 - (2r_0^3/r^3) \sin^2 \psi_0}} = \frac{dN}{dt}(R_E) \frac{R_E^3}{r_0^2} \frac{\cos \psi_0}{(2 \sin \psi_0)^{1/2}} \int_1^{x_0} \frac{dx}{x^3 \sqrt{1 - (1/x^3)}},$$

where we have put $x = (r/2^{1/3}r_0) \sin^{-1/2} \psi_0$. The upper limit can be made infinite without serious error and then the value of the integral is about .86. For comparison with eq. (44) we put $(dN/dt)(R_E)R_E^3 = (dN/dt)(r_0)r_0^3$ and have

$$(47) \quad n(\psi_0, r_0) = t \frac{dN}{dt}(r_0) r_0 \begin{cases} .86 \frac{\cos \psi_0}{[2 \sin^2 \psi_0]^{1/2}}, & \psi_0 \text{ small,} \\ 2.74 \cos \psi_0, & \psi_0 \approx \frac{\pi}{2}. \end{cases}$$

For r_0 very large, the distribution at the equator will be strongly peaked near the critical value ψ_m .

At large radii then, near the equator, there are large numbers of particles moving nearly perpendicular to the equatorial plane, in both directions. Such a situation arises because of the $1/r^3$ dependence of the source density which implies that most of the particles were created in trapped orbits near the earth, and so have small pitch angles when they cross the equator. Such a situation, with charged particles moving in opposite directions through each other, is unstable against plasma oscillations. But in this case it seems likely that the plasma oscillations act at least as much to increase the pitch angles as otherwise and so do not throw the particles out of the trapping zone. In any case, the particles will not return to near the earth, but will be thrown out, or confined nearer the equatorial plane.

5. - Summary.

The earth is a source of neutrons which are produced in the atmosphere by the cosmic rays. Neutrons which leave the atmosphere and decay will often leave the decay proton and electron in trapped orbits in the earth's magnetic field. We compute an upper limit of the density of trapped particles and show these may be the particles observed by VAN ALLEN and co-workers in satellites. Reasons are given for believing that there may be few or no particles near the magnetic poles, the boundary of the distribution occurring near the auroral zone. If the auroral zone is actually the boundary of the radiation zone, then it seems possible that the aurora is a manifestation of instabilities occurring at the outside of the zone, triggered in some way by solar phenomena.

* * *

The author would like to thank T. GOLD, Harvard University, and PAMELA ROTHWELL, Imperial College, London, who are responsible for the central idea of this paper. His debt to them has been mentioned more fully in the text. He would also like to thank E. P. NEY, C. J. WADDINGTON and J. R. WINCKLER for helpful discussions, and the members of the cosmic ray group at the State University of Iowa, particularly C. E. McILWAIN, for communicating preliminary results in Explorer IV.

Supplementary note.

As this paper was being submitted for publication, the author received *Phys. Rev. Letters*, **1**, no. 5 containing two letters from S. F. SINGER dealing with the same subject. Although the present paper would have been somewhat different if Singer's letters had been read earlier, still the author feels that the topics treated in the present paper are sufficiently different from those treated by Singer to warrant its publication.

Note added in proof.

Recently results of observations in Explorer IV (satellite 1958 ϵ) have become available (*). This satellite carries four different instrument for measuring radiation. A geiger counter shows that the flux of 50 MeV protons, at the maximum altitude attained, must be at least one thousand times less than that calculated in Table III. On the other hand, a scintillator measures an energy flux of 80 erg/cm²/s of particles of range greater than 1 mg/cm². Since it is unlikely that the satellite is high enough so that the values of Table III really apply, and since it would in any case be difficult to account for the great reduction in proton flux with no reduction in electron flux, we must consider this energy flux too great to be accounted for on the present hypothesis (the relevant flux from Table III would then be the 100 erg/cm²/s due to electrons). It seems likely, therefore, that the penetrating (range greater than 5 g/cm²) part of the Van Allen radiation may be protons due to neutron decay but that some other source is necessary to account for the less penetrating part.

(*) J. A. VAN ALLEN, C. E. McILWAIN and G. H. LUDWIG: submitted for publication in *Journ. of Geophys. Res.*

RIASSUNTO (*)

Discutiamo la possibilità suggerita da P. ROTHWELL e T. GOLD in conversazioni con l'autore che la radiazione osservata da VAN ALLEN e collaboratori alle grandi altitudini sia dovuta agli elettroni e protoni di decadimento di neutroni prodotti nell'atmosfera terrestre dai raggi cosmici ed immagazzinati nel campo magnetico terrestre. Si presentano valutazioni dell'ordine di grandezza delle densità prevedibili. Si considerano solo le perdite per scattering. Assumendo una vita media di $3 \cdot 10^9$ s per scattering, si ottiene un limite superiore di 10^{-2} elettroni/cm³ vicino alla terra e $.05(R_E/r_0)^3$ elettroni/cm³ a grandi distanze r_0 nel piano equatoriale. La densità protonica a grande distanza è $.03(R_E/r_0)^2$ cm⁻³ per una vita media di 10^{12} s. Se le accelerazioni nel plasma non sono rilevanti, lo spettro elettronico sarà approssimativamente uguale a quello del decadimento β dei neutroni. I protoni sono prodotti da neutroni veloci provenienti direttamente da stelle nucleari e il loro spettro sarà approssimativamente uguale a quello dei protoni provenienti dalle stelle. La densità elettronica è sufficiente a dare un tasso di conteggio alcune volte maggiore di quello osservato, mentre la densità protonica è sufficiente a dare un tasso di conteggio 10^4 volte maggiore del limite minimo osservato. Le vite medie delle particelle immagazzinate sono pertanto probabilmente molto minori di quelle risultanti dallo scattering. Si dovrebbe rilevare un forte effetto di latitudine che si stima grossolanamente proporzionale a $\cos^6 \lambda$. Si danno ragioni che fanno ritenere che effetti collettivi riducano in vicinanza dei poli la densità al disotto di tale valore.

(*) Traduzione a cura della Redazione.

Elastic Differential Cross-Section for 60 MeV K^+ -Scattering in Emulsion.

T. G. LIM and J. P. VAN DER LINDEN

Natuurkundig Laboratorium - Universiteit van Amsterdam, The Netherlands

(ricevuto il 2 Ottobre 1958)

Summary. — By the method of the phase shift optical model analysis, the differential cross-sections for 60 MeV K^+ -mesons elastically scattered by complex nuclei in Ilford G-5 nuclear emulsion are computed. The calculations are based on the assumption that the elastic scattering is due to a symmetrical square well potential of +13 MeV, superposed on the Coulomb potential. The resultant emulsion cross section $d\sigma/d\omega = f(\theta)$ curve is obtained from the separate contributions of the cross sections for the K^+ -meson scattering by C, Ag, Br and O. Previously the resultant cross sections were computed by COSTA and PATERGNANI⁽¹⁾ on the assumption that the K^+ -mesons were scattered by the hypothetical elements ${}^{95}_{42}\text{E}$ and ${}^{14}_7\text{E}$, representing the average of the heavy and the light elements in the emulsion, respectively. It is found that the $d\sigma/d\omega = f(\theta)$ curves obtained by their method and by the present ones do not coincide but agree fairly well.

1. — Introduction.

The successful application of the optical model of the nucleus to the analysis of the π -meson scattering⁽²⁾ is well known. Assuming also the applicability of this optical model to the K^+ -scattering, the real part of the nuclear potential can be obtained by the analysis of the elastic K^+ -scattering against complex nuclei. From the analysis of the inelastic K^+ -meson scattering, it is found

⁽¹⁾ G. COSTA and G. PATERGNANI: *Nuovo Cimento*, **5**, 448 (1957).

⁽²⁾ A. PEVSNER and J. RAINWATER: *Phys. Rev.*, **100**, 1431 (1955).

experimentally that the imaginary part is small, of about a few MeV ^(1,3). The inclusion of the imaginary part of the nuclear potential has little influence on the differential cross-section in the small angle region ⁽⁴⁾. With other authors ^(1,5) we therefore only consider the real part of the complex potential in the calculations of the elastic differential cross-sections in this angle region. The real part of the nuclear potential is assumed to be represented by a constant potential throughout the nuclear volume. We further assume a homogeneous charge distribution in the nucleus, so that the total potential for the elastic K⁺-scattering is envisaged as a Coulomb potential on which is superposed a spherical and constant real potential. The interference of the electromagnetic and the nuclear scattering is expected to be strong in the region of small scattering angles. A refinement of the shape of the nuclear potential, as *e.g.* the use of a more realistic one ⁽⁶⁾ influences the $d\sigma/d\omega = f(\theta)$ curve most in the region of large angles. It may be noted that through the observation of the scattering events just in this large angle region, one can try to determine the form of the potential. However, this is more meaningful, if a separate scattering experiment could be set up using only one element ⁽⁷⁾. So, as long as we try to fix the sign and to get an estimate of the average depth value of the real part of the nuclear potential in this region, the omission of the imaginary part in the calculation seems to be justified.

2. - Computation.

The differential cross-section is computed by the method of partial waves. According to this procedure the differential cross-section in the center of mass system, due to a pure Coulomb field is ^(8,9)

$$(1) \quad \frac{d\sigma}{d\omega} = \left| \frac{\zeta}{2k \sin^2 \frac{1}{2}\theta} \exp[-i\zeta \ln(\sin^2 \frac{1}{2}\theta) + i\pi + 2i\eta_0] \right|^2.$$

The differential cross-section due to a symmetrical square well potential only,

⁽³⁾ G. COCCONI, G. PUPPI, G. QUARENI and A. STANGHELLINI: *Nuovo Cimento*, **5**, 172 (1957).

⁽⁴⁾ G. IGO, D. G. RAVENHALL, J. J. TIEMANN, W. W. CHUPP, G. GOLDBABER, S. GOLDBABER, J. E. LANNUTTI and R. M. THALER: *Phys. Rev.*, **109**, 2133 (1958).

⁽⁵⁾ T. F. HOANG, M. F. KAPLON and R. CESTER: *Phys. Rev.*, **107**, 1698 (1957).

⁽⁶⁾ J. E. LANNUTTI, S. GOLDBABER, G. GOLDBABER, W. W. CHUPP, S. GIAMBUZZI, C. MARCHI, G. QUARENI and A. WATAGHIN: *Phys. Rev.*, **109**, 2121 (1958).

⁽⁷⁾ L. T. KERTH, T. F. KYCIA and L. VAN ROSSUM: *Phys. Rev.*, **109**, 1784 (1958).

⁽⁸⁾ N. F. MOTT and H. S. W. MASSEY: *The Theory of Atomic Collisions* (Oxford, 1949).

⁽⁹⁾ W. GORDON: *Zeits. f. Phys.*, **51**, 180 (1928).

can be written as ⁽¹⁰⁾

$$(2) \quad \frac{d\sigma}{d\omega} = \left| \frac{1}{k} \sum_l (2l+1) \exp[i\delta_l] \sin \delta_l P_l(\cos \theta) \right|^2.$$

We assume the elastic K^+ -scattering to be due to a modified Coulomb field (*viz.* a field due to a homogeneous charge distribution on which a constant real potential is superposed), so that the differential cross-section becomes ⁽¹⁰⁾

$$(3) \quad \frac{d\sigma}{d\omega} = \left| \frac{\zeta}{2k \sin^2 \frac{1}{2}\theta} \exp[-i\zeta \ln(\sin^2 \frac{1}{2}\theta) + i\pi + 2i\eta_0] + \frac{1}{k} \sum_l (2l+1) \exp[i\delta_l + 2i\eta_l] \sin \delta_l P_l(\cos \theta) \right|^2,$$

where $\zeta = Ze^2/\hbar v$, Z : nuclear charge number, e : elementary charge, \hbar : Planck's constant, divided by 2π , v : relative velocity of the colliding particles, θ : scattering angle; η_l : phase difference between the undisturbed l -th partial wave and the corresponding wave, disturbed by a Coulomb field; δ_l : phase difference between the l -th partial wave distorted both by Coulomb potential and the symmetrical square well potential, and the corresponding wave distorted by the Coulomb field only.

With COSTA and PATERGNANI ⁽¹⁾ the evaluation of δ_l is carried out using the W.K.B. approximation ^(1,11).

The composition of the G-5 nuclear emulsion at 58% humidity ⁽¹²⁾ is given in Table I, in which the elements are arranged according to their relative abundance.

TABLE I.

Element	^1_1H	$^{12}_6\text{C}$	$^{107.9}_{47}\text{Ag}$	$^{79.9}_{25}\text{Br}$	$^{16}_8\text{O}$	$^{14}_7\text{N}$	$^{32}_{16}\text{S}$	$^{126.6}_{53}\text{I}$
Number of atoms $\cdot 10^{22}/\text{cm}^3$	3.2102	1.3401	1.0221	1.0169	0.9373	0.3141	0.0131	0.0057

Scattering of K^+ -mesons by free protons are rare in emulsion and moreover these can be distinguished from those events which are due to collisions against complex nuclei. As we only consider K^+ -scattering by complex nuclei,

⁽¹⁰⁾ L. I. SCHIFF: *Quantum mechanics* (New York, 1949).

⁽¹¹⁾ P. M. MORSE and H. FESHBACH: *Methods of Theoretical Physics*, part II (New York, 1953), p. 1101.

⁽¹²⁾ A. ROSENFELD, M. BACKUS, J. FRIEDMAN, W. F. FRY, D. HASKIN, J. LACH, R. LUX, M. ORANS, J. OREAR, E. SILVERSTEIN, W. SLATER, F. SOLMITZ, R. SWANSON and H. TAFT: *How to develop emulsion* (Chicago, 1955), ch. II.

according to Table I it is clear that a good approximation to the real situation is obtained by taking only into account the scattering by C-, Ag-, Br-, and O-nuclei, being the most abundant elements. We therefore compute the elastic differential cross-sections of the K^- -mesons against these nuclei separately and call them $(d\sigma/d\omega)_C$, $(d\sigma/d\omega)_{Ag}$, $(d\sigma/d\omega)_{Br}$ and $(d\sigma/d\omega)_O$, respectively. The resultant emulsion cross-section $d\sigma/d\omega$ per nucleus is the mean of the separate cross-section and can be obtained by the relation

$$(4) \quad \frac{d\sigma}{d\omega} = \sum_i \alpha_i \left(\frac{d\sigma}{d\omega} \right)_i,$$

where α_i is the relative number of atoms of the i -th element $i = C, Ag, Br, O$.

$$\sum_i \alpha_i = 1.$$

Previously COSTA and PATERGNANI⁽¹⁾ computed the differential cross-sections starting from the hypothetical elements $A = 95$, $Z = 42$ (57%), representing the average heavy element and $A = 14$, $Z = 7$ (43%), representing the average light element. As expression (3) is not a linear one—it namely depends in an intricate manner on the nuclear parameters—we compute the resultant differential cross-section by means of (4).

To have a comparison of the resultant cross-sections obtained by the two mentioned methods, our computations are carried out for the values of the nuclear potential and K^+ -energy, also used by COSTA and PATERGNANI⁽¹⁾. We chose for the depth of the square well nuclear potential: +13 MeV and for the K^+ -energy: 60 MeV.

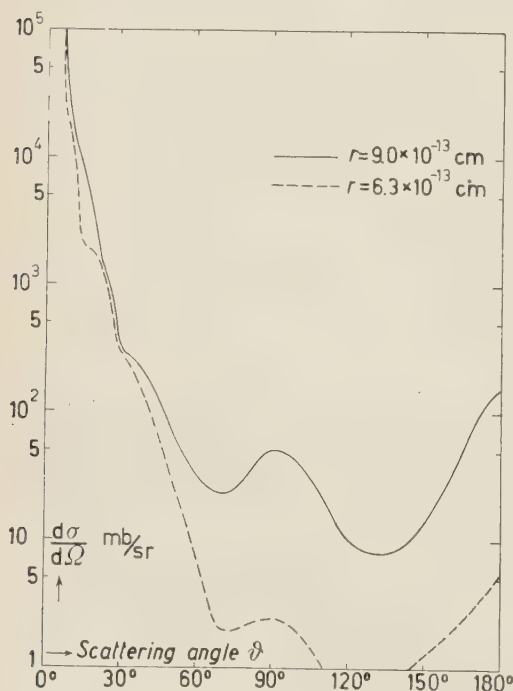


Fig. 1. - Differential cross section per nucleus versus scattering angle, for 60 MeV K^+ -mesons, elastically scattered by Ag. V : +13 MeV. Curve ----: $r = 6.3$ fermis and highest $l = 5$. Curve —: $r = 9.0$ fermis and highest $l = 8$.

From (4) it follows that the value of the resultant cross-section is strongly influenced by the greatest $\alpha_i(d\sigma/d\omega)_i$, *i.e.* by the most abundant element of high constituting differential cross-section. This leads us to investigate how the differential cross-section $d\sigma/d\omega$ varies, when the Ag-nuclear radius varies, keeping V : +13 MeV and the K^+ -energy: 60 MeV. In this way we can also obtain an idea of the spread of the theoretically expected value, as we in fact do not know the appropriate range of the nuclear potential.

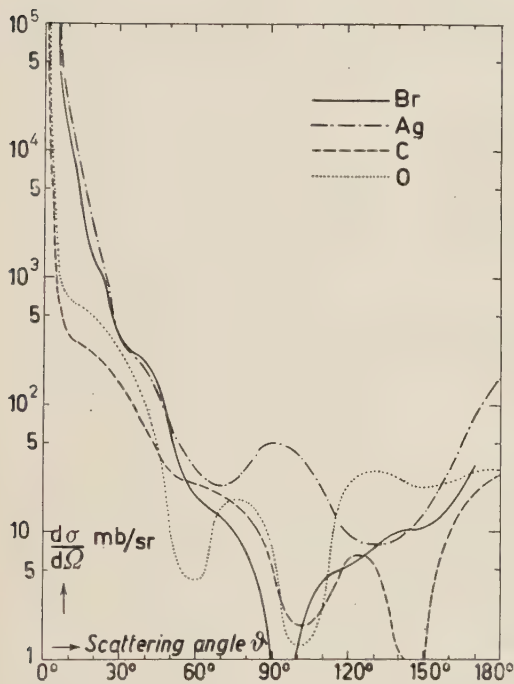


Fig. 2. — Differential cross section per nucleus versus scattering angle for 60 MeV K^+ -mesons, elastically scattered by C-, Ag-, Br- and O-nuclei, respectively. V : +13 MeV.

By way of example we varied the value of the Ag-radius from 6.3 fermis (from the neutron experiment) with its highest l -number=5 to 9.0 fermis (from the α -experiment) with its highest l -number=8. The corresponding $(d\sigma/d\omega)_{Ag}=f(\theta)$ curves are drawn in Fig. 1.

The effect of the variation of the Ag-radius is reflected in the variation of the resultant curves (Fig. 3).

To demonstrate of which components the resultant $d\sigma/d\omega=f(\theta)$ curve is built up, we draw as an example the components of curve I of Fig. 3. These $(d\sigma/d\omega)_i=f(\theta)$ curves ($i=C, Ag, Br, O$)

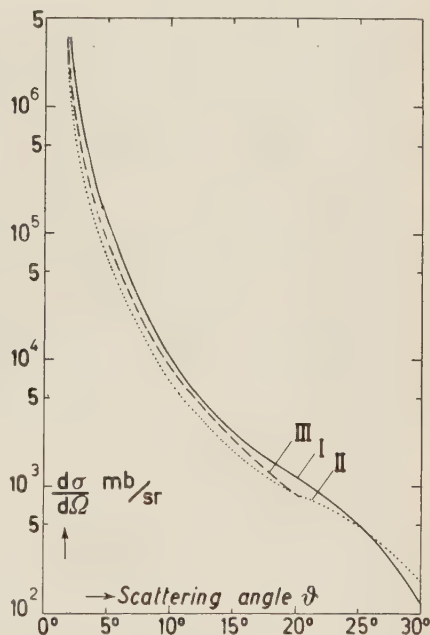


Fig. 3. — Resultant curves $d\sigma/d\omega=f(\theta)$. K^+ -energy: 60 MeV. V : +13 MeV. For curves I and II, the K^+ -mesons scatter against C-, Ag-, Br-, and O-nuclei; for curve I the Ag-radius is 9.0 fermis and for curve II the Ag-radius is 6.3 fermis. Curve III is derived from the computations of Costa and Patergnani.

are drawn separately in Fig. 2. The Ag-radius is 9.0 fermis with the highest l -number = 8; the radii of C, Br and O are taken from the neutron experiments and are 3.9 fermis, 6.0 fermis and 3.4 fermis respectively with their highest l -numbers 3, 6 and 3, respectively. The oscillatory character of the curves depends on the form of the nuclear potential, which is superposed on the Coulomb potential. This is most pronounced in the large angle region, whereas in the small angle region the oscillations are smoothed out.

In Fig. 3 the resultant curves I, II and III of $d\sigma/d\omega = f(\theta)$ are drawn for the small angle region. Curves I and II are obtained by considering the scattering of K^+ -mesons to take place against C-, Ag-, Br-, and O-nuclei; for curve I the radius of Ag is taken 9.0 fermis and for II it is taken 6.3 fermis. Curve III is derived from the computation of COSTA and PATERGNANI, where the K^+ -scatterings are assumed to take place against the hypothetical elements $A = 95$, $Z = 42$ and $A = 14$, $Z = 7$ only (¹). We note that curve III does not differ very much from the curves I and II and that it lies within the spread of the resultant cross-sections with the corresponding Ag-radius 9.0 and 6.3 fermis, respectively.

* * *

This work is part of the Research Program of the Netherlands Institution of Fundamental Research of Matter (F.O.M.), financially supported by the Netherlands Foundation for Pure Scientific Research (Z.W.O.). Many thanks are due to Professor Dr. G. W. RATHENAU for his stimulating suggestions and criticisms. The valuable discussions with Mr. F. ARTMANN, Dr. F. BRUIN (*) and Dr. M. BRUIN (*) are here gratefully acknowledged. Miss C. J. VAN ALBADA and Mr. S. BOSGRA are thanked for their help in the tedious computations.

(*) Now at the American University, Beirut.

RIASSUNTO (*)

Si calcolano col metodo dell'analisi degli spostamenti di fase nel modello ottico le sezioni d'urto differenziali pei mesoni K^+ da 60 MeV diffusi elasticamente dai nuclei complessi dell'emulsione nucleare Ilford G-5. I calcoli sono basati sull'assunzione che lo scattering elastico sia dovuto ad una buca di potenziale quadrata simmetrica di +13 MeV sovrapposta al potenziale coulombiano. La curva che rappresenta la sezione d'urto $d\sigma/d\omega = f(\theta)$ risultante per l'emulsione si ottiene dai contributi separati delle sezioni d'urto dello scattering del mesone K^+ su C, Ag, Br e O. Le sezioni d'urto risultanti erano state precedentemente calcolate da COSTA e PATERGNANI nell'ipotesi che i mesoni K^+ fossero diffusi dagli elementi ipotetici ${}^{95}_{42}\text{E}$ e ${}^{14}_7\text{E}$, rappresentanti, rispettivamente, le medie degli elementi pesanti e leggeri dell'emulsione. Si trova che le curve $d\sigma/d\omega = f(\theta)$ ottenute col loro metodo e col presente non coincidono ma si accordano soddisfacentemente.

(*) Traduzione a cura della Redazione.

Three Body Forces in Hypernuclei (*).

G. G. BACH

Istituto di Fisica dell'Università - Roma

(ricevuto il 15 Ottobre 1958)

Summary. — An investigation is made to ascertain the relative importance of the two-body and three-body Λ -nucleon potentials which have the same order of coupling constant. The three-body potential, which is derived using perturbation theory from a pseudoscalar interaction, is found to be weakly singular and hence, much smaller than the two-body potential. In addition, the largest terms are non-central. In the hypertriton, where correlations are large, it is found that three-body forces are repulsive for S states and may amount to 4%. Suitable D state admixture could lead to a repulsive three-body force of nearly 6%. In heavy hypernuclei, the relative importance of three-body forces is about $\frac{1}{2}\%$ if correlations are neglected, and may be as large as $7\frac{1}{2}\%$ if correlations are as strong as they are in the hypertriton. It is also found that by omitting the Feynman graphs with bare lines the three-body contributions are negligible.

1. — It was first pointed out by DALITZ ⁽¹⁾ that the hypernuclear force between a Λ -particle and a nucleon could be brought about through a double pion exchange. If this is the case, it then seems likely that the three-body hypernuclear potential may be important since it would have the same order of coupling constant as the two-body hypernuclear potential. Calculations have been made by SPITZER ⁽²⁾ on the relative importance of this three-body potential.

In this paper, a quantitative estimate is made of the relative importance of the three-body force for the case of the hypertriton, where one would expect

(*) This paper forms part of a thesis, which was presented at McGill University in April, 1958, in partial fulfilment of the requirements for the degree of Doctor of Philosophy.

(1) R. H. DALITZ: *Phys. Rev.*, **99**, 1475 (1955).

(2) R. SPITZER: *Phys. Rev.*, **110**, 1190 (1958).

correlations to be quite strong, and in heavy hypernuclei, where one would expect correlations to be quite weak. In Sect. 2, the three body-potential is derived and examined for its relative magnitude. It is found that without correlations, the more singular parts vanish since they are non-central. A self consistent calculation is then carried out in Sect. 3 on the hypertriton to obtain a wave function with correlations as well as a two-body Λ -nucleon potential which will give a Λ separation energy (binding energy) near zero. Then, in Section 4, using this wave function and two-body potential as well as the three-body potential, which is derived in Section 2, a direct calculation of $\langle V(3\text{-body}) \rangle / \langle V(2\text{-body}) \rangle$ is made. The sensitivity of $\langle V(3\text{-body}) \rangle$ with D state admixture is also calculated. Following these considerations, heavy hypernuclei are treated in Section 5.

2. - If one assumes pseudoscalar coupling with the spins of all baryons $\frac{1}{2}$ and the Λ and Σ particles with the same relative parity, the lowest order terms of the interaction hamiltonian are

$$(1) \quad H_{\text{int}} = \frac{g}{2m} \int d^3z \bar{\psi}_N \boldsymbol{\tau}_i \boldsymbol{\sigma} \psi_N \cdot \nabla \varphi_i + \left[\frac{g_\Lambda}{2m_\Lambda} \int d^3z \bar{\Sigma}_i \boldsymbol{\sigma} \Lambda \cdot \nabla \varphi_i + \text{conjugate} \right] + \\ + \frac{g^2}{2m} \int d^3z \bar{\psi}_N \psi_N \varphi^2 + \frac{g_\Lambda^2}{2m_\Lambda} \int d^3z \bar{\Lambda} \Lambda \varphi^2,$$

where we have set $M_\Sigma = M_\Lambda$. Here Σ , Λ , ψ and φ are the wave functions for the three baryons and the π -meson.

To evaluate the three-body potentials, we use ordinary perturbation theory and assume that the baryon wave functions are δ functions. In the energy denominators, we neglect the quantity $\Delta = M_\Sigma - M_\Lambda$ in comparison with ω_k , the energy of the meson, in the intermediate states corresponding to graphs in Fig. 1a. The calculation of the three-body potentials is then straightforward and the results for the three type of graphs in Fig. 1 are as follows: From Fig. 1a:

$$(2) \quad V_{NB} = -i \frac{g^2}{4\pi} \frac{\mu^2}{4m^2} \cdot \frac{g_\Lambda^2}{4\pi} \frac{\mu^2}{4m_\Lambda^2} \cdot \frac{2}{\pi} \frac{(\boldsymbol{\tau}_1 \cdot \boldsymbol{\tau}_2)}{3} \left\{ S_{12,xy} \left[\frac{e^{-x}}{3x^3y} (2k_1(y) + yk_0(y))(x^2 + 3x + 3) + \right. \right. \\ \left. \left. + \frac{e^{-y}}{3xy^3} (2k_1(x) + xk_0(x))(y^2 + 3y + 3) \right] - \right. \\ \left. - S_{12,x} \left[\frac{e^{-x}}{x^3y} k_1(y)(x^2 + 3x + 3) + \frac{e^{-y}}{xy^3} (2k_1(x) + xk_0(x))(y + 1) \right] - \right. \\ \left. - S_{12,y} \left[\frac{e^{-y}}{xy^3} k_1(x)(y^2 + 3y + 3) + \frac{e^{-x}}{x^3y} (2k_1(y) + yk_0(y))(x + 1) \right] - \right. \\ \left. - \frac{\boldsymbol{\sigma}_1 \cdot \boldsymbol{\sigma}_2}{3xy} [e^{-x} (k_1(y) - yk_0(y)) + e^{-y} (k_1(x) - xk_0(x))] \right\}.$$

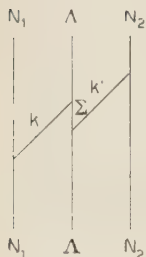


Fig. 1a.

From Fig. 1b:

$$(3) \quad V_B = -\mu \frac{g^2}{4\pi} \cdot \frac{\mu^2}{4m^2} \cdot \frac{g_\Lambda^2}{4\pi} \cdot \frac{\mu^2}{4m_\Lambda^2} \cdot \frac{\mu}{\Lambda} \cdot \frac{2(\boldsymbol{\tau}_1 \cdot \boldsymbol{\tau}_2)}{3} \frac{e^{-x-y}}{x^3 y^3} \cdot \\ \cdot \left\{ 3S_{12,xy} \left(1 + x + \frac{x^2}{3} \right) \left(1 + y + \frac{y^2}{3} \right) - 3S_{12,x} \left(1 + x + \frac{x^2}{3} \right) (1 + y) - \right. \\ \left. - 3S_{12,y} \left(1 + y + \frac{y^2}{3} \right) (1 + x) + (\boldsymbol{\sigma}_1 \cdot \boldsymbol{\sigma}_2) \frac{x^2 y^2}{3} \right\}.$$

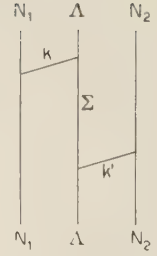


Fig. 1b.

From Fig. 1c:

$$(4) \quad V_P = \lambda \mu \frac{g^2}{4\pi} \cdot \frac{\mu^2}{4m^2} \cdot \frac{g_\Lambda^2}{4\pi} \cdot \frac{\mu^2}{4m_\Lambda^2} \cdot \\ \cdot (\boldsymbol{\sigma}_1 \cdot \mathbf{x})(\boldsymbol{\sigma}_2 \cdot \mathbf{y})(\boldsymbol{\tau}_1 \cdot \boldsymbol{\tau}_2)(1 + x)(1 + y) \frac{e^{-x-y}}{x^3 y^3}.$$

In these formulas, units of pion Compton wavelength are used and $S_{12,x}$ and $S_{12,y}$ are the usual tensor operators formed with the vector \mathbf{x} or \mathbf{y} .



Fig. 1c.

$$S_{12,xy} = q \frac{(\mathbf{x} \cdot \mathbf{y})(\boldsymbol{\sigma}_1 \cdot \mathbf{x})(\boldsymbol{\sigma}_2 \cdot \mathbf{y})}{x^2 y^2} - (\boldsymbol{\sigma}_1 \cdot \boldsymbol{\sigma}_2).$$

The factor λ multiplies V_P in accordance with BRUECKNER and WATSON⁽³⁾ who introduced this damping factor for pair terms.

It is interesting to notice that the more singular parts of the potentials are non-central and with no correlations between spin and direction or between directions, only the weakly singular central parts survive. Also V_P then averages to zero. Comparing V_{NB} and V_B , we see that V_B is larger than V_{NB} by a factor of approximately $\pi\mu/\Lambda \simeq 6$. To get orders of magnitude from these potentials then, we examine V_B with no correlations and consider the two nucleons in a spatially symmetric state so that $\langle(\boldsymbol{\tau}_1 \cdot \boldsymbol{\tau}_2)(\boldsymbol{\sigma}_1 \cdot \boldsymbol{\sigma}_2)\rangle = -3$. Then setting $(g^2/4\pi)(\mu^2/4M^2) = 0.08$ and $g_\Lambda = g$, we obtain

$$(5) \quad V_B \text{ (no correlations)} = 0.74 \frac{e^{-x-y}}{xy} \text{ MeV}.$$

Examining equation (5), we see that V_B with no correlations is very small and can be neglected in comparison with the two-body potential. Also, V_{NB} ,

(3) K. A. BRUECKNER and K. W. WATSON: *Phys. Rev.*, **92**, 1023 (1953).

which is about $\frac{1}{6}$ of this can certainly be neglected for this case. This result cannot be reconciled with Spitzer's ⁽²⁾ where $V_{\pi B}$ was calculated and found to have a comparable magnitude with the two-body potential when there were no correlations.

3. - The form of the three-body potentials derived in Section 2 show that without correlations in the wave function of the hypernucleus, one would not expect that they would be very important. However, since the non-central parts are more singular, it is worth-while to consider a particular hypernucleus in some detail to see if correlations can make three-body forces important. The simplest hyperfragment which can be considered for this purpose is the hypertriton. A complete calculation on any heavier hyperfragment would be much more complex.

To calculate the expectation value of the three-body Λ -nucleon potential for the hypertriton, a wave function with correlations is required as well as a knowledge of the core, ε , of this three-body potential. It is also necessary to have a Λ -nucleon two-body potential so that one may calculate the ratio $\langle V(3\text{-body}) \rangle / \langle V(2\text{-body}) \rangle$. Finally, one requires that the value of B_Λ , the Λ separation energy, be near zero.

We therefore consider first a trial wave function

$$(6) \quad \psi_s = \chi_s \exp \left[-\frac{\alpha}{2}(x+y) - \frac{\beta \rho}{2} \right],$$

where we let α be the variational parameter and choose $\beta = 1.4$ inverse meson units,

$$(7) \quad \chi_s = -\sqrt{\frac{2}{3}}\alpha(1)\alpha(2)\beta(\Lambda) + \sqrt{\frac{1}{6}}(\alpha(1)\beta(2) + \beta(1)\alpha(2))\alpha(\Lambda),$$

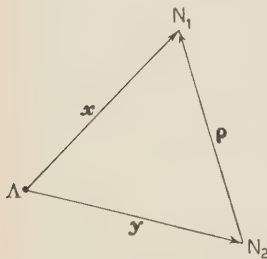


Fig. 2.

which is a spin wave function with $J = \frac{1}{2}$ and $M_J = \frac{1}{2}$. This choice of χ_s is made so that the two nucleons are in a mutual triplet spin state and also in accordance with evidence that the Λ -nucleon interaction is more attractive in the singlet state ⁽⁴⁾.

We next may write the hypertriton hamiltonian (omitting three-body forces) as

$$(8) \quad H = T + V_d + V(\Lambda, N_1) + V(\Lambda, N_2),$$

where T is the total kinetic energy of the system excluding the motion of the center of mass, V_d is the two-body nucleon-nucleon potential and $V(\Lambda, N_1)$,

⁽⁴⁾ R. H. DALITZ and B. W. DOWNS: *Phys. Rev.*, **111**, 967 (1958).

$V(\Lambda, N_2)$ are the Λ -nucleon two-body potentials. If one calculates the expectation value of H and adds to it the binding energy of the deuteron (2.226 MeV), one obtains approximately the binding energy B_Λ of the Λ -particle. We choose a form of the Λ -nucleon two-body potential such that it requires a core ε' . We then write

$$(9) \quad B_\Lambda(\alpha, \varepsilon') = \langle H \rangle + 2.226 \text{ MeV}$$

and setting $\partial B_\Lambda / \partial \alpha = 0$ when $B_\Lambda = 0$ determines an α and a core ε' . Since we need a core ε for the Λ -nucleon three-body potential for the calculation of $\langle V(3\text{-body}) \rangle / \langle V(2\text{-body}) \rangle$, the Λ -nucleon two-body potential is chosen which can be derived in a similar manner as the three-body potentials so that we can assume $\varepsilon = \varepsilon'$.

DALLAPORTA and FERRARI⁽⁵⁾ and LICHTENBERG and ROSS⁽⁶⁾ have derived Λ -nucleon two-body potentials in a similar manner as the three-body potentials are derived here. DF considered only graphs where there were no bare lines while LR considered only bare line graphs. Bare lines (refers to the nucleon lines) means a graph where an intermediate state exists with no mesons present; in other words a graph where no meson lines are allowed to cross. Of these two potentials, we note that the one derived by DF is more attractive in the singlet state. This potential is given by equation (5) in that paper. We therefore select the one derived by DF.

V_D , the nucleon-nucleon potential, is taken to be (7)

$$(10) \quad \begin{cases} V_D = -V_c \frac{e^{-\gamma \varrho}}{\gamma \varrho} - S_{12} V_\pi \frac{e^{-\gamma' \varrho}}{\gamma' \varrho}, & \varrho > .283, \\ = 0, & \varrho < .283, \end{cases}$$

where $V_c = 100.7$ MeV, $V_\pi = 257$ MeV and γ and γ' are 1.735 and 1.696 inverse meson units. We see that equation (10) differs from that mentioned in reference 16 in the paper by GAMMEL and THALER⁽⁷⁾ in that the latter has a hard core at $\varrho = .283$. It is modified by putting $V_D = 0$ so that it will be more suitable for the wave function ψ_s . The most suitable wave function would be zero at the hard core. This is further discussed in the conclusions.

Equation (9) is plotted in Fig. 3. It is seen that the minimum for B_Λ with respect to α is very close to zero when $\varepsilon = .388$. From this, we take

$$(11) \quad \begin{cases} \varepsilon = .386 \text{ meson units} \\ \alpha = 1.8 \text{ inverse meson units} \end{cases}$$

(5) N. DALLAPORTA and F. FERRARI: *Nuovo Cimento*, **5**, 111 (1957).

(6) D. B. LICHTENBERG and M. ROSS: *Phys. Rev.*, **103**, 1131 (1956).

(7) J. L. GAMMEL and R. M. THALER: *Phys. Rev.*, **107**, 1337 (1957).

and using these values of α and ε , we get

$$(12) \quad \left\{ \begin{array}{l} \langle T \rangle = 58 \text{ MeV}, \\ \langle V_d \rangle = -14.2 \text{ MeV}, \\ \langle V(\Lambda N_1) \rangle + \langle V(\Lambda N_2) \rangle = -46 \text{ MeV}. \end{array} \right.$$

It is interesting to notice that the size of the parameter $\alpha = 1.8$ is larger than the deuteron parameter ($\beta = 1.4$). This may seem objectionable, since

it infers that the Λ -nucleon parts of the wave function are more concentrated at the origin than the deuteron part is, which appears to contradict the assumption that the Λ -particle is loosely bound. To explain this, we note that the true Λ -nucleon and deuteron parts of the wave function are themselves composed of two parts; one is in the region of the potential and the other is in the tail region. The latter is the part on which depends how loosely bound the particles are. The trial wave function given by equation (6) corresponds more to the part in the region of the potential since it is there that the parameters are determined. The value obtained for α thus reflects the fact that the

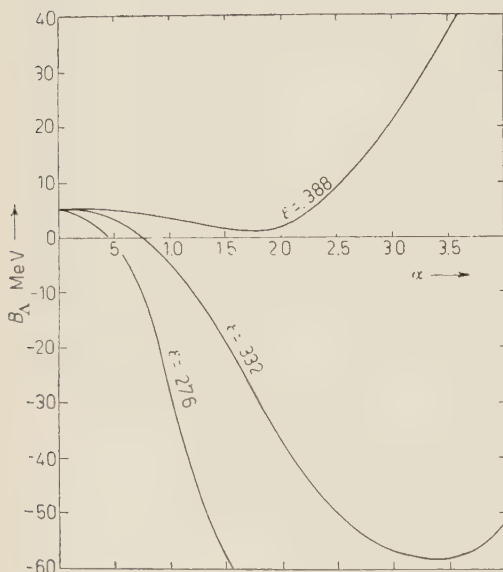


Fig. 3.

effective range of the Λ -nucleon potential is smaller than the nucleon-nucleon potential.

4. - It is of interest to examine the sensitivity of $\langle V(3\text{-body}) \rangle$ with D state admixture in the wave function. We rewrite the wave function for the hypertriton as

$$(13) \quad \psi = \cos \varphi \frac{\psi_s}{\sqrt{N_s}} + \sin \varphi \frac{\psi_d}{\sqrt{N_d}},$$

where ψ_s is given by equation (6), and N_s and N_d are normalization constants. ψ_d , the D state admixture is assumed to be

$$(14) \quad \psi_d = \chi_d \exp \left[-\frac{\alpha}{2}(x+y) - \frac{\beta \rho}{2} \right],$$

where

$$(15) \quad \chi_D = (x^2 S_{1\Lambda, x} + y^2 S_{2\Lambda, y}) \chi_s$$

and the percentage of D state is given by $100 \sin^2 \varphi$. The D state part of the spin wave function is chosen as shown since it is felt that the one spatially symmetric between the two nucleons will give the largest contribution to the binding energy.

We now calculate $\langle V(3\text{-body}) \rangle$ using this wave function obtaining

$$(16) \quad \langle V_{NB} \rangle = .108 \cos^2 \varphi + .119 \sin \varphi \cos \varphi - .106 \sin^2 \varphi \text{ MeV},$$

$$(17) \quad \langle V_{NB} + V_B \rangle = 2.00 \cos^2 \varphi - 3.09 \sin \varphi \cos \varphi - .719 \sin^2 \varphi \text{ MeV},$$

where V_{NB} and V_B are given by equations (2) and (3). Note that $\langle V_p \rangle = 0$ for this case,

$$\langle V_{NB} \rangle / \langle V(2\text{-body}) \rangle \quad (\text{no bare lines})$$

and

$$\langle V_{NB} + V_B \rangle / \langle V(2\text{-body}) \rangle \quad (\text{bare lines included})$$

are plotted against percent D state in Fig. 4. $\langle V(2\text{-body}) \rangle$ is taken to be -46 MeV (equation (12)) so that the ratios are valid for small φ . For the

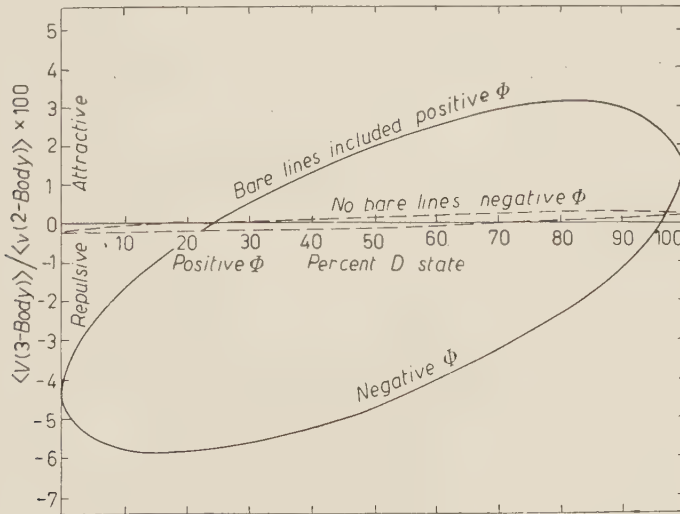


Fig. 4.

larger values of φ , the ratios only show the sensitivity of the three-body force with D state.

5. — The results of Section 4 (see Fig. 4) lead us to expect that three-body forces may be as large as 6% and repulsive when compared to the two body Λ -nucleon forces for the case of the hypertriton. In a heavy hypernucleus with one Λ -particle present, one expects that the three-body Λ -nuclear forces would be more important since the Λ -particle will not be governed by the Pauli principle and could be in the vicinity of a large number of nucleons. This might lead one to expect that the relative importance of three-body forces would be proportional to A with large A .

If we again look at the heavy hypernucleus problem from another point of view, we can see that three-body Λ -nuclear forces may not be important since the more singular non-central parts of the potential would tend to average out to zero coherently when the Λ -particle interacts with many pairs of neighboring nucleons. In other words, one would expect that the effect of correlations would be small.

The following consideration of the three-body problem follows in many respects the work reported by DRELL and HUANG⁽⁸⁾. We consider a large hypernucleus consisting of A nucleons and one Λ -particle contained in a volume v . We write the volume as

$$(18) \quad v = \frac{4\pi}{3} \left(\frac{\eta}{\mu} \right)^3 A,$$

where $\mu^{-1} = 1.42 \cdot 10^{-13}$ cm, which is a meson Compton wavelength, and η is a parameter which determines the nuclear density.

We then assume that the wave function for the A nucleons is given by the Slater determinant

$$(19) \quad \psi = \frac{1}{\sqrt{A!}} \begin{vmatrix} \varphi_1(1) & \dots & \varphi_1(A) \\ \vdots & \ddots & \vdots \\ \varphi_A(1) & \dots & \varphi_A(A) \end{vmatrix},$$

where $\varphi_i(j) = (1/\sqrt{v}) \exp[i\mathbf{k}_i \cdot \mathbf{r}_j] \chi_i(\sigma_j) \nu_i(\tau_j)$ which are all mutually orthogonal. $\chi_i(\sigma_j)$ and $\nu_i(\tau_j)$ are the spin and isotopic spin variables assigning the i -th spin and isotopic spin state to the j -th nucleon in the spatial state \mathbf{k}_i .

Since the Λ -particle is not governed by the Pauli principle here, we write the total wave function for the system as

$$(20) \quad \Phi = \psi \cdot \varphi(\Lambda),$$

where we put

$$(21) \quad \varphi(\Lambda) = \frac{1}{\sqrt{V}} \exp[i\mathbf{k}_\Lambda \cdot \mathbf{r}_\Lambda] \chi_\Lambda(\sigma_\Lambda).$$

⁽⁸⁾ S. D. DRELL and K. HUANG: *Phys. Rev.*, **91**, 1527 (1953).

For the Λ -nucleon two-body potential, we again use the one derived by DF. The expectation value is

$$(22) \quad \langle V(2\text{-body}) \rangle = \sum_{i=1}^A \int \Phi^* V_{DF}(iA) \Phi d\tau^{A+1}.$$

Notice that the $(\sigma_i \cdot \sigma_A)$ and tensor terms of V_{DF} vanish so that only the spin independent part need be evaluated. We therefore get

$$\langle V(2\text{-body}) \rangle = \frac{A(A-1)!}{A!} \sum_{i=1}^A \int \varphi_i^*(1) \psi^*(A) V_{DF}(1A) \varphi_i(1) \psi(A) d\tau_1 d\tau_A,$$

where the factor $1/A!$ comes from the normalization and $(A-1)!$ from the fact that every term in the sum contains $(A-1)!$ permutations of the remaining $A-1$ factors which integrate to unity.

Therefore, since

$$(23) \quad \left\{ \begin{aligned} \sum_{i=1}^A \varphi_i^*(1) \psi^*(A) \varphi_i(1) &= \frac{A}{v^2}, \\ \langle V(2\text{-body}) \rangle &= \frac{A}{v^2} \int V_{DF}(1A) d\tau_1 d\tau_A, \\ &= \frac{A}{v} \int V_{DF}(1A) d\tau. \end{aligned} \right.$$

In the calculation of the three-body expectation values, only the $(\sigma_1 \cdot \sigma_2)(\tau_1 \cdot \tau_2)$ term survives so that we get

$$(24) \quad \begin{aligned} \langle V(3\text{-body}) \rangle &= \sum_{\text{pairs}} \int \Phi^* V(ijA) (\tau_i \cdot \tau_j) (\sigma_i \cdot \sigma_j) \Phi d\tau^{A+1}, \\ &= \binom{A}{2} \frac{(A-2)!}{A!} \sum_{i,j=1}^A \int \varphi_i^*(1) \varphi_j^*(1) \psi^*(A) V(12A) (\tau_1 \cdot \tau_2) (\sigma_1 \cdot \sigma_2) \cdot \\ &\quad \cdot \psi(A) (\varphi_i(1) \varphi_j(2) - \varphi_j(1) \varphi_i(2)) d\tau_1 d\tau_2 d\tau_A. \end{aligned}$$

Since the three-body potentials do not contain the spin of the Λ -particle, we can put $|\psi(A)|^2 = 1/v$.

The spin-isotopic spin part is done as follows: It has been assumed that the system consists of $A/2$ protons and $A/2$ neutrons each having equal numbers of spin up and down. Therefore, $5/8$ of the nucleon pairs are antisymmetric and $3/8$ are symmetric in interchange of their spatial co-ordinates. The table below gives the values for $\langle (\sigma_1 \cdot \sigma_2)(\tau_1 \cdot \tau_2) \rangle$ for the various possibilities.

Space	Spin triplet	1	Spin singlet	9
antisymmetric	I-Spin triplet		I-Spin singlet	
Space	Spin triplet	-3	Spin Singlet	-3
symmetric	I-Spin singlet		I-Spin Triplet	

From this, equation (24) becomes

$$(25) \quad \langle V(3\text{-body}) \rangle = -\frac{9}{8v^3} \sum_{i,j=1}^A \int \exp[i(\mathbf{k}_i - \mathbf{k}_j) \cdot (\mathbf{r}_1 - \mathbf{r}_2)] V(12A) d\tau_1 d\tau_2 d\tau_A,$$

$$= -\frac{9}{8} \frac{A^2}{v^3} \int D^2(k_m r_{12}) V(12A) d\tau_1 d\tau_2 d\tau_3,$$

where

$$(26) \quad D^2(k_m r_{12}) = \left[\frac{3j_1(k_m r_{12})}{k_m r_{12}} \right]^2,$$

and $k_m = 1.52\mu/\eta$ or the largest momentum of the highest filled level for the free particle states in the nuclear well. Here, we use the same notation as DRELL and HUANG⁽⁸⁾.

From equations (23) and (25), $\langle V(3\text{-body}) \rangle / \langle V(2\text{-body}) \rangle$ can be evaluated. Using the three-body potential with no bare lines or V_{NB} (equation (2)), this ratio is

$$(27) \quad R_{NB} = \frac{A}{12v} \cdot \frac{\int_{y \geq \varepsilon} D^2(\lambda \varrho)(e^{-x/xy})(k_1(y) - y k_0(y)) d^3x d^3y}{\int_{x \geq \varepsilon} (e^{-x/x^3})[(4 + 4x + x^2)(k_1(x)/x) + (2 + 2x + x^2)k_0(x)] d^3x},$$

and the result, using the potential V_B (equation (3)), is

$$(28) \quad R_B = -\frac{\pi}{24} \cdot \frac{\mu}{A} \cdot \frac{A}{v} \cdot \frac{\int_{x,y \geq \varepsilon} D^2(\lambda \varrho)(e^{-x-y/xy}) d^3x d^3y}{\int_{x \geq \varepsilon} (e^{-x/x^3})[(4 + 4x + x^2)(k_1(x)/x) + (2 + 2x + x^2)k_0(x)] d^3x},$$

where we have changed to meson units in equations (27) and (28) and put $\lambda = k_m/\mu$. Since $|R_B|$ will be larger than R_{NB} , we evaluate R_B . The numerator of equation (28) becomes, apart from the factor $-(\pi/24)(\mu/A)(A/v)$,

$$\frac{9}{\lambda^2} \int_{x,y \geq \varepsilon} j_1^2(\lambda \varrho) \frac{e^{-x-y}}{\varrho^2 xy} d^3x d^3y = \frac{72\pi^2}{\lambda^2} \int_{\varepsilon}^{\infty} j_1^2(\lambda \varrho) \frac{e^{-\varrho}}{\varrho} (\varrho - 2\varepsilon) d\varrho,$$

This integral and the denominator of equation (28) were evaluated numerically for various values of η , using $\varepsilon = 0.386$ (equation (11)). The results are shown in the table below,

η	0.8	1.0	1.2
R_B	-0.0051	-0.0047	-0.0043

Since R_{NB} , which is given by equation (27), is of opposite sign, it will tend to reduce the ratio if included. However, the calculations in Section 4 (see equations (16) and (17)) show that R_{NB} will be much smaller than $|R_B|$.

It is interesting to notice here that the ratio R_B does not vary as A as one would expect it would, but rather increases in a complicated manner as the nuclear density increases. The reason for this can be clearly seen as follows: First consider the Λ -particle and a particular nucleon N_1 . The two-body potential will be described by $V(\Lambda N_1)$ and the three-body potential with these two baryons will be $\sum_{i=2}^A V(N_1 N_i)$. If we now assume that A and r are infinite, a measure of the relative importance of the three-body to the two-body potential is

$$(29) \quad R = \frac{\sum_{i=2}^{\infty} V(\Lambda N_i N_i)}{V(\Lambda N_1)},$$

which we see is finite since the range of the three-body force is finite. In other words, the numerator of equation (29) will only consist of a finite number of terms, the number of which will depend on the nuclear density and the range of the Λ -nucleon three-body potential.

The above table therefore shows that three-body forces are not likely to contribute more than about $\frac{1}{2}\%$ in heavy hypernuclei if the correlations are not present. From that table, a qualitative upper estimate of the size of three-body forces in heavy hypernuclei can be obtained if correlations are present to the extent that they are in the hypertriton. This can be done by estimating the values of η , corresponding to a heavy hypernucleus and the hypertriton, and then by obtaining values of R_B from the table for these values of η . The ratio of these values of R_B multiplied by 6%, which is an upper estimate of the relative importance of three-body forces in the hypertriton, gives then a qualitative estimate of the size of three-body forces in heavy hypernuclei if correlations are as strong as they are in the hypertriton.

For heavy nuclei and the deuteron, it is estimated that η is 0.94 and 1.48 respectively. We therefore get

$$R_B(\eta = 0.94) = -0.0048,$$

$$R_B(\eta = 1.48) = -0.0038.$$

From this, we conclude that with correlations in heavy hypernuclei, the relative importance of three body forces may be as large as $7\frac{1}{2}\%$ and repulsive.

6. — It must be admitted that there are many weak points in the foregoing derivations and subsequent calculations. To begin with, if the spins of Λ and Σ were not $\frac{1}{2}$ or if their relative parities were different, the form of the inter-

action hamiltonian would change. Also, if the K-meson plays the more important role in hypernuclear forces, we would expect that three-body forces would be about as important as they are in ordinary nuclei. Another question is the use of perturbation theory. Furthermore, approximations were made in the perturbation theory, the most important of which was the assumption that the baryon wave functions were δ -functions and neglecting the recoil. These assumptions will be in error for mesons of large momentum. On the other hand, disregarding the mass difference $\Delta = M_\Sigma - M_\Lambda$ in the energy denominators, introduced errors for mesons of small momentum. If we examine all of these items, it seems likely that the most critical factor is the form of the interaction hamiltonian, since once it has been chosen the qualitative form of the potentials is fixed.

The next item open to criticism is the method of determining the wave function for the hypertriton and core ε associated with the Λ -nucleon three-body potential. To begin with, the choice of the two-body potential V_{DF} may be criticized. Also the trial wave function (equation (6)) is not suitable for use with the phenomenological nucleon-nucleon potential since the deuteron part of the wave function does not vanish at the hard core. In addition, the value chosen for β may be poor.

To make the comparison of the two and three-body forces, one must have a two-body potential which has all of the desirable features; *i.e.* it should be more attractive in the singlet state. Further, since the core ε , associated with the three-body potential is desired, a two-body Λ -nucleon potential is required which is derived in a similar manner as the three-body potential; *i.e.* it also must have a core associated with it which, for consistency, we assume is equal to the core associated with the three-body potential. These considerations lead to the choice of V_{DF} .

As for the choice of the trial wave function, we see that since it does not vanish at the hard core, errors are introduced into the value of $\langle H \rangle$. It tends to make the kinetic energy term too small since the trial wave function is too smooth near the core. Again, since the trial wave function is finite and not zero at the core boundary, it tends to make the value of $|\langle V(N_1 N_2) \rangle|$ too large. Both of these errors which are in the same direction are estimated to make $\langle H \rangle$ too small by about 4.5 MeV. If we examine the graph in Fig. 3, it is seen that α would not be greatly changed since the minimum is quite shallow. ε , the Λ -nucleon core radius, will be reduced somewhat, approximately from 0.386 to 0.380 meson units.

From the foregoing remarks, it is of interest to estimate the changes in $V(3\text{-body})$ with small variations in the quantities α , β and ε . By writing $E_\Lambda(\alpha, \beta, \varepsilon) = \langle V(3\text{-body}) \rangle$, we have for small variations in the parameters

$$(30) \quad E_\Lambda(\alpha, \beta, \varepsilon) = E_\Lambda(\alpha_0, \beta_0, \varepsilon_0) + \frac{\partial E_\Lambda}{\partial \alpha} \delta\alpha + \frac{\partial E_\Lambda}{\partial \beta} \delta\beta + \frac{\partial E_\Lambda}{\partial \varepsilon} \delta\varepsilon,$$

where α_0 , β_0 and ε_0 equal 1.8, 1.4 and 0.386 and the derivatives are evaluated at these values of the parameters. If we consider only the S state trial wave function (equation (6)) and the three-body potential V_{NB} (equation (2)), the result is

$$(31) \quad E_{\Lambda NB} = 0.108 + 0.205\delta\alpha + 0.096\delta\beta - 0.977\delta\varepsilon \text{ MeV}$$

and when bare line graphs are included (equations (2) and (3)), we get

$$(32) \quad E_{\Lambda B} + E_{\Lambda NB} = 2.00 + 3.61\delta\alpha + 2.49\delta\beta - 8.46\delta\varepsilon \text{ MeV}.$$

The variations expected in the parameters are small. For example, a better value for ε may be 0.38 and perhaps β should be nearer 1.52 say. If α remains unchanged, we see from equation (32) that the three-body expectation value would go from 2 to 2.35 MeV which is a change of 17%. It is further expected that the two-body expectation value would also vary so that the ratio $\langle V(3\text{-body}) \rangle / \langle V(2\text{-body}) \rangle$ would not be greatly affected.

In Section 5, three-body forces are considered in heavy hypernuclei. An obvious assumption made there is that only one Λ -particle is present and effects due to the heavier Σ -particle are ignored. The Σ -particle probably plays an important role in heavy hypernuclei because the binding energies involved become more comparable to $\Delta = M_\Sigma - M_\Lambda$. However, since a complete calculation of that nature was not within the scope of this work, a qualitative estimate of the importance of three-body forces was made considering only one Λ -particle in a large nucleus.

We may summarize the conclusions as follows:

a) Since the Λ -nucleon potential can be obtained by a consideration of a double pion exchange, one would expect that the two and three-body Λ -nucleon potentials, which have the same order of coupling constant, would have comparable magnitudes. It is found, however, that the three-body potential is much smaller than the two-body potential due to its weak singularity.

b) The largest terms in the Λ -nucleon three-body potential are non-central whereas the central part is small.

c) For the hypertriton, where correlations are expected to be large, three-body forces are repulsive for S states and have a relative importance of about 4%. Suitable D state admixtures could make them further repulsive and perhaps large as 6%.

d) In heavy hypernuclei, two factors play an important part in determining the magnitude of three-body Λ -nucleon forces. The first factor is the increased nuclear density which enhances the effect of the three-body force

and the second factor is the reduced amount of correlations in the nucleus. The latter effect is the more important since the most singular parts of the Λ -nucleon three-body potential are non-central. It is expected that with no correlations, the relative importance of three-body to two-body Λ -nucleon forces is only about $\frac{1}{2}\%$. With correlations as strong as in the hypertriton, it may be as large as $7\frac{1}{2}\%$. In either case the contribution is repulsive.

e) If the three-body potential can only be represented by graphs with no bare lines, then the relative importance of three to two-body forces in hypernuclei is less than $\frac{1}{2}\%$ even with correlations present.

* * *

The author wishes to thank Dr. R. T. SHARP for suggesting this problem and rendering valuable assistance in the preliminary stages thereof. Special thanks are due to Dr. E. L. LOMON who, in Dr. SHARP's absence, directed the major part of the work. Finally, financial assistance in the form of Studentships for the years 1956-57 and 1957-58, given by the Canadian National Research Council, is gratefully acknowledged.

RIASSUNTO

Si studia l'importanza relativa che hanno le forze tra due e tre corpi nel potenziale Λ -nucleone. Il potenziale proveniente dalle forze tra tre corpi, è ottenuto con un calcolo perturbativo con interazione pseudoscalare all'ordine più basso. Si trova che esso è poco singolare e quindi assai più debole di quello generato dalle forze tra due corpi. Nell'ipertritio, dove le correlazioni sono forti, si trova che le forze tra tre corpi sono repulsive per stati S e possono dare fino il 4% del totale delle forze; una conveniente introduzione di stato D può portare a forze repulsive del 6%. Negli ipernuclei pesanti, l'importanza relativa delle forze tra tre corpi è di circa $\frac{1}{2}\%$ se si trascurano le correlazioni e può giungere fino a 7.5% se le correlazioni sono forti come nell'ipertritio. Si trova anche che le forze tra tre corpi sono trascurabili e si omettono i grafici di Feynman che contengono stati intermedi senza mesoni π .

On the Renormalization of a Parity Non-Conserving Interaction.

K. SEKINE

Department of Physics, University of Tokyo - Tokyo

(ricevuto il 10 Novembre 1958)

Summary. — An exact formulation is given of the renormalization method in a parity non-conserving theory. Equations determining the renormalization constants are obtained and, among other things, the internal consistency of the theory is examined.

Introduction.

Although the parity non-conservation is well established experimentally ⁽¹⁾, it does not seem that its theoretical implications have been fully exhausted.

As is well known, the present quantum theory of fields is based on certain general assumptions such as Lorentz invariance, the existence of the energy-momentum four vector, asymptotic conditions, and so on. So far the invariance of the theory under space inversion has been one of them. However, now that the parity non-conservation is established experimentally, the invariance mentioned must be ruled out from the number of fundamental postulates of quantum field theory.

In this way, a problem is to be put forward to reformulate the theory without assuming its invariance under space inversion. This problem was partly taken up by SOLOVIEV, GUPTA and ISO ⁽²⁾, who have attempted to classify inter-

⁽¹⁾ T. D. LEE and C. N. YANG: *Phys. Rev.*, **104**, 254 (1957); C. S. WU *et al.*: *Phys. Rev.*, **105**, 1413 (1957); **106**, 1361 (1957); R. L. GARWIN, L. M. LEDERMAN and M. WEINRICH: *Phys. Rev.*, **105**, 1415 (1957); J. I. FRIEDMAN and V. L. TELEGI: *Phys. Rev.*, **105**, 1681 (1957); F. S. CRAWFORD, M. CRESTI, M. L. GOOD, K. GOTTSTEIN, E. M. LYMAN, F. T. SOLMITZ, M. L. STEVENSON and H. K. TICO: *Phys. Rev.*, **108**, 1102 (1957); F. EISLER, R. PLANO, A. PRODELL, N. SAMIOS, M. SCHWARTZ, J. STEINBERGER, P. BASSI, V. BORELLI, G. PUPPI, G. TANAKA, P. WALOSCHEK, V. ZOBOLI, M. CONVERSI, P. FRANZINI, I. MANNELLI, R. SANTANGELO and V. SILVESTRINI: *Phys. Rev.*, **108**, 1353 (1957); and other papers.

⁽²⁾ V. G. SOLOVIEV: *Žu. Ėksp. Teor. Fiz.*, **33**, 537, 796 (1957); *Nucl. Phys.*, **6**, 618 (1958); S. N. GUPTA: *Can. Journ. Phys.*, **35**, 1309 (1957); C. ISO: *Progr. Theor. Phys.*, **20**, 410 (1958).

actions assuming only the CP invariance of the theory. These authors, however, have not made a penetrating analysis of the mathematical structure of quantum field theory.

A question seems to be open as to whether the usual theory can still remain as a consistent formalism when we have taken away the requirement of its invariance under space inversion. Especially, it will be of great interest to investigate how the renormalization is carried through for parity non-conserving interactions in the framework of the conventional S -matrix theory.

D'ESPAGNAT and PRENTKI⁽³⁾ have first investigated the problem of renormalizing parity non-conserving theories. These authors carried out the renormalization of a CP invariant theory according to Dyson's method⁽⁴⁾, and concluded that the theory is renormalizable in the sense of removing divergencies. They also have pointed out that the ways of renormalization are not unique. However, the equations determining the renormalization constants have not been given explicitly, nor examined the question as to whether the equations permit a consistent solution.

It is the aim of this paper to investigate systematically the above mentioned problems which seem to be of great importance from the point of view of principles.

In the first section we start with an unrenormalized Lagrangian which contains a parity non-conserving interaction. Without the use of power series expansion, we try to obtain the equations defining renormalization constants and find that the result is given without any ambiguities. In terms of these constants, we can formally carry out the renormalization according to KÄLLÉN⁽⁵⁾. In Section 2 the Lagrangian will be rewritten using only renormalized quantities. Formulae are given which express the renormalization constants in terms of Lehmann's spectral functions⁽⁶⁾.

Finally, the problem is solved explicitly in the lowest order approximation of perturbation theory and it will be shown that the above obtained equations permit a consistent solution only when the theory is parity conserving.

1. – Equations for the renormalization constants.

Let us consider a system with three kinds of particles which we call nucleons, hyperons and mesons. To each kind of particles corresponds a field which

⁽³⁾ B. D'ESPAGNAT and J. PRENTKI: *Nuovo Cimento*, **6**, 2989 (1957).

⁽⁴⁾ F. J. DYSON: *Phys. Rev.*, **75**, 1736 (1948); A. SALAM: *Phys. Rev.*, **79**, 910 (1950); J. C. WARD: *Phys. Rev.*, **84**, 897 (1951); P. T. MATTHEWS and A. SALAM: *Phys. Rev.*, **94**, 185 (1954); and other papers.

⁽⁵⁾ G. KÄLLÉN: *Helv. Phys. Acta*, **25**, 417 (1952); *Physica*, **19**, 850 (1953).

⁽⁶⁾ H. LEHMANN: *Nuovo Cimento*, **11**, 342 (1954).

will be denoted by ψ , χ and φ , respectively. We assume the system to be described by the following unrenormalized Lagrangian:

$$(1.1) \quad \mathcal{L} = \mathcal{L}_0 + \mathcal{L}_1,$$

$$(1.2) \quad \mathcal{L}_0 = -\bar{\psi}(x)(\gamma\partial + m_1)\psi(x) + \delta m_1 \bar{\psi}(x)\psi(x) - \bar{\chi}(x)(\gamma\partial + m_2)\chi(x) + \\ + \delta m_2 \bar{\chi}(x)\chi(x) + \varphi^*(x)(\square - \mu^2)\varphi(x) + \delta\mu^2 \varphi^*(x)\varphi(x),$$

$$(1.3) \quad \mathcal{L}_1 = -g[\bar{\psi}(x)(\alpha + \beta\gamma_5)\chi(x)\varphi^*(x) + \text{h. c.}].$$

From the above Lagrangian we obtain the following equations of motion for the field operators in the Heisenberg representation

$$(1.4) \quad \begin{cases} (\gamma\partial + m_1)\psi(x) = g(\alpha + \beta\gamma_5)\chi(x)\varphi^*(x) + \delta m_1\psi(x) \equiv f(x), \\ (\gamma\partial + m_2)\chi(x) = g(\alpha^* - \beta^*\gamma_5)\psi(x)\varphi(x) + \delta m_2\chi(x) \equiv g(x). \end{cases}$$

The condition of reproducing the right and left asymmetry:

$$(1.5) \quad \text{Re}(\alpha^*\beta) \neq 0,$$

is to be fulfilled. For reasons of simplicity, however, we shall discuss exclusively a special case of CP invariance, that is, both α and β are assumed to be real in what follows. Furthermore, to avoid inessential complications, we put $m_1 = m_2$. It is easy to introduce the mass difference into the formalism if required.

We now solve the equation (1.4) in view of the following asymptotic conditions:

$$(1.6) \quad \begin{cases} \lim_{x_0 \rightarrow -\infty} \psi(x) = \psi^{(0)}(x), \\ \lim_{x_0 \rightarrow -\infty} \chi(x) = \chi^{(0)}(x). \end{cases}$$

The incoming fields are to satisfy the free field equations

$$(1.7) \quad \begin{cases} (\gamma\partial + m)\psi^{(0)}(x) = 0, \\ (\gamma\partial + m)\chi^{(0)}(x) = 0, \end{cases}$$

and the covariant commutation relations

$$(1.8) \quad \begin{cases} \{\psi^{(0)}(x), \bar{\psi}^{(0)}(x')\} = -iS(x - x') \\ \{\chi^{(0)}(x), \bar{\chi}^{(0)}(x')\} = -iS(x - x'). \end{cases}$$

On the other hand, as for the operators ψ and χ of interacting fields, it can be deduced from the Lagrangian that the anticommutators for equal times have the following form:

$$(1.9) \quad \begin{cases} \{\psi(x), \bar{\psi}(x')\}_{x_0=x'_0} = \gamma_4 \delta(\mathbf{x} - \mathbf{x}') , \\ \{\chi(x), \bar{\chi}(x')\}_{x_0=x'_0} = \gamma_4 \delta(\mathbf{x} - \mathbf{x}') . \end{cases}$$

It is well known that by virtue of the equations (1.7) and (1.8) it becomes possible to define the « particle number ». We consider the complete set of state vectors $|z\rangle$ as eigenstates of the number of incoming particles. Finally we assume the existence of the energy-momentum four vector P_μ which has the property

$$(1.10) \quad [P_\mu, F(x)] = i \partial_\mu F(x)$$

and of the vacuum $|0\rangle$ characterized by the lowest eigenstate of P_0 .

Under the above assumptions we can prove the general formula

$$(1.11) \quad \langle 0 | F(x) | q \rangle = \\ = i \int_{-\infty}^{\infty} \theta(x - x') \langle 0 | \{F(x), \bar{f}(x')\} | 0 \rangle dx' \langle 0 | \psi^{(0)}(x') | q \rangle + \langle 0 | \frac{\partial F(x)}{\partial \psi(x)} | 0 \rangle \langle 0 | \psi^{(0)}(x) | q \rangle ,$$

where $F(x)$ is an arbitrary operator and $|q\rangle$ denotes a state with one particle with energy-momentum vector q . We shall not describe here the proof explicitly, which is quite similar to that in parity conserving theories (⁷).

Putting $F(x) = \psi(x)$ in (1.11) gives

$$(1.12) \quad \langle 0 | \psi(x) | q \rangle = \\ = i \int_{-\infty}^{\infty} \theta(x - x') \langle 0 | \{\psi(x), \bar{f}(x')\} | 0 \rangle dx' \langle 0 | \psi^{(0)}(x') | q \rangle + \langle 0 | \psi^{(0)}(x) | q \rangle ,$$

where $\theta(x - x') \langle 0 | \{\psi(x), \bar{f}(x')\} | 0 \rangle$ can be expanded as

$$(1.13) \quad \theta(x - x') \langle 0 | \{\psi(x), \bar{f}(x')\} | 0 \rangle = \\ = \int_{-\infty}^{\infty} dp \exp[ip(x - x')] [A(p) + i\gamma_\mu p_\mu B(p) + i\gamma_5 \gamma_\mu p_\mu B'(p)] .$$

(⁷) G. KÄLLÉN: *Handb. d. Phys.*, **5**, 169 (1958).

Clearly the last term results from the violation of the invariance under space inversion. The absence of the term $A'\gamma_5$ is due to the CP invariance.

Substituting (1.13) into (1.12) leads to

$$(1.14) \quad \langle 0 | \psi(x) | q \rangle = (N + N'\gamma_5) \langle 0 | \psi^{(0)}(x) | q \rangle,$$

where N and N' are the constants defined by

$$N = 1 + A - mB,$$

$$N' = -mB'.$$

The fact that $A(q)$, etc., are universal constants independent of x and q , is easily verified in a way similar to that in parity conserving cases.

Similarly, for the hyperon field,

$$(1.14a) \quad \langle 0 | \chi(x) | q \rangle = (N - N'\gamma_5) \langle 0 | \chi^{(0)}(x) | q \rangle.$$

It should be remarked that the reality of the constants N and N' are verified by virtue of the CP invariance.

Next we put $F(x) = f(x)$ in (1.11). Considering the equation

$$\begin{aligned} \langle 0 | f(x) | q \rangle &= (\gamma \partial + m) \langle 0 | \psi(x) | q \rangle, \\ &= 2mN'\gamma_5 \langle 0 | \psi^{(0)}(x) | q \rangle, \end{aligned}$$

we obtain

$$\begin{aligned} (1.15) \quad \delta m_1 \langle 0 | \psi^{(0)}(x) | q \rangle &= \\ &= -i \int_{-\infty}^{\infty} \theta(x-x') \langle 0 | \{f(x), \bar{f}(x')\} | 0 \rangle dx' \langle 0 | \psi^{(0)}(x') | q \rangle + 2mN'\gamma_5 \langle 0 | \psi^{(0)}(x) | q \rangle, \end{aligned}$$

where the expansion analogous to (1.13) is possible:

$$\begin{aligned} (1.16) \quad \langle 0 | \{f(x), \bar{f}(x')\} | 0 \rangle &= \\ &= \frac{-1}{(2\pi)^3} \int dp \exp[ip(x-x')] \varepsilon(p) [\Sigma_1(p^2) + (i\gamma p + m)\Sigma_2(p^2) + i\gamma_5(\gamma p)\Sigma_3(p^2)]. \end{aligned}$$

It can be proved that the expansion coefficients are all real. Substituting (1.16) into (1.15) and performing the x integration, we have

$$(1.17) \quad \delta m_1 = \bar{\Sigma}_1(-m^2) + \gamma_5 m [2N' - \bar{\Sigma}_1(-m^2)],$$

with

$$\bar{\Sigma}_i(-m^2) = P \int_0^\infty \frac{\Sigma_i(-a)}{a - m^2} da.$$

Similarly

$$(1.17a) \quad \delta m_2 = \bar{\Sigma}_1(-m^2) - \gamma_5 m [2N' - \bar{\Sigma}_3(-m^2)].$$

The above equations implicitly define the mass renormalization.

To obtain the definitions for the constants N and N' , we utilize the fact that the anticommutator for equal times is one and the same for the free field and for the interacting field.

Integrating the fundamental equation (1.4) in view of the initial condition (1.6) follows

$$\psi(x) = \psi^{(0)}(x) - \int S_R(x - x') f(x') dx',$$

and

$$\bar{\psi}(x) = \bar{\psi}^{(0)}(x) - \int \bar{f}(x') S_A(x' - x) dx'.$$

In terms of this, the anticommutator can be brought into the form

$$\begin{aligned} \{\psi(x), \bar{\psi}(x')\} &= \{\psi^{(0)}(x), \bar{\psi}^{(0)}(x')\} + \{\psi^{(0)}(x), \bar{\psi}(x') - \bar{\psi}^{(0)}(x')\} + \\ &+ \{\psi(x) - \psi^{(0)}(x), \bar{\psi}^{(0)}(x')\} + \int S_R(x - x'') \{f(x''), \bar{f}(x''')\} S_A(x''' - x') dx'' dx'''. \end{aligned}$$

We now put $x_0 = x'_0$, and take the vacuum expectation values of both sides. Considering the definition of a matrix product and Eq. (1.14), we obtain

$$\begin{aligned} \gamma_4 \delta(\mathbf{x} - \mathbf{x}') &= (2N - 1) \gamma_4 \delta(\mathbf{x} - \mathbf{x}') + [\bar{\Sigma}_2(-m^2) + 2m \bar{\Sigma}'_1(-m^2)] \gamma_4 \delta(\mathbf{x} - \mathbf{x}') + \\ &+ m[2N' - \bar{\Sigma}_3(-m^2)] \gamma_5 \gamma_4 \delta(\mathbf{x} - \mathbf{x}') \end{aligned}$$

and hence

$$(1.18) \quad N = 1 - \frac{1}{2} [\bar{\Sigma}_2(-m^2) + 2m \bar{\Sigma}'_1(-m^2)],$$

$$(1.19) \quad N' = \frac{1}{2} \bar{\Sigma}_3(-m^2),$$

where

$$\bar{\Sigma}'_1(-m^2) = - \int_0^\infty da \frac{\Sigma_1(-a)}{(a - m^2)^2}.$$

These equations define N and N' respectively. Using the result (1.19), Eqs. (1.17) and (1.17a) can be reduced to a simpler expression

$$(1.20) \quad \delta m_i = \bar{\Sigma}_1(-m^2) \quad i = 1, 2,$$

from which we can see that the mass correction δm is a real c -number not involving γ_5 . It is remarked that the equality of the constants for the nucleon and for the hyperon is merely a consequence of the assumption $m_1 = m_2$.

Thus, the equations which determine the renormalization constants are given without any ambiguities. The equations for N and δm are exactly the same if the parity non-conserving terms were absent. On the other hand, the third renormalization constant introduced on account of the parity non-conservation, is uniquely determined from the requirement that the anticommutators for equal times of the interacting field operators are to be identical with those for the free field, that is to say, they cannot contain any γ_5 terms. This requirement is necessary, as KÄLLÉN has emphasized (⁷), for being able to define consistently the «particle number» at arbitrary time. It is of interest that this very condition assures of obtaining δm as a c -number.

Before closing this section, it should be mentioned that, without solving explicitly, we cannot be sure of the internal consistency of the above obtained equations.

2. - Renormalized field equations and commutation relations.

Once the renormalization constants have been determined, the renormalization can be performed very simply. We construct the renormalized field operators

$$(2.1) \quad \begin{cases} \psi'(x) = (N + N'\gamma_5)^{-1}\psi(x), \\ \chi'(x) = (N - N'\gamma_5)^{-1}\chi(x), \end{cases}$$

which, as is easily seen, fulfil the renormalization conditions of KÄLLÉN (^{5,7})

$$(2.2) \quad \begin{cases} \langle 0 | \psi'(x) q | \rangle = \langle 0 | \psi^{(0)}(x) | q \rangle, \\ \langle 0 | \chi'(x) | q \rangle = \langle 0 | \chi^{(0)}(x) | q \rangle. \end{cases}$$

Here, it is to be remarked that

$$(2.3) \quad N^2 - N'^2 \neq 0$$

is necessary for the existence of the inverse operators in (2.1), which can be

explicitly given by

$$(2.4) \quad (N \pm N'\gamma_5)^{-1} = \frac{N \mp N'\gamma_5}{N^2 - N'^2}.$$

If we introduce new notations:

$$(2.5) \quad Z_2 = N^2 - N'^2,$$

$$(2.6) \quad a = NZ^{-\frac{1}{2}}, \quad b = N'Z^{-\frac{1}{2}},$$

then the expression (2.1) is brought into the form

$$(2.7) \quad \begin{cases} \psi'(x) = Z_2^{-\frac{1}{2}}(a + b\gamma_5)\psi(x), \\ \chi'(x) = Z_2^{-\frac{1}{2}}(a - b\gamma_5)\chi(x). \end{cases}$$

Let us now rewrite the original Lagrangian (1.1-3) in terms of the renormalized field operators. Then, the following expressions are obtained

$$(2.8) \quad \mathcal{L} = \mathcal{L}'_0 + \mathcal{L}'_1,$$

$$(2.9) \quad \begin{aligned} \mathcal{L}'_0 = & -Z_2\bar{\psi}'(a + b\gamma_5)(\gamma\partial + m)(a - b\gamma_5)\psi' - \\ & -Z_2\bar{\chi}'(a - b\gamma_5)(\gamma\partial + m)(a + b\gamma_5)\chi' + Z_3\varphi^{*'}(\square - \mu^2)\varphi', \end{aligned}$$

$$(2.10) \quad \mathcal{L}'_1 = Z_2\delta m[\bar{\psi}'\psi' + \bar{\chi}'\chi'] - gZ_2Z_3^{\frac{1}{2}}[\bar{\psi}'(\alpha' + \beta'\gamma_5)\chi'\varphi^{*'} + \text{h. c.}],$$

where

$$(2.11) \quad \begin{cases} \alpha' = (a^2 + b^2)\alpha + 2ab\beta, \\ \beta' = 2ab\alpha + (a^2 + b^2)\beta. \end{cases}$$

We have used, in the above, the well known expression for the renormalized meson operator:

$$(2.12) \quad \varphi'(x) = Z_3^{-\frac{1}{2}}\varphi(x).$$

The definitions for the constants Z_3 and $\delta\mu$ will not be described here, since they are exactly the same as those in the usual theories.

Putting

$$(2.13) \quad g' = Z_1^{-1}Z_2Z_3^{\frac{1}{2}}g,$$

leads to the coupling constant renormalization

$$(2.14) \quad \begin{cases} g\alpha \rightarrow Z_1 g' \alpha' , \\ g\beta \rightarrow Z_1 g' \beta' . \end{cases}$$

It is to be noted that, considering a and b are real, the transformation (2.11) is unimodular but not unitary.

In what follows we drop the dash on the renormalized operator, since the corresponding unrenormalized operator will not be used again.

The Lagrangian (2.8-10) follows the equations of motion for the renormalized fields

$$(2.15) \quad \begin{cases} (a + b\gamma_5)(\gamma\partial + m)(a - b\gamma_5)\psi = \delta m\psi - Z_1 g(\alpha + \beta\gamma_5)\chi\varphi^* , \\ (a - b\gamma_5)(\gamma\partial + m)(a + b\gamma_5)\chi = \delta m\chi - Z_1 g(\alpha - \beta\gamma_5)\psi\varphi , \end{cases}$$

and the anticommutators for equal times

$$(2.16) \quad \begin{cases} \{\psi(x), \bar{\psi}(x')\}_{x_0=x'_0} = Z_2^{-1}(a + b\gamma_5)\gamma_4(a - b\gamma_5)\delta(\mathbf{x} - \mathbf{x}') , \\ \{\chi(x), \bar{\chi}(x')\}_{x_0=x'_0} = Z_2^{-1}(a - b\gamma_5)\gamma_4(a + b\gamma_5)\delta(\mathbf{x} - \mathbf{x}') . \end{cases}$$

If we now put

$$(2.17) \quad \gamma_\mu^{(\pm)} = (a \pm b\gamma_5)\gamma_\mu(a \mp b\gamma_5) ,$$

it can be verified that the $\gamma_\mu^{(\pm)}$ satisfy Dirac's relations as well as γ_μ :

$$(2.18) \quad \gamma_\mu^{(\pm)}\gamma_\nu^{(\pm)} + \gamma_\nu^{(\pm)}\gamma_\mu^{(\pm)} = 2\delta_{\mu\nu}$$

and

$$(2.19) \quad \gamma_5^{(+)} = \gamma_5^{(-)} = \gamma_5 .$$

With the use of these expressions, (2.15) and (2.16) can be rewritten as

$$(2.15a) \quad \begin{cases} (\gamma^{(+)}\partial + m)\psi = \delta m\psi - Z_1 g(\alpha + \beta\gamma_5)\chi\varphi^* , \\ (\gamma^{(-)}\partial + m)\chi = \delta m\chi - Z_1 g(\alpha - \beta\gamma_5)\psi\varphi , \end{cases}$$

$$(2.16a) \quad \begin{cases} \{\psi(x), \bar{\psi}(x')\}_{x_0=x'_0} = Z_2^{-1}\gamma_4^{(+)}\delta(\mathbf{x} - \mathbf{x}') , \\ \{\chi(x), \bar{\chi}(x')\}_{x_0=x'_0} = Z_2^{-1}\gamma_4^{(-)}\delta(\mathbf{x} - \mathbf{x}') . \end{cases}$$

From the above, we can conclude as follows:

In the renormalization of a system where parity non-conserving interactions are present, i) there appears a certain difference in the γ -representation between the physical and the bare particles, apart from the mass and the coupling constant renormalizations carried out in the conventional way. ii) As far as the γ -representation is taken to be equal for the two kinds of bare particles, then occurs a definite relative difference in the γ -representation between the physical nucleons and the physical hyperons (*). iii) These differences in the representation is non-unitary because of the reality of a and b , and hence it is impossible to give γ_μ , $\gamma_\mu^{(+)}$ and $\gamma_\mu^{(-)}$ unitary representations at the same time.

The renormalized propagator is now given by

$$(2.20) \quad \langle 0 | T\psi(x)\bar{\psi}(x') | 0 \rangle = -\frac{1}{2}S'_F(x - x').$$

According to LEHMANN⁽⁶⁾, we introduce the spectral representation

$$(2.21) \quad S'_F(p) = -2i \int_0^\infty d\kappa^2 \frac{i\gamma^{(+)}p\varrho_1(\kappa^2) + \varrho_2(\kappa^2) + i\gamma_5\gamma^{(+)}p\varrho_3(\kappa^2)}{p^2 + \kappa^2 - i\varepsilon},$$

from which we get the expression

$$(2.22) \quad \langle 0 | \{\psi(x), \bar{\psi}(x')\} | 0 \rangle_{x_0=x'_0} = \left[\int \varrho_1(\kappa^2) d\kappa^2 + \gamma_5 \int \varrho_3(\kappa^2) d\kappa^2 \right] \gamma_4^{(+)} \delta(\mathbf{x} - \mathbf{x}'),$$

for the anticommutator for equal times. Comparing this with (2.16a) leads to

$$(2.23) \quad Z_2^{-1} = \int_0^\infty \varrho_1(\kappa^2) d\kappa^2,$$

and

$$(2.24) \quad 0 = \int_0^\infty \varrho_3(\kappa^2) d\kappa^2.$$

An inequality

$$(2.25) \quad 0 \leq Z_2 \leq 1,$$

(*) On the contrary, to obtain the equal representation for the two kinds of *physical* particles, it is necessary to take certain shifted representations in the corresponding unrenormalized quantities. This means, however, that the *free* part of the unrenormalized Lagrangian also violates parity.

can also be proved in a way similar to that in parity conserving theories. Here, $N^2 > N'^2$ has been assumed. The alternative case $N^2 < N'^2$ must be excluded because the negative sign appears on the right hand side of the anti-commutator. This is a situation similar to the ghost in Lee's model ⁽⁸⁾.

The mass renormalization is given by

$$(2.26) \quad \delta m = Z_2 \int_0^\infty [m \varrho_1(\kappa^2) + \varrho_2(\kappa^2)] d\kappa^2.$$

And it is to be noted that here use has been made of the condition (2.24).

3. - Perturbation theory in the lowest order approximation.

So far we have discussed the problem without the use of expansions in the coupling constant. In this section, we shall solve it explicitly in the lowest order approximation of perturbation theory to see in more detail the properties of the renormalized field.

Now, in the equation

$$(3.1) \quad (\gamma^{(+)} \partial + m)(\gamma^{(+)\tau} \partial' - m) \langle 0 | \psi(x) \bar{\psi}(x') | 0 \rangle = \\ = g^2 (\alpha + \beta \gamma_5) \langle 0 | \chi^{(0)}(x) \bar{\chi}^{(0)}(x') | 0 \rangle (\alpha - \beta \gamma_5) \langle 0 | \varphi^{(0)*}(x) \varphi^{(0)}(x') | 0 \rangle,$$

we expand

$$(3.2) \quad \langle 0 | \psi(x) \bar{\psi}(x') | 0 \rangle = \\ = \int d^4 k \theta(k_0) \int d\kappa^2 [i \gamma^{(+)} k \varrho_1(\kappa^2) + \varrho_2(\kappa^2) + i \gamma_5 \gamma^{(+)} k \varrho_3(\kappa^2)] \delta[k^2 + \kappa^2],$$

$$(3.3) \quad \langle 0 | \chi^{(0)}(x) \bar{\chi}^{(0)}(x') | 0 \rangle = \int d^4 q \theta(q_0) (i \gamma^{(-)} q - m) \delta[q^2 + m^2].$$

Hence, the Fourier transform of (3.1) is

$$(3.4) \quad \theta(k_0) (i \gamma^{(+)} k + m) (i \gamma^{(+)} k \varrho_1 + \varrho_2 + i \gamma_5 \gamma^{(+)} k \varrho_3) (i \gamma^{(+)} k + m) = \\ = - \frac{g^2}{(2\pi)^3} \int d^4 q \theta(k_0 - q_0) \theta(q_0) \delta[q^2 + m^2] \delta[(k - q)^2 + \mu^2] \cdot \\ \cdot (\alpha + \beta \gamma_5) (i \gamma^{(-)} q - m) (\alpha - \beta \gamma_5).$$

⁽⁸⁾ T. D. LEE: *Phys. Rev.*, **95**, 1329 (1954); G. KÄLLÉN and W. PAULI: *Dan. Mat. Fys. Medd.*, **30** no. 7 (1955).

We multiply this first by unity, by $i\gamma^{(-)}k$ from the right, and then by γ_5 from the left. Taking trace in each step gives respectively

$$(3.5) \quad \begin{cases} 2m\kappa^2 \varrho_1 + (m^2 + \kappa^2) \varrho_2 = -m(\alpha^2 - \beta^2)I, \\ (m^2 + \kappa^2)A \varrho_1 + 2mA \varrho_2 + (m^2 - \kappa^2)B \varrho_3 = (\alpha^2 + \beta^2)J, \\ (m^2 + \kappa^2)B \varrho_1 + 2mB \varrho_2 + (m^2 - \kappa^2)A \varrho_3 = 2\alpha\beta J, \end{cases}$$

where

$$(3.6) \quad \begin{aligned} I &= -\frac{g^2}{(2\pi)^3} \int d^4q \theta(k_0 - q_0) \theta(q_0) \delta[q^2 + m^2] \delta[(k - q)^2 + \mu^2] = \\ &= \frac{g^2}{16\pi^2} \frac{\sqrt{(\kappa^2 - m^2 - \mu^2)^2 - 4\mu^2 m^2}}{\kappa^2}, \\ J &= -\frac{g^2}{(2\pi)^3} \int d^4q \theta(k_0 - q_0) \theta(q_0) (k \cdot q) \delta[q^2 + m^2] \delta[(k - q)^2 + \mu^2] = \\ &= \frac{1}{2} (\mu^2 - m^2 - \kappa^2) I, \end{aligned}$$

and in addition the following abbreviation is used

$$(3.7) \quad \begin{cases} A = (a^2 + b^2)^2 + (2ab)^2, \\ B = 2(2ab)(a^2 + b^2). \end{cases}$$

Solving the simultaneous equations (3.5), we have

$$(3.8) \quad \varrho_3(\kappa^2) = \frac{1}{m^2 - \kappa^2} J(\kappa^2) [2\alpha\beta A - (\alpha^2 + \beta^2)B].$$

In order to satisfy the condition (2.24), it must be

$$(3.9) \quad 2\alpha\beta A = (\alpha^2 + \beta^2)B,$$

i.e.

$$(3.10) \quad \alpha = a^2 + b^2, \quad \beta = 2ab.$$

By using this, the other spectral functions $\varrho_1(\kappa^2)$ and $\varrho_2(\kappa^2)$ are completely determined, from which the renormalization constants Z_2 and δm can be calculated with the aid of the formulae (2.23) and (2.26). The explicit expression for them will not be given here.

The point to be remarked is rather the very relation (3.10). This shows that, not only the integral of the form (2.24), but the function $\varrho_3(\kappa^2)$ itself is identically zero at least as far as the lowest order approximation is concerned.

In other words, there is no room in the spectral decomposition of the renormalized propagator to introduce consistently the third q function characteristic of the violation of parity.

On the other hand, the renormalized Lagrangian

$$(3.11) \quad \begin{aligned} \mathcal{L} = & -Z_2 \bar{\psi}(a + b\gamma_5)(\gamma\partial + m)(a - b\gamma_5)\psi \\ & -Z_2 \bar{\chi}(a - b\gamma_5)(\gamma\partial + m)(a + b\gamma_5)\chi \\ & -Z_1 g \bar{\psi}(\alpha + \beta\gamma_5)\chi\varphi^* - \text{h. c.} \end{aligned}$$

is rewritten, in view of (3.10),

$$(3.12) \quad \begin{aligned} \mathcal{L} = & -Z_2 \bar{\psi}(\gamma\partial + m)\psi \\ & -Z_2 \bar{\chi}(\gamma\partial + m)\chi \\ & -Z_1 g \bar{\psi}\chi\varphi^* - \text{h. c.} \end{aligned}$$

in terms of the conventional canonical variables

$$(3.13) \quad \begin{cases} \psi(x) = (a - b\gamma_5)\psi(x), \\ \chi(x) = (a + b\gamma_5)\chi(x), \end{cases}$$

which satisfy

$$(3.14) \quad \begin{cases} \{\psi(x), \bar{\psi}(x')\}_{x'_0=x_0} = \gamma_4 \delta(\mathbf{x} - \mathbf{x}') \\ \{\chi(x), \bar{\chi}(x')\}_{x'_0=x_0} = \gamma_4 \delta(\mathbf{x} - \mathbf{x}') \end{cases}$$

As can be seen, the above obtained Lagrangian does not contain any terms which violate parity. We have found a parity *conserving* Lagrangian by renormalizing the parity *non-conserving* one. This means, however, that the original Lagrangian also cannot contain parity violating terms in order that the theory be consistent. The theory is thus reduced to the usual parity conserving one.

Here may be raised an argument that we shall be able to have a renormalized parity non-conserving Lagrangian, if we take, at the outset, certain shifted representations between the two kinds of unrenormalized particles (see the footnote of the previous section). To examine this possibility, suppose that, instead of (3.11), a renormalized Lagrangian of the form

$$(3.15) \quad \begin{aligned} \mathcal{L} = & -Z_2 \bar{\psi}(\gamma\partial + m)\psi \\ & -Z_2 \bar{\chi}(\gamma\partial + m)\chi \\ & -Z_1 g \bar{\psi}(\alpha + \beta\gamma_5)\chi - \text{h. c.} \end{aligned}$$

be given. This Lagrangian follows the anticommutator for equal times

$$(3.15) \quad \{\psi(x), \bar{\psi}(x')\}_{x_0=x'_0} = Z_2^{-1} \gamma_4 \delta(\mathbf{x} - \mathbf{x}').$$

On the other hand, the renormalized propagator

$$(3.16) \quad S'_F(p) = -2i \int_0^\infty dK^2 \frac{i\gamma p \varrho_1(\kappa^2) + \varrho_2(\kappa^2) + i\gamma_5 \gamma p \varrho_3(\kappa^2)}{p^2 + \kappa^2 - i\varepsilon},$$

leads to

$$(3.17) \quad \{\psi(x), \bar{\psi}(x')\}_{x_0=x'_0} = \left[\int \varrho_1(\kappa^2) d\kappa^2 + \gamma_5 \int \varrho_3(\kappa^2) d\kappa^2 \right] \gamma_4 \delta(\mathbf{x} - \mathbf{x}').$$

Comparing this with (3.15) gives

$$(3.18) \quad \int_0^\infty \varrho_3(\kappa^2) d\kappa^2 = 0.$$

Now, let us calculate ϱ_3 in the lowest order approximation of perturbation theory. Then we find

$$(3.19) \quad \varrho_3(\kappa^2) = \frac{2\alpha\beta}{m^2 - \kappa^2} J(\kappa^2),$$

which is inconsistent with the condition (3.18), unless $\alpha\beta = 0$.

4. - Concluding remarks.

Opinions will be divided on the interpretation of the revealed phase of the theory. First of all, it might be possible to consider that the inconsistency mentioned is only a result of the unjustified use of perturbational calculations, and there will exist an exact solution which cannot be expanded in powers of the coupling constant.

If, contrary to this expectation, it turns out that the inconsistency is inherent to the theory, then we shall conclude that the present formalism of quantum field theory is to be drastically changed in order to reconcile the notion of renormalization with the fact of parity non-conservation.

The third point of view is also possible which asserts that the notion of renormalization cannot be applied to the parity non-conserving interaction.

In view of the fact that parity violates only in weak interactions associated with the decay of elementary particles, it may be reasonable to presume that there exists a *complementarity* between the concept of the dressed particle and the fact that the particle decays spontaneously.

* * *

The author wishes to thank Mr. T. YOSHIMURA for stimulating discussions and criticisms.

RIASSUNTO (*)

Si dà una formulazione esatta del metodo di rinormalizzazione in una teoria non conservante la parità. Si ottengono equazioni che determinano le costanti di rinormalizzazione, e, fra l'altro, si esamina la compatibilità interna della teoria.

(*) Traduzione a cura della Redazione.

NOTE TECNICHE

Detection of High Energy μ -Mesons by an Air Čerenkov Counter (*).

R. GIACCONI (+), W. BLUM (+) and G. T. REYNOLDS

Palmer Physical Laboratory, Princeton University - Princeton, N. J.

(ricevuto il 16 Settembre 1958)

Summary. — An investigation of the properties of air Čerenkov counters is described. A quantitative interpretation of the results is given.

1. — Introduction.

The interest in high energy particles selectors has led various groups ^(1,2) in the past to study the properties of Čerenkov counters filled with gases. In order to obtain a better understanding of the possibilities of these counters as reliable ultrarelativistic particle detectors, it was felt necessary to repeat, with the improved photomultipliers now available, some of the experiments already performed and to present a more detailed interpretation of the data obtained. The purpose of this paper is to describe such an experiment and to present a quantitative analysis of the results.

2. — Experimental arrangement and procedure.

2.1. The experiment was performed at sea level with μ -mesons (energy > 280 MeV) of the cosmic radiation. The apparatus consisted of a light tight box with a parabolic mirror at the bottom. The Čerenkov light produced by single particles in the air contained in the box was focused on the cathode of a photomultiplier. The geometry of the box and mirror and the dispo-

(*) Sponsored by the joint program of the U.S. Office of Naval Research and the U.S. Atomic Energy Commission.

(+) Fulbright fellows.

(1) A. ASCOLI BALZANELLI and R. ASCOLI: *Nuovo Cimento*, **11**, 562 (1954).

(2) F. R. BARCLAY and J. V. JELLEY: *Nuovo Cimento*, **11**, 26 (1955).

sition of the G.M. counters, absorber and phototube are shown in Fig. 1. A Dumont 6263 photomultiplier with 12.5 cm cathode diameter was used. The amplitude of the solid angle and the height at which the phototube was placed were selected according to the results of an empirical focusing pro-

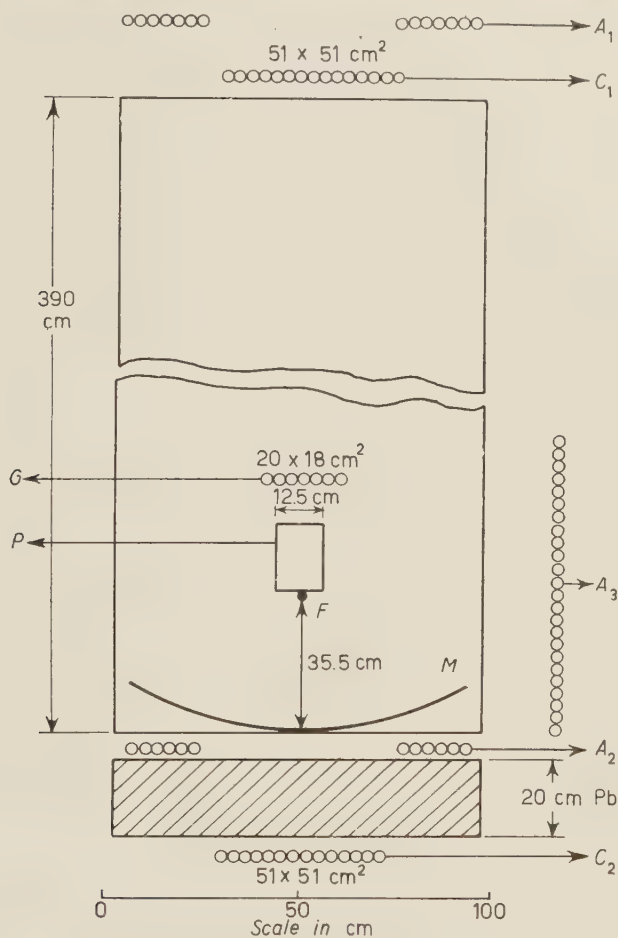


Fig. 1. — Essential features of the apparatus.

cedure in order to assure complete light collection for all possible paths of the incoming particles. The 18×20 cm² G.M. tray (G) on top of the phototube prevents the acceptance of pulses produced by particles passing through the photomultiplier itself.

2.2. The experiment consisted in recording simultaneously the rates of coincidences of the type $C_1 C_2 P \bar{G} \bar{A}_1 \bar{A}_2 \bar{A}_3 \equiv N_p$ and $C_1 C_2 G \bar{A}_1 \bar{A}_2 \bar{A}_3 \equiv N_\mu$. The resolving time of both coincidences was approximately $2 \cdot 10^{-6}$ s. Time constants of $2 \cdot 10^{-7}$ s were used in the circuit of the phototube amplifier. The signal from this amplifier was fed through a single channel differential pulse

height analyzer to the coincidence circuit. For each setting of the discriminator the N_p rate was measured, once with the photocathode surface uncovered, $(N_p)_o$, and the second time with the photocathode surface covered by a shutter, $(N_p)_c$, to obtain the rate of background counts. This latter rate was of the order of 30% of the total counting rate and was in agreement with the expected chance coincidence value due to the noise of the phototube and amplifier and to the rather poor time resolution. All measurements were started from some minimum value of the discriminator setting below which the statistical fluctuations of the number of background counts became large compared to the difference between the total and background counts. Since, even at larger values of the discriminator bias, the background was a considerable fraction of the total number of counts, care has been taken to avoid the effects of slow changes of the noise level by taking the counts with shutter open and closed, for the same pulse height interval, one immediately after the other. In order to measure the possible influence of fast changes of the noise, various counts for a given discriminator setting were repeated. The difference between total number of counts and background were found to be constant for the same pulse height interval within the statistical errors.

2.3. Between measurements, periodic checks of the overall amplification of the photomultiplier circuit were performed using a ^{137}Cs and a plastic scintillator with constant geometry. The peak given by the 624 keV electrons was determined with 20% resolution.

2.4. The pulse height of a single photoelectron pulse was calculated from the experimentally measured noise spectrum of the phototube ⁽³⁾. This value depends on the overall amplification of the photomultiplier and associated circuit. Since the experiment was repeated with two phototubes and it was felt desirable to be able to compare directly the results, the voltage applied to the tubes was adjusted so that both would give the same pulse height for the electron peak of the ^{137}Cs source. Under these conditions the amplitudes of the single photoelectron pulse height, V_o , were found to be $V_{o1} = 3.5$ and $V_{o2} = 1.5$ V. It can be shown that $V_{o1}/V_{o2} = \varepsilon_{ph2}/\varepsilon_{ph1}$, where ε_{ph} represents the quantum efficiency of the phototube.

3. — Results.

Because of the coincidence requirements and the thickness of the lead absorber over tray C_2 , we feel confident that our N_μ counting rate represents the flux of single particles and more specifically of μ -mesons with energy greater than 280 MeV through the detector. The corrected counting rate of 1075 ± 36 per hour is in good agreement with the value that can be calculated from Rossi's data ⁽⁴⁾. The total running time with each phototube was approximately 200 h. For each pulse height interval the measurements with shutter open and closed were extended for a period of time sufficient to collect a statistically significant number of events. The ratios $(N_p/N_\mu)_o$ with shutter open and $(N_p/N_\mu)_c$ with shutter closed were calculated for each

⁽³⁾ G. A. MORTON: *RCA Rev.*, **10**, 525 (1949).

⁽⁴⁾ B. ROSSI: *Rev. Mod. Phys.*, **3**, 537 (1948).

discriminator setting. The difference, $(N_p/N_\mu)_o - (N_p/N_\mu)_c$, represents the fraction of μ 's emitting a quantity of light corresponding to the given pulse height. In Figs. 2 and 3 the differential spectrum of the difference, $(N_p/N_\mu)_o - (N_p/N_\mu)_c$, versus pulse height is given for the two runs with different phototubes. The errors to be associated with the experimental values are of the order of 10% at all points. The electron scales attached are derived from the measured one-electron pulse height.

Fig. 2. — Differential pulse height distribution. (Photomultiplier 1).

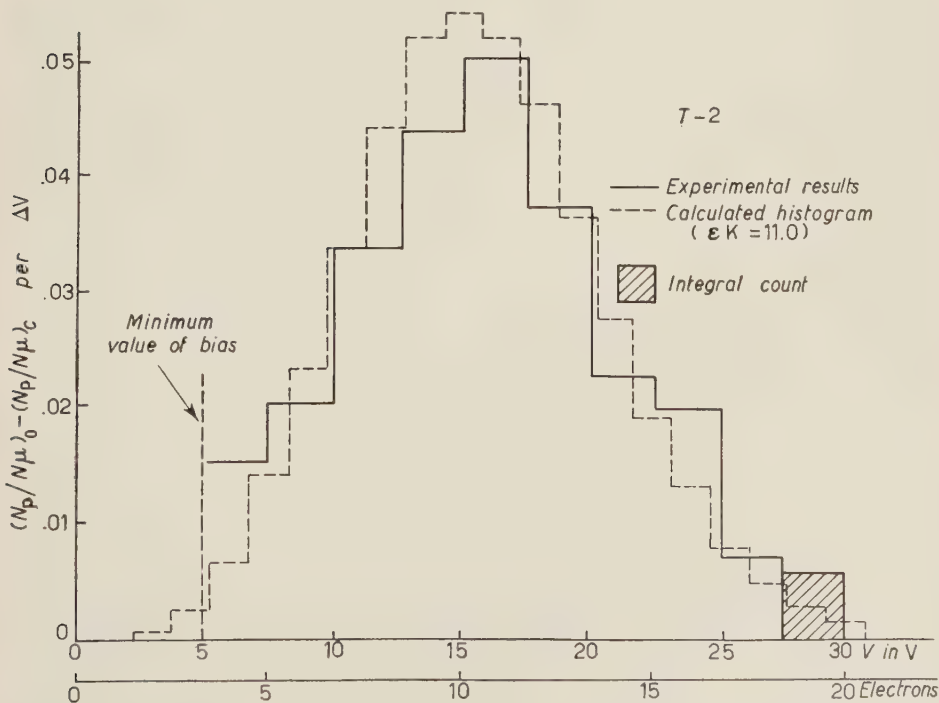
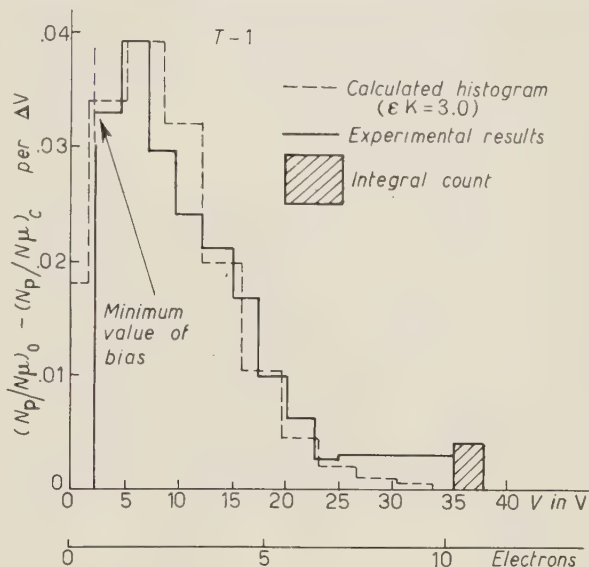


Fig. 3. — Differential pulse height distribution. (Photomultiplier 2).

The sum of $(N_p/N_\mu)_n - (N_p/N_\mu)_c$ on all pulse height intervals represents the measured value of the fraction of μ 's producing Čerenkov radiation. This value was found to be $S_1 = (19.9 \pm 2.0)\%$ and $S_2 = (25.5 \pm 3.5)\%$ for the two phototubes respectively. According to the known μ spectrum ⁽¹⁾, 27% of the μ 's which pass through the counter ($E > 280$ MeV) should produce Čerenkov light.

4. - Discussion.

A discussion of the general principles of the experiment is given in ref. ⁽²⁾. We are interested here in the derivation of the expected pulse height distribution.

From the classical treatment of Frank and Tamm, the average number of photons emitted in the wave length interval for which the photomultiplier is sensitive (approximately $3700 \div 5200$ Å) can be calculated as a function of the energy of the incident particles. Assuming, further, a given energy spectrum for the μ -mesons, namely $W(E)dE = E^{-2.0}dE$, the distribution of pulses of a given number of photons can be found. If one also knows the efficiency of collection of light, $\varepsilon_{\text{coll}}$, and the quantum efficiency of the phototube, ε_{ph} , the pulse height distribution can be directly calculated. However, since the average amount of Čerenkov light created by a single particle in air is generally small, even for distances of the order of meters, one has to take into account the statistical character of photon creation, photoelectric emission, and secondary electron emission at all dynodes.

Since the number of photoelectrons at the cathode is an order of magnitude smaller than the number of photons from the Čerenkov effect, and smaller than the number of secondary electrons at the dynodes, we have used, as a first approximation, only the statistical fluctuations in the emission of photoelectrons. For these we have assumed a Poisson distribution ⁽³⁾. It can be shown that the resulting differential distribution expressed as a function of the number of photoelectrons, i , is given by:

$$W(i) = \frac{1}{A} \frac{(\varepsilon K)^i}{i!} \sum_{n=0}^{\infty} \frac{(\varepsilon K)^n}{n!} \frac{1}{2(n-i)-1},$$

- where: ε is the product $\varepsilon_{\text{coll}} \cdot \varepsilon_{\text{ph}}$ (both quantities previously defined);
 $K = H(1 - 1/N^2)$ is a constant which represents the maximum average number of photons emitted (approximately 80);
 H is a constant of the order of 10^5 ;
 N is the index of refraction of air at 1 atm, 20 °C ($N = 1.00027$);
 A is a normalization constant;

and where the approximation $H - K \approx H$ has been used.

To compare the calculated distribution with the experimental results, the fit with various values of εK was tried using a least square method. The calculated histograms associated with the experimental results, Fig. 2 and Fig. 3, are the ones for which the best fit was obtained. The corresponding values of εK are $(\varepsilon K)_1 = 3.0$ and $(\varepsilon K)_2 = 11.0$ for the first and second photomultiplier.

Assuming $\varepsilon_{\text{coll}}$ to remain constant for the two different runs, it follows that $(\varepsilon K)_1/(\varepsilon K)_2 = \varepsilon_{\text{ph1}}/\varepsilon_{\text{ph2}} = .27$. This value should be compared with the experimentally determined $\varepsilon_{\text{ph1}}/\varepsilon_{\text{ph2}} = V_{02}/V_{01} = .43$ which has an estimated error of 40%. Using the calculated histograms, the experimental values of the fraction of μ 's producing Čerenkov light, $S_1 = (19.9 \pm 2.0)\%$ and $S_2 = (25.5 \pm 3.5)\%$, can be corrected to take into account the finite value of the minimum bias level. The corrections yield $S_1 = (21.0 \pm 2.1)\%$ and $S_2 = (25.6 \pm 3.5)\%$ to be compared with the expected 27%.

5. — Conclusions.

The agreement between calculated and experimental values seems to justify the approximations used and to indicate no appreciable discrepancy from what would be expected under the assumption that most of our light pulses were produced by Čerenkov radiation of single μ -mesons of energy ~ 4 GeV. We feel confident that with minor improvements in the electronics to reduce the background noise, our apparatus could be used as an efficient detector of particles with $\gamma = 1/(1 - \beta^2)^{1/2}$ greater than 40.

RIASSUNTO (*)

Si presenta un esame delle proprietà dei contatori Čerenkov in aria. Si dà un'interpretazione quantitativa dei risultati.

(*) Traduzione a cura della Redazione.

Grain Size and Grain Density in Ilford K-5 and L-4 Emulsions.

R. C. KUMAR (*)

Pure Physics Division, National Research Council - Ottawa

(ricevuto il 20 Settembre 1958)

Summary. — Electron micrographs of grains in unprocessed and processed Ilford K-5 and L-4 emulsions are shown. The silver bromide grain sizes in the unprocessed K-5 and L-4 plates have been measured and found to be normally distributed with mean values of $(0.210 \pm .007) \mu\text{m}$ and $(0.134 \pm .004) \mu\text{m}$ and standard deviations of $0.035 \mu\text{m}$ and $0.021 \mu\text{m}$ respectively. The electron micrographs of the silver grains in processed emulsions reveal absence of spherical shape or solid structure in case of most of these grains. The grain densities on plateau ionization tracks have been found to be approximately the same in K-5 and L-4 plates as in G-5 plates processed under similar conditions. The L-4 plates however are subject to more serious fading with delay in processing after exposure than the K-5 or G-5 ones.

1. — Grain size in unprocessed emulsion.

The size of the silver bromide grains in nuclear emulsions and its distribution is of importance in the estimation of loss of energy by ionization of charged particles in these emulsions. Electron microscope photographs of these grains have been published for Ilford G-5 emulsions (^{1,2}). Recently Ilford Ltd. have introduced two new types of emulsions — K-5 and L-4 — with smaller grain sizes, and it was thought useful to investigate grains in unprocessed and processed emulsion by electron microscopy.

The specimens for the electron microscope were prepared by dissolving a piece of dry unprocessed emulsion with warm de-ionized water, the solutions being well stirred. The emulsions used were from Ilford batch No. Z711 (April, 1958). Specimens were collected on standard holders (copper grids

(*) National Research Council Post-Doctorate Fellow; now at University College, London.

(¹) G. BARONI and C. CASTAGNOLI: *Nuovo Cimento*, **7**, 394 (1950).

(²) E. PICKUP: *Can. Journ. Phys.*, **31**, 898 (1953).



a)

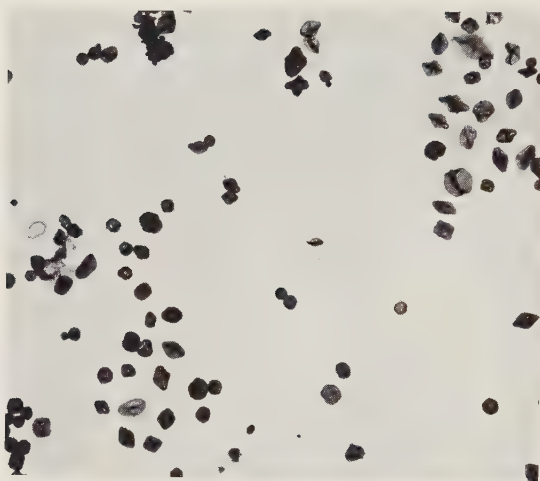


b)

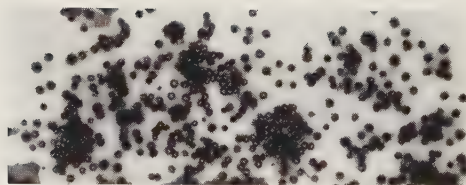


c)

Fig. 1. — Electron microscope photographs: *a)* L-4; *b)* K-5; *c)* latex grains of known uniform diameter ($0.340 \pm .005$) μm ; all at same magnification.



a)



b)

Fig. 2. — Silver grains in processed emulsions; *a)* L-4; *b)* K-5: magnification approximately same as for Fig. 1.

covered with Formvar films) for use in a 50 kV RCA electron microscope. Figs. 1a and 1b show reproductions of the silver bromide grains in L-4 and K-5 emulsions respectively. Fig. 1c shows some latex grains of known uniform size ($0.340 \pm .005$) μm under the same magnification. Measurements on 300 grains gave mean grain diameters of ($0.134 \pm .004$) μm and ($0.210 \pm .007$) μm for L-4 and K-5 emulsions respectively, where the errors quoted are standard errors. The distributions of the grain sizes shown in Figs. 3a and 3b were found to be normal with standard deviations of 0.021 μm and 0.035 μm for L-4 and K-5 emulsions respectively.

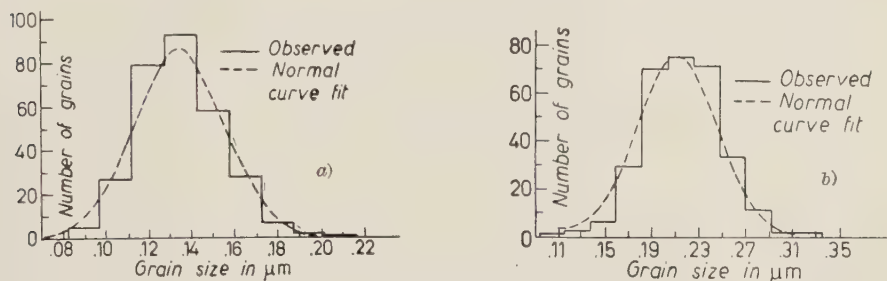


Fig. 3. — Grain size distributions: a) L-4; b) K-5.

It will be noticed that in Figs. 1a and b there are groups of grains in addition to what appear to be single resolved grains. It is not certain whether these groups represent grains as they were originally packed in the emulsion or whether they were formed while preparing the specimens. Measurements were made only on resolved grains. Besides, some of the single grains showed some structure at the edges. This is due to the action of the electron beam on the silver bromide grains causing migration of silver ions in the grains; similar phenomena have been observed for Ilford C-2 and G-5 emulsions (^{3,2}). In making measurements of the diameter, such grains showing any structure at the edges were ignored. Care was also taken, while making the electron microscope exposures, not to use too intense an electron beam, or a long time of exposure such that visual observation indicated structural changes in the grains.

2. — Grain density.

Two stacks of stripped emulsions, each containing G-5, K-5 and L-4 pellicles, were exposed to electrons and positrons of energy (300 ÷ 700) MeV at the Cornell synchrotron. These stacks were processed at different times, the first two days and the second fourteen days after the exposure. Prior to development and after exposure, the emulsions were transported and stored at low temperature, about 32° F. The usual temperature development method was employed, the temperature of the hot bath being 78° F and the time of development 40 min.

(³) L. WINAND: *Fundamental Mechanisms of Photographic Sensitivity* (London, 1951), p. 286.

The grain density on the electron (positron) tracks of plateau ionization was found to be approximately the same in G-5, K-5 and L-4 emulsions of the first stack, being about 26 blobs/100 μm . The second stack had undergone obvious fading; the grain density on electron (positron) tracks of plateau ionization was about 18 blobs/100 μm in the G-5 and K-5 plates and the L-4 plates showed no tracks at all.

3. - Grains in processed emulsion.

Figs. 2a and 2b show electron micrographs of silver grains in processed L-4 and K-5 emulsions at approximately the same magnification as in Fig. 1. In contrast with the undeveloped silver bromide crystals, most of the silver grains do not possess either a regular spherical shape or a solid structure. This agrees with previous findings ⁽⁴⁾ that the developed silver grain consists of a mass of tangled filaments. However, it is not certain that the structure of the grains was not somewhat modified in the process of centrifuging that was found necessary in preparing specimens for the electron microscope due to the relatively sparse concentration of grains in the processed emulsion. The mean grain size was not measured for the processed grains because of the difficulty of assigning a parameter common to all (such as the diameter in case of spherical grains). Visually the size of the developed silver grains appeared to be larger than that of the silver bromide grains in the unprocessed emulsion as a comparison of Figs. 1 and 2 will show. The distribution in size of the silver grains was less regular than that of the silver bromide grains. This may be due to the presence of the smaller background grains, in addition to those forming tracks in the emulsion.

* * *

The author is greatly indebted to Dr. E. PICKUP for valuable advice and to Dr. S. T. BAYLEY of the Applied Biology Division for kindly making the electron microscope exposures. Thanks are due to Drs. B. JUDEK and J. G. McEWEN for help in processing the plates.

(4) C. E. HALL and A. L. SCHOEN: *Journ. Opt. Soc. Amer.*, **31**, 281 (1941).

RIASSUNTO (*)

Si presentano micrografie elettroniche di granuli di emulsioni Ilford K-5 e L-4 sviluppate e non sviluppate. Si sono misurate le dimensioni dei granuli di bromuro d'argento delle lastre K-5 e L-4 non sviluppate e si sono trovate normalmente distribuite con valori medi di $(0.210 \pm .007) \mu\text{m}$ e $(0.134 \pm .004) \mu\text{m}$ e scostamenti di $0.035 \mu\text{m}$ e $0.021 \mu\text{m}$ rispettivamente. Le micrografie elettroniche dei granuli d'argento delle lastre sviluppate rivelano per la maggioranza dei granuli assenza di forma sferica o di struttura solida. Si è trovato che la densità dei granuli delle tracce mostranti ionizzazione massima è nelle lastre K-5 e L-4 approssimativamente uguale a quella delle lastre G-5 sviluppate in condizioni simili. Le lastre L-4, tuttavia, sono soggette, tardando a svilupparle dopo l'esposizione, a maggior sbiadimento che le K-5 o le G-5.

(*) Traduzione a cura della Redazione.

LETTERE ALLA REDAZIONE

(La responsabilità scientifica degli scritti inseriti in questa rubrica è completamente lasciata dalla Direzione del periodico ai singoli autori)

Presence of ^{57}Co in the Atmosphere (*).

L. MARQUEZ, N. L. COSTA and I. G. ALMEIDA

Centro Brasileiro de Pesquisas Físicas - Rio de Janeiro

(ricevuto il 29 Novembre 1957)

We have established the presence of the radioisotope ^{57}Co in the atmosphere. It has been done by collecting a few thousand liter of rain water, adding Co carrier to it, and passing it through an ion exchange column to retain the cations. The technique is similar to the one we used to determine ^{22}Na in the atmosphere and it has been described already (1).

The cations with the Co were eluted from the column and the Co precipitated with H_2S in basic solution. The Co was dissolved, then scavenging was done with sulphides of Cu, Sb, Te, Se, Bi, and Pb; with sulphate of Ba; and with hydroxides of Fe and La. The Co extracted from thiocyanate solution with a mixture of amyl alcohol and ethyl ether, returned to H_2O phase, precipitated in solution of HCl with 1-Nitroso-2-Naphtol, and ignited to the oxide. The procedure described is specific for Co, and the chemical yield ranged from 15 to 60%.

The Co was counted in a well crystal scintillation spectrometer Model 516, built by Baird-Atomic, Inc., Cambridge,

Mass., which we calibrated for energy measurements and for efficiency. The spectrum obtained showed one peak with an energy of (125 ± 5) keV corresponding to the tabulated γ -rays of ^{57}Co of 123 keV and 173 keV. We observed, of course, one peak only due to the poor resolution of the spectrometer. The counting efficiency at the photoelectric peak was 65%.

We carried out three experiments and the results are shown in Table I. The average activity of ^{77}Co for these three experiments is 0.020 dpm/liter.

TABLE I.

Date 1957	Amount of rain water in liters	Absolute specific activity in dpm/liter
June	8 500	0.016
September	3 500	0.011
October	3 000	0.040

One does not expect that ^{57}Co will be formed with appreciable yield in nuclear tests, whether they derive their energy from fusion or from fission. To see that, we will write the reactions that

(*) This work was done under the auspices of the Conselho Nacional de Pesquisas of Brazil.

(1) L. MARQUEZ, N. L. COSTA and I. G. ALMEIDA: *Nuovo Cimento* (to be published).

can produce ^{57}Co in decreasing order of likelihood. They are $^{57}\text{Fe}(\text{p}, \text{n})^{57}\text{Co}$; $^{56}\text{Fe}(\text{p}, \gamma)^{57}\text{Co}$; $^{56}\text{Fe}(\text{d}, \text{n})^{57}\text{Co}$; $^{58}\text{Fe}(\text{p}, 2\text{n})^{57}\text{Co}$; $^{58}\text{Ni}(\text{n}, 2\text{n})^{57}\text{Ni}$; $^{59}\text{Co}(\text{n}, 3\text{n})^{57}\text{Co}$; etc.

Examining these reactions, one arrives at the conclusion that nuclear tests having mostly fission could not account for the ^{57}Co observed, since all the reactions indicated produced by neutrons require threshold of 12 MeV or greater, and one can calculate that this is not compatible with the amount of the fission product ^{137}Cs in rain water which is 1.2 dpm/liter ⁽²⁾.

The two first reactions written are the most likely to produce ^{57}Co in a test having mostly fusion. They should be hindered by the potential barrier. The only thermonuclear reaction giving protons with energy greater than the barrier in Fe is the reaction $^3\text{He}(\text{d}, \alpha)\text{p}$; but in a device where this reaction takes place, the reaction $\text{d}(\text{d}, ^3\text{He})\text{n}$ will be more prominent and give a large number of neutrons. In any case, in a fusion nuclear test where protons with a few MeV are produced, it is likely that more neutrons will be produced, and since there might be iron in the device, we decided to look for the radioisotopes formed in iron by neutron capture, namely ^{55}Fe and ^{59}Fe . One expects that (n, γ) will be more

probable than (p, n) and (p, γ) in iron in a nuclear test.

A sample of 3000 liters of rain water was processed, and the iron purified with a chemical yield of 50%. The sample was counted with a Geiger counter and no detectable activity was found, giving an upper limit of 1 cpm. We corrected this upper limit for absorption, self-absorption, back-scattering, geometry, efficiency and yield and it gives an upper limit for ^{56}Fe of 0.010 dpm/liter. The corresponding upper limit for ^{53}Fe is 0.003 dpm/liter. Both upper limits are lower than the activity of ^{57}Co .

In conclusion, the presence of ^{57}Co in the atmosphere has been proven. The present evidence from theoretical considerations and from the absence of radioisotopes of iron seems to indicate that it is not likely to come from a nuclear test, although this point is not definite yet. The systematic observation of ^{77}Co in rain water and the radioisotopes in its neighborhood during three or four years will help to decide its origin.

Note. — We have made more measurements from January to July, 1958 on ^{57}Co and ^{54}Mn . These measurements indicate that the bulk of ^{57}Co is produced in thermonuclear tests ⁽³⁾.

⁽²⁾ L. MARQUEZ, N. L. COSTA and I. G. ALMEIDA: *An. Acad. Bras. Ciencias* (to be published).

⁽³⁾ L. MARQUEZ, N. L. COSTA and I. G. ALMEIDA: *Proceedings of the Second International Conference on the Peaceful Uses of Atomic Energy*.

A New Type of Particle Detector: the «Discharge Chamber».

S. FUKUI and S. MIYAMOTO

Department of Physics, Osaka University - Osaka

(ricevuto il 26 Settembre 1958)

Recently, the devices based on gaseous discharges which can determine the trajectory of ionizing particles, such as the hodoscope chamber⁽¹⁾ or the triggered spark counter⁽²⁾ have been reported. However, these have some inherent imperfections, in spite of their wide usefulness as detectors. Regarding the former, even taking into account the considerations of F. ASHTON *et al.*⁽³⁾, one cannot expect a *very precise determination* of the trajectory of the particle, owing to the finite dimensions of the glass tubes and their dead spaces, and in the latter it is difficult

to determine all trajectories when more than two particles pass through simultaneously, because the discharge, which grows in advance of others, decreases the intensity of the electric field very rapidly. We describe here the possibility of constructing a new type of detector also based on the gaseous discharge. This detector secures the precision of the trajectory of the particle and works for a group of particles.

The chamber consists of glass boxes filled with a mixture of neon and argon gases at atmospheric pressure. Each glass box is constructed of glass plates glued with Araldite adhesives. The inner size of the box used for the test is $8.5 \text{ cm} \times 13 \text{ cm} \times 2 \text{ cm}$ or $\times 1 \text{ cm}$ and the thickness of the glass plates is 0.5 mm or 2 mm. Metal plates or conductive glass plates (Nesa) are used as electrodes. We also constructed the boxes with Nesa whose outer surfaces were conductive.

A pulsed, intense electric field is applied across the spaces immediately after the passage of the ionizing particle. If the intensity and the duration of the electric field are properly chosen, tiny luminous discharges occur along the

⁽¹⁾ M. CONVERSI and A. GOZZINI: *Nuovo Cimento*, **2**, 189 (1955); M. CONVERSI, S. FOCARDI, C. FRANZINETTI, A. GOZZINI and P. MURTAS: *Suppl. Nuovo Cimento*, **4**, 234 (1956); G. BARSANTI, M. CONVERSI, P. MURTAS, C. RUBBIA and G. TORELLI: *Report at the Geneva International Conference* (1956); M. GARDENER, S. KISDNASAMI, E. RÖSSLE and A. W. WOLFENDALE: *Proc. Phys. Soc.*, B **70**, 687 (1957); S. FUKUI and S. MIYAMOTO: *INS-TCA*, **10** (1957) and **11** (1958), (Technical reports at the Institute for Nuclear Study, University of Tokyo).

⁽²⁾ T. E. CRANSHAW and J. F. DE BEER: *Nuovo Cimento*, **5**, 1107 (1957).

⁽³⁾ F. ASHTON, S. KISDNASAMI and A. W. WOLFENDALE: *Nuovo Cimento*, **8**, 615 (1958).

trajectory of the particle and can be photographed. When the electric field is kept longer than a certain time at an intensity sufficient to cause discharges, successive discharges occur at random places. It seems that these spurious discharges are caused by the photo-electrons freed by photons emitted from excited atoms inside the streamers initially produced. Therefore, the time width of the high voltage pulse must be very short in order to prevent spurious discharges.

The arrangements of the chamber for the test are shown schematically in Fig. 1 and the circuits of the triggered high voltage pulse generator is shown in Fig. 2. As seen in Fig. 2, the pulse has an exponential shape with time constant CR . We can obtain good

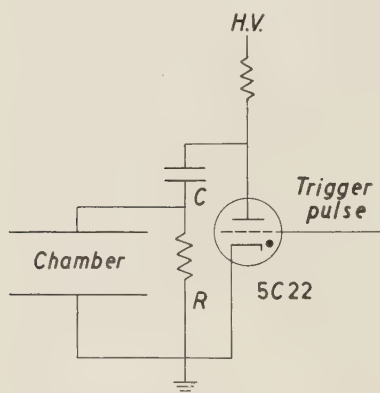


Fig. 1. - The arrangements of the chamber for test are shown schematically. In Arr. A, tracks are photographed through the conductive glass and in Arr. B, through the side of the box.

tracks when we employ the value of 10^{-7} s for the time constant, *i.e.* $C = 0.001 \mu\text{F}$ and $R = 100 \Omega$. From the results of the present investigation the value of CR must be shorter than 10^{-6} s. Some typical examples of photographs are presented in Fig. 3. Fig. 3a shows the two photographs taken with Arr. A and Fig. 3b is the one taken with Arr. B of Fig. 1, respectively.

Specifications of these chambers for the present test are as follows. The time constant of the voltage pulse is

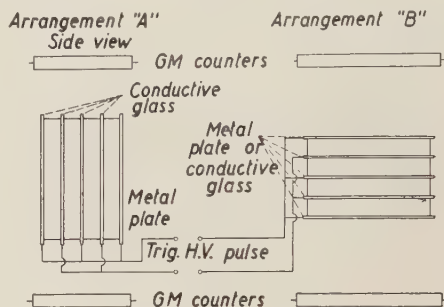
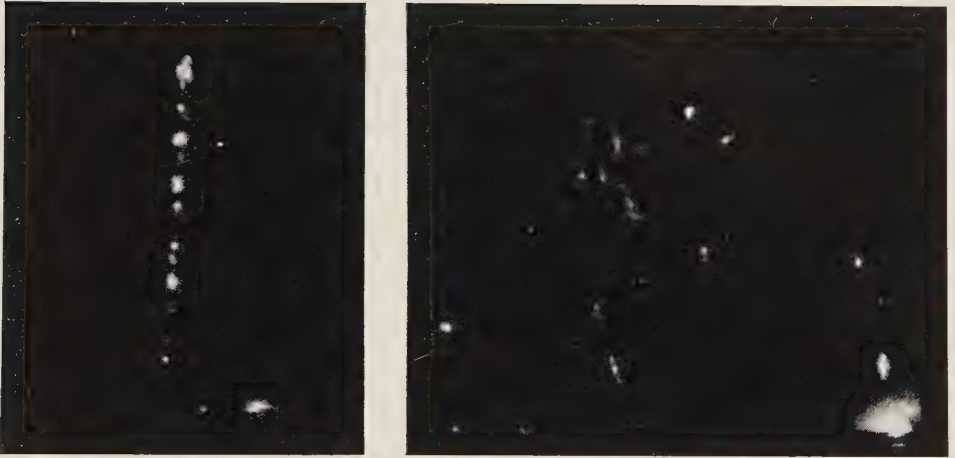


Fig. 2. - The circuit of triggered high voltage pulse generator.

fixed at the value of 10^{-7} s throughout the investigation. The efficiency for the formation of the track is not changed by the value of the applied voltage from 12.5 kV/2 cm to 15 kV/2 cm in the case of the box of 2 cm width and from 8 kV/1 cm to 12 kV/1 cm in the case of the box of 1 cm width. The efficiency of the chamber placed in Arr. A is almost 100% except at the spaces near the glass plates when the time delay between the passage of the particle and the application of the voltage pulse is shorter than $2 \mu\text{s}$. When the time delay is about $10 \mu\text{s}$, discharges showing the track do not occur and randomly separated discharges occur at a few places in the chamber. Therefore, the maximum sensitive time of the chamber is expected to be $10 \mu\text{s}$. The inefficient space close to the glass plate, which is somewhat larger near the positive electrode, is caused by the discharge mechanism and depends slightly on the pulse height. Its width is about 3 mm along the surface of the plate of the positive electrode in the case of Arr. A. The width of the track is ~ 2 mm and the average number of discharge columns (this quantity is like the drop density of the cloud chamber track) is 2.6/cm. The width of the track in the case of



(a)



(b)

Fig. 3. — Examples of photographs taken with the discharge chamber. (a) shows the two taken in Arr. A; one is a track of a penetrating particle and the other shows tracks of an electron shower. (b) is a photograph taken in Arr. B, a track of a penetrating particle. These were taken under the condition of $CR = 10^{-7}$ s, $E_{\text{peak}} = 13$ kV/2 cm $t_{\text{delay}} = 1$ μ s.

Arr. B is ~ 3 mm. The recovery time was determined experimentally to be 0.1 s. As one sees in Fig. 3a, this chamber can detect many particles passing the same box simultaneously and the spatial resolution is expected to be ~ 2 mm.

The details of this investigation will be reported elsewhere in the near future. As described above, this detector is simple in construction and stable in

operation, and also has a very short resolving time ($10 \mu\text{s}$) and a short recovery time (0.1 s). As it can be made easily in a large size, it may be a useful instrument in cosmic ray experiments as well as in research with accelerators.

This work was performed in one of the branches of the Air Shower Project of the Institute for Nuclear Study, University of Tokyo.

Symmetry Properties of Racah's Coefficients.

T. REGGE

Istituto Nazionale di Fisica Nucleare, Sezione di Torino - Torino

(ricevuto il 9 Ottobre 1958)

We have shown in a previous letter ⁽¹⁾ that the true symmetry of Clebsh-Gordan coefficients is much higher than that is was before believed. A similar result has been now obtained for Racah's coefficients. Although no direct connection has been established between these wider symmetries it seems very probable that it will be found in the future. We shall merely state here the results which can be checked very easily with the help of the well known Racah's formula:

$$(1) \quad \left\{ \begin{matrix} a & b & c \\ d & e & f \end{matrix} \right\} = \left[\frac{(a+b-c)! (a+c-b)! (b+c-a)! (d+b-f)! (d+f-b)! (f+b-d)! \cdot (d+e-c)! (e+c-d)! (c+d-e)! (a+e-f)! (a+f-e)! (f+e-a)!}{(a+b+c+1)! (a+e+f+1)! (d+e+c+1)! (b+d+f+1)!} \right]^{\frac{1}{2}}$$

$$\sum_z (-1)^z \frac{(z+1)!}{(a+b+d+e-z)! (b+c+e+f-z)! (a+c+d+f-z)! \cdot (z-a-b-c)! (z-a-e-f)! (z-b-d-f)! (z-d-e-e)!}.$$

From the usual tetrahedral symmetry group of $\left\{ \begin{matrix} a & b & c \\ d & e & f \end{matrix} \right\}$ we know already that:

$$(2) \quad \left\{ \begin{matrix} a & b & c \\ d & e & f \end{matrix} \right\} = \left\{ \begin{matrix} b & a & c \\ e & d & f \end{matrix} \right\} = \left\{ \begin{matrix} a & e & f \\ d & b & c \end{matrix} \right\} = \left\{ \begin{matrix} c & e & d \\ f & b & a \end{matrix} \right\} = \text{etc.}$$

⁽¹⁾ T. REGGE: *Nuovo Cimento*, **10**, 544 (1958).

Our results can be put into the following form:

$$\begin{aligned}
 (3) \quad \left\{ \begin{matrix} a & b & c \\ d & e & f \end{matrix} \right\} &= \left\{ \begin{matrix} a & \frac{b+e+c-f}{2} & \frac{b+c+f-e}{2} \\ d & \frac{b+e+f-c}{2} & \frac{c+e+f-b}{2} \end{matrix} \right\} = \\
 &= \left\{ \begin{matrix} \frac{a+c+f-d}{2} & b & \frac{a+c+d-f}{2} \\ \frac{c+d+f-a}{2} & e & \frac{a+d+f-c}{2} \end{matrix} \right\} = \left\{ \begin{matrix} \frac{a+b+e-d}{2} & \frac{a+b+d-e}{2} & c \\ \frac{b+d+e-a}{2} & \frac{a+d+e-b}{2} & f \end{matrix} \right\} = \\
 &= \left\{ \begin{matrix} \frac{b+e+c-f}{2} & \frac{a+f+c-d}{2} & \frac{a+d+b-e}{2} \\ \frac{b+f+e-c}{2} & \frac{c+d+f-a}{2} & \frac{a+d+e-b}{2} \end{matrix} \right\} = \\
 &= \left\{ \begin{matrix} \frac{b+c+f-e}{2} & \frac{a+c+d-f}{2} & \frac{a+b+e-d}{2} \\ \frac{c+e+f-b}{2} & \frac{a+d+f-c}{2} & \frac{d+e+b-a}{2} \end{matrix} \right\}.
 \end{aligned}$$

Only the first of these symmetries is essentially new, the others can be obtained from it and (2). We see therefore that there are 144 identical Racah's coefficients. These new symmetries should reduce by a factor 6 the space required for the tabulation of W . It should be pointed out that this wider 144-group is isomorphic to the direct product of the permutation groups of 3 and 4 objects.

The Effect of Long and Short Range Order on Residual Resistivity.

A. CORCIOVEI

Institutul de Fizică Atomică - Bucuresti

(ricevuto il 3 Novembre 1958)

It is well known that an ordered alloy has a smaller residual resistivity than a disordered one. Various workers have discussed the effect of ordering on resistivity, namely MUTO ⁽¹⁾ has considered long range order, MURAKAMI ⁽²⁾ and GIBSON have taken into account short range order, KRIVOGLAZ and MATYSINA ⁽⁴⁾ have discussed the effects of both long and short range order. There exists also a large experimental material, which deals with this problem ⁽⁵⁾.

The purpose of the present letter is to point out a different method of treatment of this effect, in which the basic and periodic potential $U_0(\mathbf{r})$ is not that of Nordheim. We are dealing with a binary alloy, with equal atom fractions of constituents A and B . We have supposed that the lattice of the alloy can be separated into two impenetrating sublattices, with equal number of points, and that each atom contributes a single electron to the conduction band. The potential of a conduction electron is U_A in the field of an A ion, and U_B in the field of a B ion.

For complete ordering, and in the particular case of equal number of A and B ions, the A ions are occupying the points j of the first sublattice, and the B ions are occupying the points k of the second sublattice. In this manner we can choose the following basic, static, and periodic potential $U_0(\mathbf{r})$, for the electron in the \mathbf{r} position:

$$(1) \quad U_0(\mathbf{r}) = \sum_j U_A(\mathbf{r} - \mathbf{r}_j) + \sum_k U_B(\mathbf{r} - \mathbf{r}_k),$$

where \mathbf{r}_j , \mathbf{r}_k are the vectors of the j , k points. Resolving the Schrödinger equation of a conduction electron with the potential $U_0(\mathbf{r})$, we can find the solutions in the well known form

$$(2) \quad \psi_{\mathbf{x},l}(\mathbf{r}) = \exp[i\mathbf{x}\mathbf{r}]u_{\mathbf{x},l}(\mathbf{r}).$$

⁽¹⁾ T. MUTO: *Sci. Papers Inst. Phys. Chem. Research* (Tokio) **30**, 99 (1936).

⁽²⁾ T. MURAKAMI: *Journ. Phys. Soc. Japan*, **8**, 458 (1953).

⁽³⁾ J. B. GIBSON: *Journ. Phys. Chem. Solids*, **1**, 27 (1956).

⁽⁴⁾ M. A. KRIVOGLAZ and Z. A. MATYSINA: *Journ. Exp. Theor. Phys.*, **28**, 61 (1955).

⁽⁵⁾ T. MUTO and Y. TAKAGI: *Solid State Physics*, **1**, p. 193.

Restricting us to a single band, we can omit the index l . In this band we can write approximately

$$(2') \quad \psi_{\mathbf{x}}(\mathbf{r}) = \exp [i\mathbf{x}\mathbf{r}] u_{\mathbf{x}}(\mathbf{r}).$$

Now we introduce the parameters μ_j and μ_k as follows

$$(3) \quad \left\{ \begin{array}{l} \mu_j = \left\{ \begin{array}{l} 1 \\ -1 \end{array} \right. \quad \text{when } j \text{ is occupied by an } \frac{-1}{B} \text{ atom,} \\ \mu_k = \left\{ \begin{array}{l} 1 \\ 1 \end{array} \right. \quad \text{when } k \text{ is occupied by an } \frac{1}{B} \text{ atom.} \end{array} \right.$$

In this manner the potential of a conduction electron, in the field of the ions of the lattice is

$$(4) \quad U(\mathbf{r}) = \frac{1}{2} \sum_j [(1 + \mu_j) U_A(\mathbf{r} - \mathbf{r}_j - \mathbf{u}_j) + (1 - \mu_j) U_B(\mathbf{r} - \mathbf{r}_j - \mathbf{u}_j)] + \\ + \frac{1}{2} \sum_k [(1 - \mu_k) U_A(\mathbf{r} - \mathbf{r}_k - \mathbf{u}_k) + (1 + \mu_k) U_B(\mathbf{r} - \mathbf{r}_k - \mathbf{u}_k)],$$

where we have taken into account the fact that the ions are in movement with respect of the lattice points, \mathbf{u}_j and \mathbf{u}_k being the corresponding displacements. The difference between the actual potential $U(\mathbf{r})$, and the basic potential $U_0(\mathbf{r})$, used to determine the zero order states (2') is the perturbing potential $H^{v,r}$, which will produce transitions between the basic states. Knowing the matrix of the perturbing potential we can calculate the resistivity of the material, using the actual formalism of the theory of electric resistivity (6).

With the notations

$$(5) \quad \nabla U_A = \mathbf{W}^A(\mathbf{r}), \quad \nabla U_B = \mathbf{W}^B(\mathbf{r}), \quad \frac{1}{2} (U_A - U_B) = U, \quad \nabla U = \mathbf{W},$$

and performing the series expansions with respect to \mathbf{u}_j , \mathbf{u}_k the calculation leads to

$$(6) \quad H^{v,r} = H^v + H^d + H^m = \left[- \sum_j \mathbf{u}_j \mathbf{W}^A(\mathbf{r} - \mathbf{r}_j) - \sum_k \mathbf{u}_k \mathbf{W}^B(\mathbf{r} - \mathbf{r}_k) \right] + \\ + \left[\sum_j (1 - \mu_j) U(\mathbf{r} - \mathbf{r}_j) - \sum_k (1 - \mu_k) U(\mathbf{r} - \mathbf{r}_k) \right] + \\ + \left[\sum_j \mathbf{u}_j (\mu_j - 1) \mathbf{W}(\mathbf{r} - \mathbf{r}_j) - \sum_k \mathbf{u}_k (\mu_k - 1) \mathbf{W}(\mathbf{r} - \mathbf{r}_k) \right].$$

We see that the perturbing potential is the sum of a vibrational term H^v , a disordering term H^d , and a mixed term H^m . We note that the resistivity is proportional to an integral in which appears $|H_{\mathbf{x}\mathbf{x}'}^{\text{per}}|^2$ (3). In this way it is clear that the correct treatment of the problem must take into account not only the contribution of $|H_{\mathbf{x}\mathbf{x}'}^v|^2$, which gives a term ϱ_v (the thermal resistivity) and $|H_{\mathbf{x}\mathbf{x}'}^d|^2$ which gives a term ϱ_d (the residual resistivity), but also of $|H_{\mathbf{x}\mathbf{x}'}^m|^2$ and the other mixed terms, which all give a correcting term ϱ_m . Thus

$$(7) \quad \varrho = \varrho_v + \varrho_d + \varrho_m.$$

(6) A. H. WILSON: *The Theory of Metals* (Cambridge, 1953), p. 193.

The calculation of these terms is very difficult. We must begin with an evaluation of the terms which appear in $|H_{\mathbf{x}\mathbf{x}'}^{\text{par}}|^2$. We have performed it, making some approximations. We have done some averages on the vibrations of the lattice and on the order parameters. It is not here the place to discuss the calculus (*). We have shown that $\varrho_m > 0$, and also that $\varrho_v, \varrho_d > \varrho_m$. Thus the formula (7) shows that $\varrho > \varrho_v + \varrho_d$, in accordance with KOHLER (7), the term ϱ_m giving the deviation from the Mathiessen law. Complete quantitative calculations have not been performed for ϱ_m .

We note that in ϱ_v and ϱ_m appear the mean values of u_j^2 and u_k^2 , quantities which vanish when the temperature is very small compared to the Curie temperature of the alloy. Thus for small temperatures only the term $|H_{\mathbf{x}\mathbf{x}'}^d|^2$ contributes to the resistivity. Its mean expression, for equal number of A and B ions, is

$$(8) \quad |H_{\mathbf{x}\mathbf{x}'}^d|^2 = N |U_{\mathbf{x}\mathbf{x}'}|^2 \{ (1 - R^2) - z\gamma_k(\sigma - R^2) \},$$

where $U_{\mathbf{x}\mathbf{x}'} = \int_{\Omega} \psi_{\mathbf{x}}^*(\mathbf{r}) U(\mathbf{r}) \psi_{\mathbf{x}'}(\mathbf{r}) d\tau$, the integration being performed in one cell. N is the number of lattice points in the alloy, R and σ are the long respectively the short range order (8), $\gamma_k = (1/z) \sum_{i_i} \exp[i\mathbf{k}\mathbf{r}_i]$, $\mathbf{k} = \mathbf{x} - \mathbf{x}'$, the sum being performed on the z nearest neighbours \mathbf{r}_i of an arbitrary ion. The residual resistivity at low temperatures will be

$$(9) \quad \varrho_{\text{res}} = \varrho_0 \{ (1 - R^2) - z\gamma(\sigma - R^2) \},$$

where ϱ_0 is the residual resistivity calculated by NORDHEIM (9) for complete disorder of the alloy. The quantity $z\gamma$ is usually smaller than unity.

(*) Details will appear in «Studii și Cercetări de Fizică» 10, (1959).

(7) M. KOHLER: *Zeits. Phys.*, **126**, 495 (1949).

(8) TER HAAR: *Elements of Statistical Mechanics* (Reinehart, 1955), p. 251.

(9) L. NORDHEIM: *Ann. Phys. Lpz.* (5), **9**, 607 (1931).

Angular Momentum Distributions for the Thomas-Fermi Field.

T. TIETZ

University Łódź, Department of Theoretical Physics - Łódź

(ricevuto il 3 Novembre 1958)

As known the number of electrons N_l which have an angular momentum of $l(l+1)\hbar^2$ for the Thomas-Fermi field ⁽¹⁾ can be written as

$$(1) \quad N_l = 2(2l+1) \int_0^\infty \frac{dx}{x} \int dt t J_{l+\frac{1}{2}}^2(t) \cdot \Phi^{\frac{1}{2}x^{\frac{1}{2}}}$$

In the last formula for N_l the symbol $J_{l+\frac{1}{2}}$ denotes the Bessel function, Φ is the Thomas-Fermi function for the free neutral atom and α is given by $\alpha = (\frac{3}{4}\pi Z)^{\frac{1}{3}}$ where Z is the atomic number. GOLDEN ⁽²⁾ has shown that the integral of eq. (1) can be evaluated in terms of Bessel functions, his result for N_l is

$$(2) \quad N_l = (2l+1)\alpha^3 \left\{ \frac{J_{l+\frac{1}{2}}^2(y) - J_{l-\frac{1}{2}}(y)J_{l+\frac{3}{2}}(y)}{y} \right\}$$

where y appearing in eq. (2) is given by

$$(3) \quad y^{2n} = \alpha^{2n} \int_0^\infty dx \Phi^{\frac{1}{2}x^{\frac{1}{2}}} (\Phi x)^n = \alpha^{2n} \langle (\Phi x)^n \rangle_{\text{av}}.$$

The integral in eq. (3) was carried out numerically by Golden for $n=1, 2, 3, 4$ with the Thomas-Fermi field values given by GOMBAS ⁽³⁾. In this note we evaluate anal-

⁽¹⁾ J. H. D. JENSEN and J. M. LUTTINGER: *Phys. Rev.*, **86**, 107 (1952); T. A. OLIPHANT: *Phys. Rev.*, **100**, 954 (1956); S. GOLDEN: *Phys. Rev.*, **110**, 1349 (1958). See also P. GOMBAS: *Die statistische Theorie des Atoms und ihre Anwendungen* (Wien, 1944).

⁽²⁾ See reference ⁽¹⁾.

⁽³⁾ See reference ⁽¹⁾.

ytically the above mentioned integral with the approximate solution of the Thomas-Fermi function for the free neutral atom given by the author (4).

$$(4) \quad \Phi(x) = (1 + ax + bx^2)^{-\frac{3}{2}}, \quad a = 0.7105, \quad b = 0.03919.$$

In order to compare the results for N_l in our case with the numerical results of Golden we evaluate the integral of eq. (3) with the help of eq. (4) only for $n = \frac{1}{2}, \frac{3}{2}, \frac{5}{2}, \frac{7}{2}, \frac{9}{2}$.

It is necessary to stress that for every n the above mentioned complicated integral may be evaluated analytically by means of our approximated $\Phi(x)$ given by eq. (4). The values $n = \frac{1}{2}, \frac{3}{2}, \frac{5}{2}, \frac{7}{2}, \frac{9}{2}$, were chosen because then the integral of eq. (3) is given by elementary functions suitable for practical calculations. The results for

$$I_n = \int_0^\infty dx \Phi^{\frac{3}{2}} x^{\frac{1}{2}} (\Phi x)^n \quad \text{and} \quad (I_n)^{1/2n},$$

are given in Table I.

TABLE I. — Values of the integral I_n and $(I_n)^{1/2n}$ for several n .

n	$\frac{1}{2}$	$\frac{3}{2}$	$\frac{5}{2}$	$\frac{7}{2}$	$\frac{9}{2}$
I_n	0.60360	0.233795	0.097294	0.041773	0.019260
$I_n^{1/2n}$	0.60360	0.616044	0.627505	0.635309	0.64477

Table I shows that a relatively uniform value of $\bar{y} = \alpha \{ \langle (\Phi x)^n \rangle_{av} \}^{1/2n}$ is obtained for $n \leq \frac{9}{2}$. For the mean value $\bar{y} = 0.62545\alpha$ we calculate for $Z = 6, 12, 18, 24$ the number of electrons N_l given by Golden's formula eq. (2). In Table II we have a comparison of the numerical results of Golden with our results and the experimental values for N_l .

Table II shows that the results for N_l calculated with our mean value according to eq. (3) agree very well with the numerical results for N_l of Golden. This good agreement may be explained by the fact that our approximate solution for $\Phi(x)$ eq. (4) is very accurate as also that the Thomas-Fermi field values used by Golden are not the best ones, hitherto known (5). The steps of argument x in the numerical table used by Golden are little convenient for the numerical integration and therefore the error is quite a big one. Further Table II shows that the Thomas-Fermi model explains roughly in a simple way the experimental facts concerning the angular momentum distributions (6).

(4) T. TIETZ: *Nuovo Cimento*, **4**, 1192 (1956).

(5) S. KOBAYASHI and T. TAIMA: *Table of the exact values of T.F. function*. Memoirs of the Faculty of Liberal Arts and Educations Kagawa University. Part III, no. 33.

(6) G. HERZBERG: *Atomic Spectra and Atomic Structure* (New York, 1944), pp. 140-142.

TABLE II. — *A comparison of angular momentum distributions for the Thomas-Fermi field in our case with the numerical results and experimental results.*

		$Z = 6$	$Z = 12$	$Z = 18$	$Z = 24$
N_0	numerical results of Golden	3.8	5.8	6.9	7.5
	our approximation eq. (4)	3.78	5.76	6.90	7.54
	experimental	4	6	6	7
N_1	numerical results of Golden	2.0	5.1	8.6	11.9
	our approximation eq. (4)	1.97	5.14	8.55	11.85
	experimental	2	6	12	12
N_2	numerical results of Golden	0.2	1.0	2.3	3.9
	our approximation eq. (4)	0.22	1.00	2.27	3.95
	experimental	0	0	0	5
N_3	numerical results of Golden	0.0	0.1	0.2	0.6
	our approximation eq. (4)	0.0	0.1	0.2	0.6
	experimental	0	0	0	0
N_4	numerical results of Golden	0.0	0.0	0.0	0.1
	our approximation eq. (4)	0.0	0.0	0.0	0.1
	experimental	0	0	0	0

Compound Model and the Relative Parity of Baryons.

Y. OISHI

Takeshima-cho - Kochi-shi

(ricevuto il 15 Novembre 1958)

Compound models of the strongly interacting particles (baryon, π and K) have been already discussed by many authors.

One of the common and basic assumptions of them is that the strangeness of the compound is simply the sum of the strangenesses of their component particles. This implicitly postulates the charge independence of the interaction inside the compounds.

Here, we wish to explore the possibility of obtaining the outlook of the structure of the strong interaction by assuming that all compounds are coupled in S -state and the intrinsic parities (*) of the compounds are simply the products of the intrinsic parities of the component particles.

Of course, it is impossible to give a reliable base for such a crude assumption, but it is most reasonable if all baryons have spin $\frac{1}{2}$ as is commonly assumed.

Though the type of the compound model has many varieties, here we consider only the compound models which consider only the Fermions as

basic particles along the line of the original idea of Fermi and Yang ⁽¹⁾.

In the following considerations, we further assume that the spinors of the basic particles are transformed generally as $\psi \rightarrow \pm \gamma_4 \psi$ for space reflection, for it is suggested from the quaternion formalism of Gürsey ⁽²⁾ that the transformations such as $\psi \rightarrow \pm i\gamma_4 \psi$ might be attributed only to the space reflection combined with the inversion through origin in the isotopic spin space (so to say, combined reflection).

First, we consider the compound model that has been given by SAKATA ⁽³⁾, which treats the nucleon and the Λ as basic particles. In this model the π -meson is regarded as the compound of a nucleon and an antinucleon, as in the theory of Fermi and Yang, and the pseudo-scalar nature of this particle immediately follows from the above assumption.

The N - Ξ and Λ - Σ relative parities become both odd. And furthermore the K - Λ relative parity becomes odd relative

⁽¹⁾ C. N. YANG and E. FERMI: *Phys. Rev.*, **76**, 1739 (1949).

⁽²⁾ F. GÜRSEY: *Nuovo Cimento*, **3**, 988 (1956); **7**, 411 (1958).

⁽³⁾ S. SAKATA: *Progr. Theor. Phys.*, **16**, 686 (1956).

(*) The word "intrinsic parity" is used in the sense of P. T. MATTHEWS: *Nuovo Cimento*, **6**, 642 (1957).

to the nucleon and the $K-\Sigma$ relative parity becomes even relative to the nucleon, which just coincides with Barshay's conjecture⁽⁴⁾ concerning K -nucleon scattering and associated production.

This result is very tempting, although Barshay's conjecture is based on the Yukawa type interaction, considering the recent work of IHARA and HATANO⁽⁵⁾ that shows a possibility of deriving field theoretically a result equivalent to the Yukawa type interaction from a reasonable Fermi type interaction concerning π -nucleon interaction.

In the model which is considered here, the K -particle could become both pseudo-scalar and scalar according as the $N-\Lambda$ relative parity is even or odd. But this does not give an observable effect in the charge-independent theory.

Next, we consider the compound model that was discussed by KING and PEASLEE⁽⁶⁾ which treats Ξ and Λ as the basic particles. In this case, the $N-\Xi$ and $\Lambda-\Sigma$ relative parities are still odd, but the $K-\Lambda$ relative parity becomes even relative to the nucleon and the $K-\Sigma$ relative parity becomes odd relative to the nucleon, and does not coincide with Barshay's conjecture.

That is, when we consider the Yukawa type interaction including the compounds, we have an obvious disparity according as we treat nucleon and Λ or Ξ and Λ as the basic particles.

We have no *a priori* theoretical reason to take either of them, but it is more favourable to take nucleon and

Λ as the basic particles, if Barshay's conjecture is valid.

Thus we have met a possibility to obtain the tempting outlook on the structure of the strong interaction from the compound model.

This result, however, might not be necessarily regarded as a direct support of the compound model in its conventional meaning.

For, in the compound model which treats the nucleon and Λ as the basic particles, the $K-\Lambda$ relative parity is even relative to the Ξ and the $K-\Sigma$ relative parity is odd relative to the Ξ and just gives the Lagrangian which is considered by KATSUMORI⁽⁷⁾ (it differs from Gürsey's Lagrangian⁽⁸⁾) and gives a reasonable possibility to explain the mass level ordering of baryons as a self-energy effect (*), and it seems incompatible with the standpoint of the conventional theory of the compound model that attempts to explain the mass level of baryons in connection with the binding energies among the component particles.

About these points, we expect further theoretical or experimental investigation in the future.

(⁴) R. W. KING and D. C. PEASLEE: *Phys. Rev.*, **106**, 360 (1957).

(⁷) H. KATSUMORI: *Progr. Theor. Phys.*, **19**, 342 (1958).

(⁸) F. GÜRSEY: *Phys. Rev. Lett.*, **1**, 98 (1958).

(*) Though the baryon self-energies are, as was noted by PAIS [A. PAIS: *Phys. Rev.*, **110**, 574 (1958)], not in general the even functions of the coupling constants, the relations of the coupling constants that are stated by him [*Phys. Rev.*, **110**, 1480 (1958)] are just the necessary and sufficient conditions for the mass degeneracy of the Λ and Σ , when $\Lambda-\Sigma$ relative parity is even and Λ and Σ both interact in equal strength either with π or K .

(⁴) S. BARSHAY: *Phys. Rev. Lett.*, **1**, 97 (1958).

(⁵) C. IHARA and S. HATANO: *Progr. Theor. Phys.*, **20**, 368 (1958).

Discrete States for Non-Singular and Singular Potential Problems.

T. TIETZ

University of Łódź, Department of Theoretical Physics - Łódź

(ricevuto il 15 Novembre 1958)

This paper concerns the discrete states for non singular and singular potential problems of the Schrödinger equation. We write first the one-dimensional Schrödinger equation in the following form,

$$(1) \quad \frac{d^2 u}{dx^2} + \left[\frac{2m}{\hbar^2} (E - V(x)) - \frac{l(l+1)}{x^2} \right] u = 0.$$

and suppose that the potential $V(x)$ is continuous for $x \neq 0$ and for $x = 0$ it may be infinite (singular potential) and if we suppose that: (I) $V(x) \rightarrow \infty$ as $x \rightarrow \infty$ and (II) $V(x) \rightarrow 0$ as $x \rightarrow \infty$ then the two above mentioned cases (I) and (II) exhaust all possibilities appearing in the quantum mechanics for the infinite interval. Let us consider first the case (I). In this case the coefficient [], of u in eq. (1) tends to ∞ for every fixed E . It follows, therefore, from a theory of Kneser⁽¹⁾ that there belongs to every E a solution u satisfying $u(x) \rightarrow 0$ as $x \rightarrow \infty$, while every solution linearly independent of this particular solution tends to ∞ . The case (I) implies that eq. (1) is ultimately majorized by the differential equation $u'' - C^2 u = 0$, where C is any given positive constant, the bounded solution of eq. (1) ultimately majorized by $\exp[-C]$. This implies that the bounded solution of eq. (1) must satisfy the (L^2) -condition

$$(2) \quad \int_0^\infty u^2(x) dx < \infty.$$

In case (II) we see directly from eq. (1) that there exists for every E a solution $u(x)$ satisfying $u(x) \rightarrow 0$ as $x \rightarrow \infty$, while every solution linearly independent of this particular solution tends to ∞ .

(¹) A. KNESER: *Journ. für die reine und angewandte Mathem.*, **116**, 178 (1926); see also P. HARTMAN and A. WINTNER: *Amer. Journ. of Mathem.*, **70**, 462 (1948).

This implies that the bounded solution in case (II) must satisfy also the (L^2) -condition. The (L^2) -condition eq. (2), where E is arbitrary, cannot of course be interpreted that every E is an eigenvalue. The eigenvalues are selected only by a boundary condition assigned for $x = 0$, if the point $x = 0$ is a limit circle point (Grenzkreis type). As pointed by VON NEUMANN ⁽²⁾ and others ⁽³⁾ all normalizable solutions of the quantum mechanical wave equation are meaningful and acceptable and they are sufficient to give correct results if problems associated with the ordinary continuous spectrum are excluded. This assumption as will be shown in this paper is fulfilled for non singular and singular potentials if we require that the Wronskian of the unbounded solution $u_1(x)$ and of the bounded solution $u_2(x)$ vanishes. The vanishing of the Wronskian gives us correct eigenvalues and eigenfunctions. The vanishing of the Wronskian causes that the unbounded solution $u_1(x)$ passes, for such E_n which are eigenvalues, to the solution $u_2(x)$ bounded for every E . The eigenvalues E_n are determined by the zeros of the Wronskian. Further the vanishing of the Wronskian causes that

$$(3) \quad \int_0^{\infty} u_n(x) dx < \infty.$$

At first we give two examples for non singular potential. In case of the one-dimensional harmonic oscillator the Schrödinger equation is as known

$$(4) \quad -\frac{\hbar^2}{2m} \frac{d^2 u}{dx^2} + \frac{1}{2} kx^2 u = Eu.$$

Putting $z = \alpha x$ we have then to solve the equation

$$(5) \quad \frac{d^2 u}{dz^2} + (\lambda - z^2)u = 0,$$

where

$$(6) \quad \alpha^4 = \frac{mk}{\hbar^2} \quad \text{and} \quad \lambda = \frac{2E}{\hbar} (m/k)^{\frac{1}{2}} = 2E/\hbar\omega_c.$$

The Wronskian of eq. (5) is

$$(7) \quad W(u_1, u_2) = u_1(z)u_2'(z) - u_2(z)u_1'(z) = -(1 + \exp[-\pi i \lambda])^2 \cdot 2^{\frac{1}{2}} \cdot \lambda^{1/2} \pi^{\frac{1}{2}} \Gamma\left(\frac{1}{2} - \frac{\lambda}{2}\right).$$

This has zeros at the points $\lambda_n = 2n + 1$, they are double zeros for $n < 0$, single for $n \geq 0$ (on account of the poles of the Γ -functions). Substituting for λ_n eq. (6) we obtain the well known eigenvalues E_n ,

$$(8) \quad E_n = (n + \frac{1}{2})\hbar\omega_c, \quad \text{where } n = 0, 1, 2, 3.$$

⁽²⁾ J. VON NEUMANN: *Mathematical Foundations of Quantum Mechanics* (Princeton, 1955).

⁽³⁾ K. KOIDARA and T. KATO: *Progr. Theor. Phys.*, **3**, 439 (1948); G. FALK and H. MARSHALL: *Zeits. Phys.*, **134**, 269 (1952); T. TIETZ: *Ann. d. Phys.*, **15**, 79 (1954); *Nuovo Cimento*, **12**, 449 (1954); *Acta Phys. Hung.*, **5**, 347 (1955); *Žurn. Éxsp. Teor. Fiz. USSR*, **30**, 948 (1956); *Translation Sov. Phys.*, **3**, 777 (1956).

For the spherical harmonic oscillator the Schrödinger equation is

$$(9) \quad \frac{d^2 R_l}{dr^2} + \left[\frac{2m}{\hbar^2} \left(E - \frac{m}{2} \omega^2 r^2 \right) - \frac{l(l+1)}{r^2} \right] R_l = 0.$$

Substituting $x = \beta r$ we obtain

$$(10) \quad \frac{d^2 R_l}{dx^2} + \left[\lambda - x^2 - \frac{\alpha^2 - \frac{1}{4}}{x^2} \right] R_l = 0,$$

where

$$(11) \quad 2mE/\beta^2\hbar^2 = \lambda, \quad (m\omega/\beta^2\hbar)^2 = 1 \quad \text{and} \quad \alpha^2 = (l + \frac{1}{2})^2.$$

The Wronskian of eq. (10) is

$$(12) \quad W({}_1R_l(x); {}_2R_l(x)) = \frac{8\pi^2 \exp[(i\pi/4)(\lambda - 2\alpha - 2)]}{\Gamma[\frac{1}{4}(2\alpha + 2 - \lambda)] \Gamma[\frac{1}{4}(2\alpha + 2 + \lambda)]}.$$

Now $1/W({}_1R_l(x); {}_2R_l(x))$ has poles at the points $\lambda_{n_1} = \pm(4n_1 + 2\alpha + 2)$ where $n_1 = 0, 1, 2, 3 \dots$ Using λ_{n_1} and eq. (11) we obtain the well known eigenvalues

$$(13) \quad E_n = (n + \frac{3}{2})\hbar\omega, \quad \text{where } n = 0, 1, 2, 3 \dots$$

Next we consider the examples for discrete states of singular potential problems. For the hydrogen atom the Schrödinger equation is

$$(14) \quad \frac{d^2 R_l}{dr^2} + \left[\frac{2m}{\hbar^2} \left(E + \frac{Ze^2}{r} \right) - \frac{l(l+1)}{r^2} \right] R_l = 0.$$

The Wronskian of the two linearly independent solutions ${}_1R_l(r)$ and ${}_2R_l(r)$ is ⁽⁴⁾

$$(15) \quad W({}_1R_l, {}_2R_l) = \frac{-2\pi i (2is)^{-(2l+1)} (1 - \exp[2i\pi k])}{(l-k)(l-k-1) \dots (-l-k)},$$

where

$$(16) \quad k = \frac{1}{2} ic/s, \quad s^2 = \frac{2m}{\hbar^2} E \quad \text{and} \quad c = \frac{2m}{\hbar^2} Ze^2.$$

The zeros of $W({}_1R_l, {}_2R_l)$ are $k_{n_1} = l + n_1 + 1$ and $n_1 = 0, 1, 2 \dots$

Eq. (16) and k_{n_1} gives us the well known eigenvalues E_n .

$$(17) \quad E_n = -\frac{mZ^2e^4}{2\hbar^2n^2}, \quad \text{where } n = 1, 2, 3.$$

(4) E. C. TITCHMARSH: *Eigenfunction Expansions* (Oxford, 1946).

Further we consider the one-dimensional Schrödinger equation for an attractive potential

$$(18) \quad V(x) = -V_0 f(x) x^{-k} \quad \text{and} \quad f(0) = 1.$$

Then

$$(19) \quad u'' + [U_0 f(x) x^{-k} - \eta^2] u = 0,$$

where

$$(20) \quad U_0 = 2mV_0/\hbar^2 \quad \text{and} \quad \eta^2 = -2mE/\hbar^2, \quad (\eta = i\lambda, E > 0):$$

This equation was discussed for the first time by CASE⁽⁵⁾ and later by SCARF⁽⁶⁾ for $k=2$. We have written this Schrödinger equation in the notation of Scarf. If we adopt $f(x) = [1 + 2\nu x/U_0]$ and $k=2$ then the two linear independent solutions $w_1(x)$ and $w_2(x)$ of equation (18) are

$$(21) \quad \begin{cases} w_1(x) = \exp[-\eta x] x^{\frac{1}{2}+s} {}_1F_1(\frac{1}{2} + s - \nu/\eta; 1 + 2s; 2\eta x), \\ w_2(x) = \exp[-\eta x] x^{\frac{1}{2}-s} {}_1F_1(\frac{1}{2} - s - \nu/\eta; 1 - 2s; 2\eta x), \end{cases}$$

where $s = (\frac{1}{4} - U_0)^{\frac{1}{2}}$ and ${}_1F_1(a, c, x)$ is a confluent hypergeometric function. If $U_0 > \frac{1}{4}$ and s is imaginary ($s = iv$) then $w_1(x)$ and $w_2(x)$ are quadratic near the origin. The solutions $w_1(x)$ and $w_2(x)$ are unbounded for $x = \infty$. The Wronskian $W(w_1(x), w_2(x))$ is different from zero for every fixed E . Since both solutions $w_1(x)$ and $w_2(x)$ are quadratic integrable near the origin as also unbounded for $x = \infty$ we have to take into consideration such solutions $u_1(x)$ and $u_2(x)$ from which one would be unbounded for $x = \infty$ for such values of E which are not eigenvalues E_n and the other would be linearly independent bounded for every fixed E for $x = \infty$. The above discussed solutions $u_1(x)$ and $u_2(x)$ are

$$(22) \quad \begin{cases} u_1(x) = A_s(\eta) w_1(x) + B_s(\eta) w_2(x), \\ u_2(x) = (2\eta)^s \frac{\Gamma(\frac{1}{2} + s - \nu/\eta)}{\Gamma(1 + 2s)} w_1(x) - (2\eta)^{-s} \frac{\Gamma(\frac{1}{2} - s - \nu/\eta)}{\Gamma(1 - 2s)} w_2(x), \end{cases}$$

where $A_s(\eta)$ and $B_s(\eta)$ are constants. The Wronskian $W(u_1(x), u_2(x))$ gives us

$$(23) \quad \begin{aligned} W(u_1(x), u_2(x)) = & -W(w_1(x), w_2(x)) [A_s(\eta) \cdot (2\eta)^{-s} \frac{\Gamma(\frac{1}{2} - s - \nu/\eta)}{\Gamma(1 - 2s)} + \\ & + B_s(\eta) \cdot (2s)^s \frac{\Gamma(\frac{1}{2} + s - \nu/\eta)}{\Gamma(1 + 2s)}], \end{aligned}$$

since $W(w_1(x), w_2(x)) \neq 0$ for any η then the vanishing of $W(u_1(x), u_2(x))$ gives us

$$(24) \quad F_s(\eta) = \frac{B_s(\eta)}{A_s(\eta)} = - (2\eta)^{-2s} \frac{\Gamma(\frac{1}{2} - s - \nu/\eta) \Gamma(1 + 2s)}{\Gamma(\frac{1}{2} + s - \nu/\eta) \Gamma(1 - 2s)}.$$

⁽⁵⁾ K. M. CASE: *Phys. Rev.*, **80**, 797 (1950).

⁽⁶⁾ F. L. SCARF: *Phys. Rev.*, **109**, 2170 (1958).

In this way we obtained the well known results of Case and Scarf ⁽⁷⁾. The function $F_s(\eta)$ of eq. (24) is periodic with infinite number of poles and zeros at $(\frac{1}{2} \pm s - \nu/\eta) = -n$ where $n = 0, 1, 2, \dots$. The detailed discussions of $F_s(\eta)$ can be found in the mentioned paper of Scarf. The examples considered in this paper show that for non singular and singular potentials we obtain correct eigenvalues without any extra boundary conditions if only we assume that the Wronskian of two linearly independent solutions (one of these solutions $u_2(x)$ is bounded for $x = \infty$) should vanish. The vanishing of the Wronskian gives us also correct quadratic integrable eigenfunctions.

⁽⁷⁾ See reference ⁽⁶⁾.

Cross-Section and Polarization in Elastic Nucleon-Deuteron Scattering.

L. CASTILLEJO

Department of Mathematical Physics, University of Birmingham - Birmingham

L. S. SINGH (*)

Physics Department, University College - London

(ricevuto il 18 Novembre 1958)

There have recently been many interpretations of high energy nucleon-nucleon scattering experiments in terms of phase shifts. STAPPS *et al.* ⁽¹⁾ have obtained several sets of phase shifts which fit the proton-proton scattering data at 310 MeV and two of these sets Stapp (1) and Stapp (6) have been extended ⁽²⁾, assuming charge independence, to fit the neutron-proton scattering data. At 95 MeV and 140 MeV PHILLIPS ⁽³⁾ has similarly found several adequate sets of phase shifts (Phillips (1b), (2a), (3b), etc.). GAMMEL and THALER ⁽⁴⁾ (GT) have produced potentials which essentially reproduce one set of Stapp's phase shifts and also explain the low energy data. This potential has been used to calculate the scattering amplitudes at intermediate energies ⁽⁴⁾ and gives fair agreement with experiment. SIGNELL and MARSHAK ⁽⁵⁾ (SM) have independently found potentials which fit the data well up to 150 MeV. These investigations have shown that there is as yet no unique set of phase shifts to explain the nucleon-nucleon interaction at a given energy, though the potentials of Gammel and Thaler and of Signell and Marshak have rather similar long range parts which are most effective at these energies. It is therefore worth-while to look for other experiments which will provide further independent data. BETHE ⁽²⁾, BATTY ⁽⁶⁾ and OHNUMA ⁽⁷⁾ have discussed the scattering of protons from carbon at small angles, and the purpose of the present note is to show how far nucleon-deuteron cross sections and polarization will provide criteria for differentiating between the various sets of phase shifts. Because of the very loose structure of the deuteron the nucleon-deuteron scattering is dominated

(*) Now at the Department of Mathematical Physics, University of Birmingham.

⁽¹⁾ H. P. STAPP, T. J. YPSILANTIS and N. METROPOLIS: *Phys. Rev.*, **105**, 302 (1957).⁽²⁾ H. A. BETHE: *Ann. Phys.*, **3**, 200 (1958).⁽³⁾ R. J. N. PHILLIPS: *Proc. Phys. Soc.*, A **70**, 721 (1957); *Nuovo Cimento*, **5**, 1335 (1957).⁽⁴⁾ J. L. GAMMEL and R. L. THALER: *Phys. Rev.*, **107**, 291, 1337 (1957).⁽⁵⁾ P. S. SIGNELL and R. E. MARSHAK: *Phys. Rev.*, **109**, 1229 (1958).⁽⁶⁾ C. J. BATTY: *Proc. Phys. Soc.*, to be published.⁽⁷⁾ S. OHNUMA: *Phys. Rev.*, **111**, 1173 (1958).

by the individual nucleon-nucleon scattering over an appreciable range of angles, and should therefore provide different information from that obtained from proton-carbon scattering.

The nucleon-nucleon scattering matrix may be written ⁽⁸⁾

$$(1) \quad m = \lambda_1 + \lambda_2(\boldsymbol{\sigma}_1 + \boldsymbol{\sigma}_2) \cdot \mathbf{n}' + \lambda_3(\boldsymbol{\sigma}_1 \cdot \mathbf{K}')(\boldsymbol{\sigma}_2 \cdot \mathbf{K}') + \\ + \lambda_4(\boldsymbol{\sigma}_1 \cdot \mathbf{P}')(\boldsymbol{\sigma}_2 \cdot \mathbf{P}') + \lambda_5(\boldsymbol{\sigma}_1 \cdot \mathbf{n}')(\boldsymbol{\sigma}_2 \cdot \mathbf{n}'),$$

where the orthogonal unit vectors \mathbf{n}' , \mathbf{P}' , \mathbf{K}' are defined by

$$(2) \quad \mathbf{n}' = \frac{\mathbf{k}'_0 \times \mathbf{k}'}{|\mathbf{k}'_0 \times \mathbf{k}'|}, \quad \mathbf{P}' = \frac{\mathbf{k}'_0 + \mathbf{k}'}{|\mathbf{k}'_0 + \mathbf{k}'|}, \quad \mathbf{K}' = \frac{\mathbf{k}' - \mathbf{k}'_0}{|\mathbf{k}' - \mathbf{k}'_0|},$$

\mathbf{k}'_0 , \mathbf{k}' being the initial and final momenta of the incident nucleon in the c.m. system and $\boldsymbol{\sigma}_1$, $\boldsymbol{\sigma}_2$ the spins of the incident and target nucleons respectively.

Using the impulse approximation of Chew ⁽⁹⁾, we express the nucleon-deuteron scattering amplitude as the sum of the scattering amplitudes from the neutron and proton in the deuteron, times a form factor $S(\mathbf{q}) = \int \psi^2(\mathbf{r}) \exp[i\frac{1}{2}\mathbf{q} \cdot \mathbf{r}] d\mathbf{r}$ where \mathbf{q} is the momentum transferred in the collision and $\psi(\mathbf{r})$ is the deuteron wave function which we assume to be a pure S -state. Multiple scattering corrections and the shadowing effect discussed by GLAUBER ⁽¹⁰⁾ are neglected.

The neutron-deuteron scattering matrix for elastic scattering is then

$$(3) \quad M = G + \boldsymbol{\sigma} \cdot \mathbf{H},$$

where

$$(4) \quad \left\{ \begin{aligned} G &= \sqrt{4\pi} \left\{ A_1 Y_{00} T_{00}^+ + \frac{\sqrt{2}}{3} A_2 \sum_m Y_{1m}(\mathbf{n}) T_{1m}^+ \right\}, \\ \mathbf{H} \cdot \mathbf{K} &= \sqrt{4\pi} \left\{ \frac{\sqrt{2}}{3} A_3 \sum_m Y_{1m}(\mathbf{K}) T_{1m}^+ \right\}, \\ \mathbf{H} \cdot \mathbf{P} &= \sqrt{4\pi} \left\{ \frac{\sqrt{2}}{3} A_4 \sum_m Y_{1m}(\mathbf{P}) T_{1m}^+ \right\}, \\ \mathbf{H} \cdot \mathbf{n} &= \sqrt{4\pi} \left\{ \frac{\sqrt{2}}{3} A_5 \sum_m Y_{1m}(\mathbf{n}) T_{1m}^+ + A_2 Y_{00} T_{00}^+ \right\}. \end{aligned} \right.$$

The T_{JM} are deuteron spin operators defined by

$$\langle m | T_{JM} | m' \rangle = (-1)^{1-m'} C_{11}(m', -m; J, -M) \sqrt{3},$$

and

$$(5) \quad A_i = (\lambda_i^{\text{np}} + \lambda_i^{\text{nn}}) S(\mathbf{q}).$$

⁽⁸⁾ R. H. DALITZ: *Proc. Phys. Soc.*, A **65**, 175 (1952); L. WOLFENSTEIN and J. ASHKIN: *Phys. Rev.*, **85**, 947 (1952).

⁽⁹⁾ G. F. CHEW: *Phys. Rev.*, **80**, 196 (1950); **84**, 710, 1057 (1951).

⁽¹⁰⁾ R. J. GLAUBER: *Phys. Rev.*, **100**, 242 (1955).

The indices np and nn denote neutron-proton and neutron-neutron respectively. The A_i depend on the neutron-deuteron centre-of-mass momentum k and scattering angle θ and the λ_i on the corresponding variables k' , θ' for the nucleon-nucleon system. The connection implied in (5) is made by choosing the laboratory energy and the magnitude of momentum transfer $|\mathbf{q}|$ to be equal in both reactions, and the directions \mathbf{K} , \mathbf{P} , \mathbf{n} the same as \mathbf{K}' , \mathbf{P}' , \mathbf{n}' . This is the most convenient way to approximate to M when the λ_i are known only at one energy, and leads to $k' = \frac{3}{4}k$ and $\sin \theta'/2 = \frac{4}{3} \sin \theta/2$.

The neutron-deuteron differential cross section for elastic scattering is then

$$(6) \quad I(\theta) = \frac{1}{6} \text{Tr} (MM^+) (k/k')^2 = \frac{16}{9} \left\{ |A_1|^2 + |A_2|^2 + \frac{2}{3} (|A_2|^2 + |A_3|^2 + |A_4|^2 + |A_5|^2) \right\},$$

and the polarization of the scattered nucleon is

$$(7) \quad P(\theta) =$$

$$= \text{Tr} (MM^+ \boldsymbol{\sigma} \cdot \mathbf{n}) / \text{Tr} (MM^+) =$$

$$= \frac{16}{9I(\theta)} \left\{ 2 \text{Re} A_2^* \left(A_1 + \frac{2}{3} A_5 \right) \right\}.$$

The deuteron wave function ψ used in $S(\mathbf{q})$ was a pure S -wave with the shape given by MORAVCSIK⁽¹¹⁾, which is an approximation to the wave function for the Gartenhaus potential⁽¹²⁾. The differential

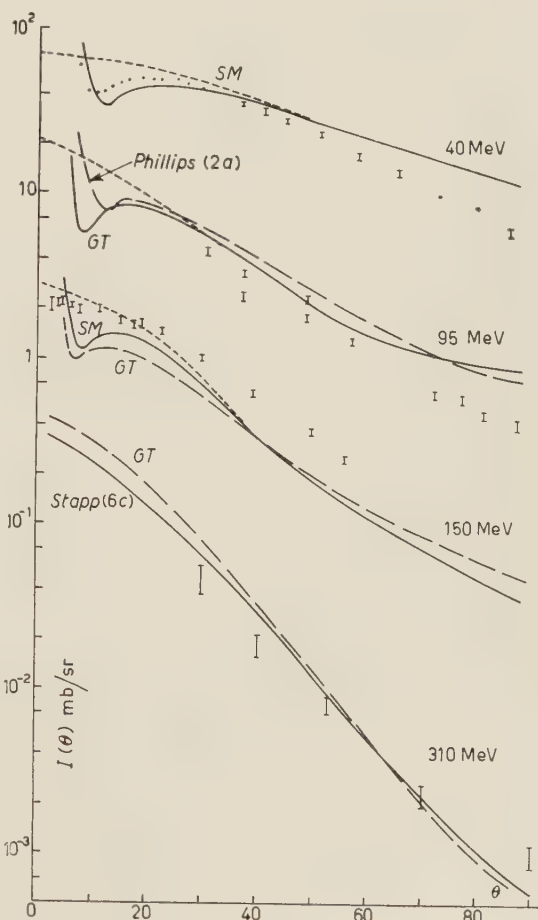


Fig. 1. — Nucleon-deuteron elastic cross sections. The curves at 95, 150 and 310 MeV are scaled by factors $\frac{1}{2}$, $1/10$, $1/50$ respectively. Those with sharp minima are for p-d the others for n-d scattering. The experimental points are: p-d at 40 MeV [WILLIAMS and BRUSSELS: *Phys. Rev.*, **110**, 136 (1958)]; p-d at 95 MeV [CHAMBERLAIN and STERN: *Phys. Rev.*, **94**, 666 (1954)]; n-d at 150 MeV [C. P. VAN ZYL: private communication]; p-d at 340 MeV [CHAMBERLAIN and CLARK: *Phys. Rev.*, **102**, 473 (1956)].

⁽¹¹⁾ M. J. MORAVCSIK: *Nucl. Phys.*, **7**, 113 (1958).

⁽¹²⁾ S. GARTENHAUS: *Phys. Rev.*, **100**, 900 (1955).

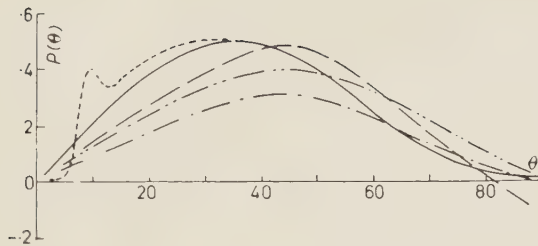


Fig. 2. — Nucleon polarization at 95 MeV. (p-d) SM ---; (n-d) SM —; (n-d) GT — — —; (n-d) PHILLIPS (2a) - · - · - (n-d) PHILLIPS (3b) · · · · ·.

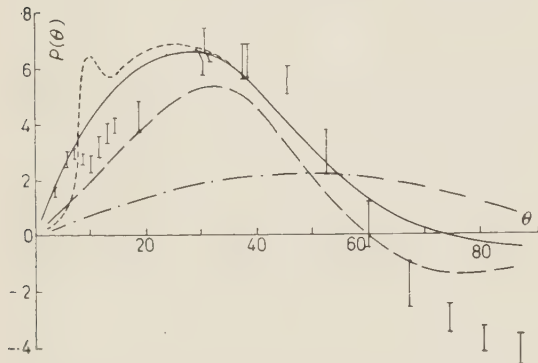


Fig. 3. — Nucleon polarization at 150 and 40 MeV. At 150 MeV: (p-d) Sm ---; (n-d) SM —; (n-d) GT — — —. At 40 MeV: (n-d) SM - · - · -. Experimental points at 147 MeV (p-d) [CORMACK *et al.* (14)].

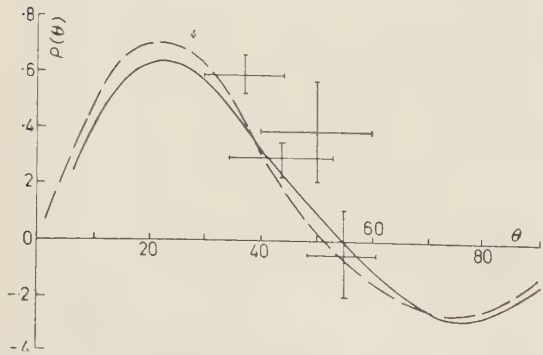


Fig. 4. — Nucleon polarization at 310 MeV; (n-d) GT —; (n-d) Stapp's solution (6c) - - - -; experimental points at 314 MeV (p-d) [MARSHALL *et al.* (13)].

cross section $I(\theta)$ depends on ψ but is sensitive to its shape only for large q . $P(\theta)$ is independent of $S(q)$.

The results for $I(\theta)$ due to various phase-shift analyses or potentials are shown in Fig. 1 for energies near 40, 95, 150 and 310 MeV. The experimental points are also plotted for comparison. Interference between the n-p and n-n scattering amplitudes is constructive for all sets of phase shifts at all angles and energies and contributes about 25% of the cross section. The Coulomb amplitude has been added to the amplitudes in (5) to give curves for p-d scattering. At large angles (above about 60°) the errors introduced by equation (5) may become appreciable and only the gross features of the curves can be relied on. Multiple scattering and other corrections will also become important for large θ .

The corresponding curves for $P(\theta)$ are plotted in Figs. 2, 3 and 4. The interference between the n-p and the n-n amplitudes is again constructive for all the curves and is large, producing about half of $P(\theta)$. There is fair agreement with experiment at 314 and 147 MeV (13,14).

Total n-d cross sections calculated from the imaginary part of the forward scattering amplitude are given in Table I, together with experimental values.

It is clear from the curves that $I(\theta)$ does not discriminate effectively between the

(13) L. MARSHALL, J. MARSHALL, D. NAGLE and W. SKOLNIK: *Phys. Rev.*, **95**, 1020 (1954).

(14) A. CORMACK, J. PALMERI, N. F. RAMSEY, R. WILSON and H. POSTMA: *Proc. Annual Conf. on High Energy Phys.* (Geneva, 1958). We are grateful for having been informed of these results before publication.

sets of phase shifts. $P(\theta)$, on the other hand, does discriminate between the various sets but this is partly because these phases predict slightly different polarization in nucleon-nucleon scattering. We therefore conclude that the measurement

TABLE I. — *Total n-d cross sections.*

Calculated			Experimental ⁽¹⁵⁾	
Model	Energy (MeV)	σ (mb)	σ (mb)	Energy (MeV)
SM	40	259	289 ± 13	42
GT	90	108	—	—
Phillips	95	113	104 ± 4	95 ± 5
SM	100	107	—	—
SM	150	82	70	153
GT	156	75	74	156
GT	310	66 }	57 ± 5	314 ± 8
Stapp (6)	310	60 }		

of n-d scattering and polarization is not a sensitive way to decide between sets of phases which fit the nucleon-nucleon data equally well. But p-d polarization is large and could perhaps be used instead of n-p polarization to obtain a best set of phases.

The effect of the D -wave in the deuteron will alter the structure of equations (4) and (5). The magnitude of this effect will be reported later.

* * *

We wish to thank Professor H. S. W. MASSEY for his encouragement and Professor R. E. PEIERLS and Dr. C. P. VAN ZYL for helpful discussions.

⁽¹⁵⁾ W. N. HESS: *Rev. Mod. Phys.*, **30**, 368 (1958).

Triple Scattering Parameters in Elastic Neutron-Deuteron Scattering.

L. CASTILLEJO

Department of Mathematical Physics, University of Birmingham - Birmingham

L. S. SINGH (*)

Physics Department, University College - London

(ricevuto il 18 Novembre 1958)

The triple scattering parameters defined by WOLFENSTEIN ⁽¹⁾ are the depolarization D and A , R , A' , R' , which describe the rotation of the direction of polarization. The measurements of these quantities in p-p scattering have been used to restrict phase shift solutions ⁽²⁾. Similar parameters can be defined for the elastic scattering of nucleons by deuterons and will depend on the interference between the scattering from the neutron and proton in the deuteron. They could give further information about the nucleon-nucleon scattering amplitudes. We report here some typical results obtained in impulse approximation from various nucleon-nucleon amplitudes which have been proposed ⁽³⁾.

The nucleon-deuteron elastic scattering matrix has been written ⁽⁴⁾

$$(1) \quad M = G + \sigma \cdot H,$$

G and the three components of H are approximated by adding neutron-proton and neutron-neutron amplitudes. But it is also necessary to decide the directions K, P, n of these approximate components of H (see I, Eq. (4)). To be consistent we should choose K, P, n to be the directions K', P', n' of I, Eq. (2) which appear in nucleon-nucleon scattering with the same magnitude of momentum transfer and laboratory energy. But it is more convenient to assume that P is the direction of the scattered nucleon in the laboratory system, $K = n \times P$ and $n = n'$. These definitions differ very little for small scattering angles.

(*) Now at the Department of Mathematical Physics, Birmingham.

⁽¹⁾ L. WOLFENSTEIN: *Phys. Rev.*, **96** 1654 (1954).

⁽²⁾ H. P. STAPP, T. J. YPSILANTIS and N. METROPOLIS: *Phys. Rev.*, **105** 302 (1957); H. A. BETHE: *Ann. Phys.*, **3** 200 (1958).

⁽³⁾ For references, see the preceding note.

⁽⁴⁾ Preceding note, referred to as I.

We then have the following results,

$$(2) \quad \begin{cases} ID(\theta) = \frac{16}{9} (\Gamma_1 + \Gamma_3), \\ IR(\theta) = \frac{16}{9} [-\Gamma_2 \sin \Theta + (\Gamma_1 + \Gamma_3) \cos \Theta], \\ IA(\theta) = \frac{16}{9} [-\Gamma_2 \cos \Theta - (\Gamma_1 + \Gamma_3) \sin \Theta], \\ IR'(\theta) = \frac{16}{9} [\Gamma_2 \cos \Theta + (\Gamma_1 + \Gamma_4) \sin \Theta], \\ IA'(\theta) = \frac{16}{9} [-\Gamma_2 \sin \Theta + (\Gamma_1 + \Gamma_4) \cos \Theta], \end{cases}$$

where Θ and θ are the scattering angles in the laboratory and c. of m. system respectively, $I(\theta)$ is the differential cross-section (I, Eq. (6)) and,

$$(3) \quad \begin{cases} \Gamma_1 = \frac{1}{6} \text{Tr} [GG^+ - \mathbf{H} \cdot \mathbf{H}^+], \\ \quad - |A_1|^2 + \frac{1}{3} |A_2|^2 - \frac{2}{3} [|A_2|^2 + |A_3|^2 + |A_4|^2 + |A_5|^2], \\ \Gamma_2 = 2 \text{Im} \frac{1}{6} \text{Tr} [G^+ \mathbf{H} \cdot \mathbf{n}] = 2 \text{Im} A_2^* \frac{2}{3} (A_5 - A_1), \\ \Gamma_3 = \frac{2}{6} \text{Tr} [(\mathbf{H} \cdot \mathbf{K})(\mathbf{H}^+ \cdot \mathbf{K})] = 2 \frac{2}{3} |A_3|^2, \\ \Gamma_4 = \frac{2}{6} \text{Tr} [(\mathbf{H} \cdot \mathbf{P})(\mathbf{H}^+ \cdot \mathbf{P})] = 2 \frac{2}{3} |A_4|^2, \\ \Gamma_5 = \frac{2}{6} \text{Tr} [(\mathbf{H} \cdot \mathbf{n})(\mathbf{H}^+ \cdot \mathbf{n})] = 2 [|A_2|^2 + \frac{2}{3} |A_5|^2]. \end{cases}$$

and the A_i are given in terms of the nucleon-nucleon amplitudes in I, Eq. (5). If the A_i are replaced by λ_i and the factors $\frac{2}{3}$, $\frac{1}{3}$ and $\frac{16}{9}$ by unity, eqs. (2) and (3) describe nucleon-nucleon scattering.

In this approximation, where the deuteron wave function is taken to be a pure s -state, these n -d triple scattering parameters are independent of the shape of this wave function. A striking feature of all the results is that those parts which arise from interference between the scattering from the two nucleons in the deuteron are about as large, and of the same sign, as the remaining terms.

In Fig. 1, $D(\theta)$, $R(\theta)$ and $R'(\theta)$ are plotted for GT (GAMMEL and THALER) ⁽⁵⁾ and Stapp's solution (6c) phases ⁽²⁾. The two curves for $D(\theta)$ differ near 40° though the corresponding results for p - p scattering are similar. But this is only partly due to interference terms as the n - p predictions of GT and STAPP (6c) also differ at the corresponding angles. The

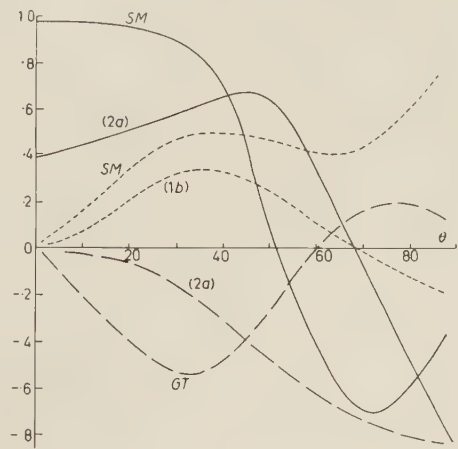


Fig. 1. — $D(\theta)$, $R(\theta)$ and $R'(\theta)$ at 310 MeV. On the curve SM stands for Stapp's solutions (6c). $D(\theta)$ - - - - - ; $R(\theta)$ — — — ; $R'(\theta)$ — — — .

⁽⁵⁾ J. L. GAMMEL and R. M. THALER: *Phys. Rev.*, **107**, 291, 1337 (1957).

curves for R , R' , A and A' are similar up to 50° and only differ where there is little experimental data to determine the nucleon-nucleon amplitudes.

At 150 MeV the results from SM (SIGNELL and MARSHAK) ⁽⁶⁾ and GT phases are compared in Fig. 2. The curves for D and R' show differences which again

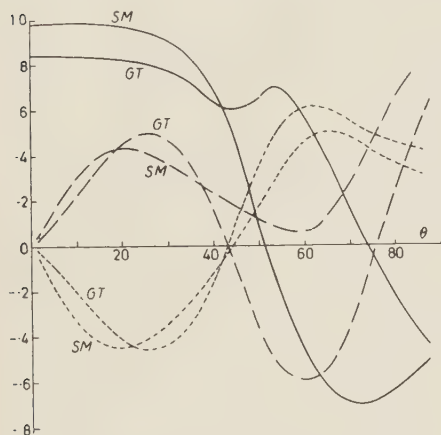


Fig. 2. — $D(\theta)$, $A(\theta)$ and $R'(\theta)$ at 150 MeV. $D(\theta)$ —; $R'(\theta)$ — — —; $A(\theta)$ — · — ·.

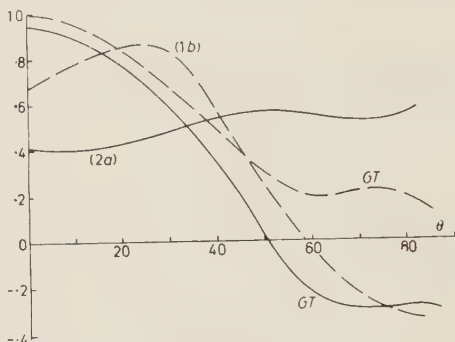


Fig. 3. — $A'(\theta)$ and $R(\theta)$ at 95 MeV. $A'(\theta)$ — · — ·; $R(\theta)$ — — —. Curves (1b) and (2a) belong to Phillip's solutions (1b) and (2a) respectively.

correspond to differences in the nucleon-nucleon predictions for D and R' . GT and SM phases produce very similar results for A , E and A' .

At 95 MeV GT and SM give very similar n-d triple scattering parameters. We

have therefore compared these with some of the results using Phillip's phase shifts ⁽⁷⁾ and in Figs. 3 and 4 show those curves which differ most from the GT or SM predictions. In all cases it is just as easy to distinguish between sets of phases by testing predictions for nucleon-nucleon scattering as to do so by studying neutron-neutron scattering. But nevertheless, the results reported here indicate that n-d scattering appears to be a useful alternative to some of the nucleon-nucleon data.

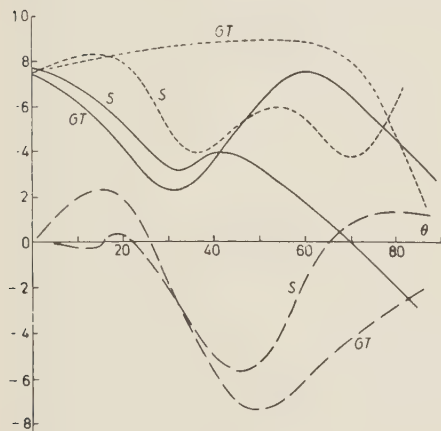


Fig. 4. — $D(\theta)$, $A(\theta)$ and $R'(\theta)$ at 95 MeV. $D(\theta)$ — — —; $R'(\theta)$ — · — ·; $A(\theta)$ — · — ·.

We thank Professors H. S. W. MASSEY and R. E. PEIERLS for their interest in this work.

⁽⁶⁾ P. S. SIGNELL and R. F. MARSHAK: *Phys. Rev.*, **109** 1229 (1958).

⁽⁷⁾ R. J. N. PHILLIPS: *Proc. Phys. Soc.*, **A70** 721 (1957).

The Debye Effect in Electrolytic and Colloidal Solutions in High Frequency Acoustic Fields.

A. CARRELLI, G. COZZA and F. GAETA

Istituto di Fisica dell'Università - Napoli

(ricevuto il 26 Novembre 1958)

The theory of Debye ⁽¹⁾ on electrolytic solutions under ultrasonic fields predicts a difference of potential between two planes of the same solutions, at the distance Δx in the direction of waves propagation. In order to understand the origin of ΔV we must think that when in a fluid ultrasonic waves are travelling in a particular direction, all the planes at the distance x from the source will move at time t in the same way across the direction of the x axis. The constituents of the fluid are moving with velocity changing from one plane to one other, and in the same plane there is a further change from time to time. Accordingly in such a fluid we have accelerations; if in the system there are ions with various masses they move with different velocity, namely the heavy particles are slow in comparison with the light particles. Furthermore if the particles with different masses are charged, their different inertia produces a separation of charges resulting in a difference of potential between planes at different x coordinates.

According to the calculations of

Debye (in the case of a binary salt), the amplitude ΔV_0 of the potential wave, produced in such a way along the x axis, is as follows:

$$(1) \quad \Delta V_0 = 1.4 \cdot 10^{-7} a_0 \frac{M_1/\varrho_1 - M_2/\varrho_2}{1/\varrho_1 + 1/\varrho_2},$$

where ϱ_1 and ϱ_2 are friction constants, a_0 is the velocity amplitude, and M_1 , M_2 are the masses of the two ions present in the solution.

It is easy to get a value for $a_0 = 1$ cm/s; consequently with salts which have large differences relative to the M/ϱ quotients, ΔV_0 may be as low as 10^{-6} V.

The calculations of Debye have been modified later by HERMANS ⁽²⁾ (but in a way which didn't affect the predicted order of magnitude of the potential). HERMANS extended this theory to the colloid solutions ⁽³⁾, predicting a difference of potential up to 10^{-3} V, even in the range of some volts, when proper assumptions are advanced in relation to the structure of these solutions, *i.e.* if the size of colloid particle is small or

⁽¹⁾ DEBYE: *Chem. Phys.*, **1**, 13 (1933).

⁽²⁾ J. J. HERMANS: *Phil. Mag.*, **7**, 426 (1938).

⁽³⁾ J. J. HERMANS: *Phil. Mag.*, **7**, 674 (1938).

large in comparison with that of the double layer surrounding the particle.

Thus in the present paper, we report an attempt to check the predicted effect which seems to be important in the theory of liquids. In this connection a suitable apparatus has been constructed to detect differences of alternate potential in the range of 10^{-6} V. The apparatus is set with an oscillator connected to a piezoelectric quartz (frequency: 495 kHz) immersed in a liquid contained in a plexiglass cell with a mirror which generates steady waves. The cell is provided with two glass windows which permit by means of an optical system to show an ultrasonic perturbation in the liquid of sufficient amplitude and that corresponding to a progressive or steady state.

Two metal pick-ups were introduced in the solution at a distance which can be modified up to 10^{-2} cm shiftings by means of a micrometer screw. The pick-ups are connected, by means of two screened wires, to an amplifier tuned to the frequency of the quartz; such an amplifier allows a gain of $3.5 \cdot 10^3$; the output current was straightened, then measured directly by a microammeter. The apparatus was calibrated in order to test satisfactory conditions. In this operations it was possible to detect differences of potential even as low as 10^{-6} V.

Using this apparatus we tested aqueous solutions of various colloids, including: gelatin, colloidal Ag, starch. In any case we could not confirm experimentally the effect predicted by the theory, also when in the same colloidal solutions were travelling progressive waves.

The investigation was extended also to when there is the permanence of the ultrasonic pattern ascribed to steady waves in colloidal solution when the vibration is over; the phenomenon consists ⁽⁴⁾ in a packing of particles at the

loops which produces a difference of static potential when the particles are charged in respect of the solvent. Also in this case we obtained negative results.

A new attempt of looking for the Debye effect in simple electrolytic solutions, which give ideal experimental conditions, did not allow us to verify the effect. We used also calcium caseinate as a salt of two ions of largely different masses, and therefore supposed to give a marked effect as predicted by the theory. The evidence, even in this case, was negative.

In order to give the theoretical value of ΔV_0 we must know the experimental value of a_0 , i.e. the amplitude of the shifting velocity of particles in the liquid which is subjected to the ultrasonic field.

From the equation

$$(2) \quad (\Delta p)_0 = \frac{2\pi}{\lambda} \gamma p s_0,$$

we can obtain s_0 .

On the other hand

$$(3) \quad (\Delta n)_0 = \frac{1}{\varepsilon} \frac{(n^2 + 2)(n^2 - 1)}{6n} (\Delta p)_0,$$

$$(4) \quad \Delta n = r \frac{\lambda'}{2\pi L},$$

where λ' is the wave length of the sodium light used, L is the diameter of the quartz employed in the equipment, r is a parameter which may be obtained experimentally by the plots by SANDERS ⁽⁵⁾, which agree with the Raman theory we used also to construct the above mentioned optical method ⁽⁶⁾. From eqs. (2), (3) and (4) we have:

$$(5) \quad \frac{2\pi}{\lambda} \gamma k p s_0 \frac{1}{\varepsilon} \frac{(n^2 + 2)(n^2 - 1)}{6n} = r \frac{\lambda'}{2L\pi}$$

By measuring r we obtain s_0 from (5)

⁽⁵⁾ H. SANDERS: *Can. Journ. Res.*, A **14**, 158 (1936).

⁽⁶⁾ C. V. RAMAN and N. S. NAGENDRA: *Nath. I, II, III, IV, V Proc. Ind. Acad. Sci.*, 2, 3 (1935-1936).

⁽⁴⁾ A. CARRELLI and F. PORRECA: *Nuovo Cimento*, **9**, 90 (1952).

and accordingly a_0 , resulting in

$$a_0 \approx 5.8 \text{ cm/s.}$$

Furthermore from (1) we have:

$$\Delta V_0 \cong 3.8 \cdot 10^{-4} \text{ V.}$$

These results do show that the measurement fit pretty well in the sensitivity of our apparatus; nevertheless we were unable to verify the predicted effect.

In order to account for the experimental failure we may think that ions in a strongly polar solvent, *i.e.* water, are surrounded by the dipoles in aggregates more or less stable.

A simple calculation, using the molecular diameter of water ($r=4 \cdot 10^{-8}$ cm) and the dipolar moment of water ($p=1.87 \cdot 10^{-18}$ e.s.u.) shows that:

$$E = \frac{e}{r^2} = \frac{4.8 \cdot 10^{-10}}{1.6 \cdot 10^{-16}} \cong \\ \cong 3.3 \cdot 10^{-5} \text{ e.s.u.} \cong 10^8 \text{ V/cm.}$$

therefore the energy of bond for each dipole to the ion will be:

$$pE = 1.87 \cdot 3.3 \cdot 10^{-13} = 6 \cdot 10^{-13} \text{ erg.}$$

We may get an idea of the stability for these aggregates by computing the thermal energy kT ; this factor is the only cause destroying the aggregates. At room temperature the product will be:

$$kT = 4 \cdot 10^{-15} \text{ erg.}$$

It follows:

$$pE/kT = 1.5 \cdot 10^{-2} \gg 1.$$

These results show that the aggregates are practically rigid. Accordingly the ion moves either because of an electrical field or mechanically under the action of acoustic waves, carrying on his surface at least one layer of dipoles of the solvent.

Since the aggregate carries on his surface only molecules of the solvent, the specific coefficient of friction (ϱ_1 in the equation of Debye) will be dependent only on the masses M_1 and M_2 of the aggregate, being practically independent of the inner ion. Namely one can think $M_1/\varrho_1 = M_2/\varrho_2$, then from (1): $\Delta V_0 = 0$.

Our results on colloidal solutions fit also in the above mentioned picture, since absorption of solvent molecules on colloidal particles occurs all over.

On the Symmetries Concerning the Scheme of Elementary Particles.

N. DALLAPORTA

Istituto di Fisica dell'Università - Padova
Istituto Nazionale di Fisica Nucleare - Sezione di Padova

(ricevuto il 6 Dicembre 1958)

The study of strong interactions has been based up to now on the Lagrangian

$$(1) \quad \mathcal{L} = g_1 \bar{N} i \gamma_5 \boldsymbol{\tau} \cdot \boldsymbol{\pi} N + g_2 [\bar{\Lambda}^0 i \gamma_5 \boldsymbol{\pi} \cdot \boldsymbol{\Sigma} + \text{h.c.}] + g_3 i (\bar{\boldsymbol{\Sigma}} i \gamma_5 \wedge \boldsymbol{\Sigma}) \cdot \boldsymbol{\pi} + g_4 \bar{\Xi} i \gamma_5 \boldsymbol{\tau} \cdot \boldsymbol{\pi} \Xi + \\ + (g_5 \bar{N} I_{N\Lambda} K \Lambda^0 + \text{h.c.}) + g_6 (\bar{N} \boldsymbol{\tau} I_{N\Sigma} \cdot \boldsymbol{\Sigma} K + \text{h.c.}) + \\ + g_7 (\bar{\Xi} \tau_2 I_{\Xi\Lambda} K^* \Lambda^0 + \text{h.c.}) + g_8 (\bar{\Xi} \tau_2 \boldsymbol{\tau} I_{\Xi\Sigma} \cdot \boldsymbol{\Sigma} K^* + \text{h.c.}),$$

used by d'Espagnat, Prentki and Salam ⁽¹⁾ in which the different baryon and meson states are grouped according to the well-known following isospin multiplets:

$$(1a) \quad \left\{ \begin{array}{l} N = \begin{vmatrix} p \\ n \end{vmatrix}, \quad \Xi = \begin{vmatrix} \Xi^0 \\ \Xi^- \end{vmatrix}, \quad \Sigma = \begin{vmatrix} \Sigma_1 \\ \Sigma_2 \\ \Sigma_3 \end{vmatrix}, \quad \begin{array}{l} \Sigma_1 = \frac{1}{\sqrt{2}} (\Sigma^+ + \Sigma^-), \\ \Sigma_2 = \frac{1}{\sqrt{2}i} (\Sigma^- - \Sigma^+), \end{array} \\ \pi = \begin{vmatrix} \pi_1 \\ \pi_2 \\ \pi_3 \end{vmatrix}, \quad \begin{array}{l} \pi_1 = \frac{1}{\sqrt{2}} (\pi + \pi^*) \\ \pi_2 = \frac{1}{\sqrt{2}i} (\pi - \pi^*), \\ \pi_3 = \pi^0, \end{array} \quad \begin{array}{l} \Sigma_3 = \Sigma^0, \\ K = \begin{vmatrix} K^+ \\ K^0 \end{vmatrix}. \end{array} \end{array} \right.$$

Another kind of Lagrangian has been proposed in a paper by PAIS ⁽²⁾, namely:

$$(2) \quad \mathcal{L} = i[G_1 \bar{N}_1 \boldsymbol{\tau} \gamma_5 N + G_2 \bar{N}_2 \boldsymbol{\tau} \gamma_5 N_2 + G_3 \bar{N}_3 \boldsymbol{\tau} \gamma_5 N_3 + G_4 \bar{N}_4 \boldsymbol{\tau} \gamma_5 N_4] \cdot \boldsymbol{\pi} + \\ + \sqrt{2} [F_1 \bar{N}_1 I_1 N_2 K^0 + F_2 \bar{N}_1 I_2 N_3 K^+ + F_3 N_4 I_3 N_2 \bar{K}^- - F_4 \bar{N}_4 I_4 N_3 \bar{K}^0 + \text{h.c.}],$$

⁽¹⁾ B. D'ESPAGNAT and J. PRENTKI: *Nucl. Phys.*, **1**, 33 (1956); A. SALAM: *Nucl. Phys.*, **2**, 173 (1956); B. D'ESPAGNAT, J. PRENTKI and A. SALAM: *Nucl. Phys.*, **3**, 446 (1957).

⁽²⁾ A. PAIS: *Phys. Rev.*, **110**, 574 (1958).

in which all baryons are grouped into isospin doublets according to the definitions

$$(2a) \quad N_1 = \begin{pmatrix} p \\ n \end{pmatrix}, \quad N_2 = \begin{pmatrix} \Sigma^+ \\ Y^0 \end{pmatrix}, \quad N_3 = \begin{pmatrix} Z^0 \\ \Sigma^- \end{pmatrix}, \quad N_4 = \begin{pmatrix} \Xi^0 \\ \Xi^- \end{pmatrix},$$

and the states Z^0 and Y^0 are defined according to Gell-Mann (), in the approximation in which the Σ - Λ mass-difference is neglected, as:

$$(3) \quad Z^0 = \frac{1}{\sqrt{2}} (\Lambda^0 + \Sigma^0), \quad Y^0 = \frac{1}{\sqrt{2}} (\Lambda^0 - \Sigma^0).$$

The relation between these two Lagrangians is the following: one could assume that fundamentally the baryons are all isospin doublets of equal mass so that expression (2) is the fundamental interaction and the coupling and interaction constants of the different terms are linked together by the fundamental symmetries which rule the scheme. If now, owing to some physical reason which mixes the neutral baryons Z^0 and Y^0 to give Λ^0 and Σ^0 we substitute in (2) the Z^0 and Y^0 states according to relation (3) we get the terms of (1) and if adequate relations between the coupling and interaction constants of (2) subsist, namely:

$$(4) \quad \begin{cases} F_1 = F_2, & F_3 = F_4, \\ G_2 = G_3, \\ F_1 = F_2, & F_3 = F_4, \end{cases}$$

then we may obtain expression (1), and the values of coupling type and of the constants in (1) are determined by the assumptions made for the couplings and the constants in (2).

Up to now all K couplings were considered to be the same ^(3,4) (all scalar or all pseudoscalar) and with the assumption (4) for the constants, the transition from (2) to (1) was always possible so that the two lagrangians in the approximation of neglecting the mass difference between Λ^0 and Σ^0 could always be considered as equivalent. However, PAIS ⁽²⁾ has shown that such an assumption appears now to be incompatible with the experimental data and he has recently examined ⁽⁵⁾ the possibility that the parities of charged K's could be opposite to the parities of the neutral ones. If such an hypothesis is introduced into (2) it is no more possible to obtain (1) from it, as this formulation considers that K^+K^0 and \bar{K}^0K^- are isospin doublets and this grouping does not subsist any more according to the new assumption; therefore, in this case, the substitution of the fictitious particles Z^0 and Y^0 with the real ones Σ^0 and Λ^0 should lead to another Lagrangian in which charge independence in the ordinary sense is no more valid for K interactions.

A possible way of obtaining such an expression may be found in an alternative way of writing the same Lagrangian of Pais ⁽²⁾, which has been previously pro-

⁽³⁾ M. GELL-MANN: *Phys. Rev.*, **106**, 1296 (1957).

⁽⁴⁾ J. SCHWINGER: *Phys. Rev.*, **104**, 1164 (1956); *Ann. Phys.*, **2**, 407 (1957).

⁽⁵⁾ A. PAIS: private information kindly communicated by Prof. M. BLOCK.

posed by the author ⁽⁶⁾:

$$(5) \quad \mathcal{P} = \bar{\psi}_{jlm} [g_n \sum_{\alpha=1,2,3} \gamma_5 \tau_\alpha \pi_\alpha + g_{K_n} \sum_{\beta=1,2} \Gamma_n \omega_\beta \chi_\beta^n + g_{K_c} \sum_{\gamma=1,2} \Gamma_c \chi_\gamma^\zeta \chi_\gamma^\zeta] \psi_{j' l' m'} .$$

This expression is based on a scheme whose main feature consists also in grouping all baryons into doublets, but of three different kinds and labelled by three quantum numbers τ_3 , ω_3 , ζ_3 ; the first of these is the third component of normal isotopic spin ruling the emission and absorption of pions, while the second and third, (which are the same numbers as S_1 and S_2 of Pais: $\omega_3=S_2$, $\zeta_3=S_1$ for mesons; $\omega_3=S_2+\frac{1}{2}$, $\zeta_3=S_1+\frac{1}{2}$ for baryons) have the same function relatively to the two other isospins ω and ζ ruling the emission and absorption of the neutral K's (χ^n), and of the charged K's (χ^c) respectively; while the three indices of the baryon functions label the different isospins states (τ_3 , ω_3 , ζ_3) on which τ , ω , and ζ respectively act; the quantum numbers thus assigned both to baryons and mesons are given in Table I and the possible transitions are visualized in Fig. 1.

TABLE I.

	C	$U = S + 1$	τ_3	ω_3	ζ_3
p	+1	+1	$+\frac{1}{2}$	$+\frac{1}{2}$	$+\frac{1}{2}$
n	0	+1	$-\frac{1}{2}$	$+\frac{1}{2}$	$+\frac{1}{2}$
Σ^+	+1	0	$+\frac{1}{2}$	$-\frac{1}{2}$	$+\frac{1}{2}$
Y^0	0	0	$-\frac{1}{2}$	$-\frac{1}{2}$	$+\frac{1}{2}$
Z^0	0	0	$+\frac{1}{2}$	$+\frac{1}{2}$	$-\frac{1}{2}$
Σ^-	-1	0	$-\frac{1}{2}$	$+\frac{1}{2}$	$-\frac{1}{2}$
Ξ^0	0	-1	$+\frac{1}{2}$	$-\frac{1}{2}$	$-\frac{1}{2}$
Ξ^-	-1	-1	$-\frac{1}{2}$	$-\frac{1}{2}$	$-\frac{1}{2}$
		$U = S$			
π^0	0	0	0	0	0
π^+	+1	0	+1	0	0
π^-	-1	0	-1	0	0
K^0	0	+1	0	+1	0
\bar{K}^0	0	-1	0	-1	0
K^+	+1	+1	0	0	+1
\bar{K}^-	-1	-1	0	0	-1

C = Charge;

U = Hypercharge;

S = Strangeness.

In reference ⁽⁶⁾ the names of Z^0 and Y^0 were interchanged with respect to those given by Gell-Mann and Pais and the hypercharge U was named strangeness S ; here we have adopted the usual definitions of these authors.

⁽⁶⁾ N. DALLAPORTA: *Proceedings of the Conference on Mesons and Recently Discovered Particles* (Padua-Venice 1957); V, 3 Mimeogr. edition; *Nuovo Cimento*, **7**, 200 (1958) and J. TROMNO: *Nuovo Cimento*, **6**, 69 (1957).

In such a scheme, the possibility of opposite parities for charged and neutral K's may be introduced in a quite natural way, as in fact it considers the K-mesons as grouped into two triplets similar to the pion triplet; the neutral K triplet and the charged K triplet in each of which the components with hypercharge ± 1 are

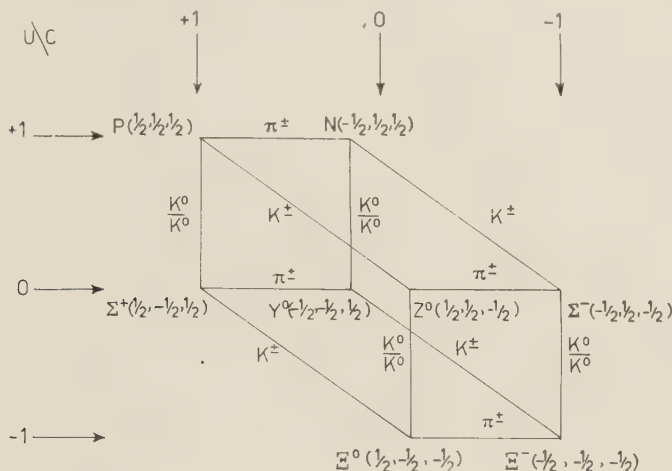


Fig. .

known while the third hypercharge component (which should possess the same quantum numbers as the π^0) is lacking or is still unknown. It is then sufficient to assume *i.e.* $I_n = i\gamma_5$, $I_c = 1$ or the reverse in order to obtain the desired effect. Now when we substitute in (5) the fictitious particles Z^0 , Y^0 by Σ^0 and Λ^0 we obtain the new expression (6)

$$\begin{aligned}
 (6) \quad \mathcal{L} = & g_\pi (N i \gamma_5 \boldsymbol{\tau} \cdot \boldsymbol{\pi} N + \bar{\Lambda}^0 i \gamma_5 \boldsymbol{\pi} \cdot \boldsymbol{\Sigma} + \text{h.c.} - i \bar{\boldsymbol{\Sigma}} i \gamma_5 \boldsymbol{\Lambda} \cdot \boldsymbol{\Sigma} \cdot \boldsymbol{\pi} + \bar{\boldsymbol{\Xi}} i \gamma_5 \boldsymbol{\tau} \cdot \boldsymbol{\pi} \boldsymbol{\Xi}) + \\
 & + g_{\tau_n} \{ \bar{J}_n \Gamma_n (\omega_1 K_{n_1} + \omega_2 K_{n_2}) \} J_n + \bar{\Lambda}^0 \Gamma_n (K_{n_1} S_{\tau_1} + K_{n_2} S_{\tau_2}) + \text{h.c.} - \\
 & - i [(S_n \Gamma_n \wedge S_n)_1 \cdot K_{n_1} + (S_n \Gamma_n \wedge S_n)_2 \cdot K_{n_2}] + [L_n \Gamma_n (\omega_1 K_{n_1} + \omega_2 K_{n_2}) L_n] \} + \\
 & + g_{K_c} \{ \bar{J}_c \Gamma_c (\zeta_1 K_{c_1} + \zeta_2 K_{c_2}) \} J_c + \bar{\Lambda}^0 \Gamma_c (K_{c_1} S_{c_1} + K_{c_2} S_{c_2}) + \text{h.c.} - \\
 & - i [(S_c \Gamma_c \wedge S_c)_1 K_{c_1} + (S_c \Gamma_c \wedge S_c)_2 K_{c_2}] + [L_c \Gamma_c (\zeta_1 K_{c_1} + \zeta_2 K_{c_2}) L_c] \} ,
 \end{aligned}$$

with the definitions

$$\begin{aligned}
 J_n = \begin{vmatrix} \mathbf{P} \\ \Sigma^+ \end{vmatrix}, \quad L_n = \begin{vmatrix} \Sigma \\ -\Xi^- \end{vmatrix}, \quad S_n = \begin{vmatrix} S_{n_1} \\ S_{n_2} \\ \Sigma^0 \end{vmatrix}, \quad S_{n_1} = \frac{1}{\sqrt{2}} (n - \Xi^0), \\
 S_{n_2} = \frac{1}{\sqrt{2}i} (-\Xi^0 - n), \\
 K_n = \begin{vmatrix} K_{n_1} \\ K_{n_2} \\ K_{n_3} \end{vmatrix}, \quad K_{n_1} = \frac{1}{\sqrt{2}} (K_n^* + K_n), \\
 K_{n_2} = \frac{1}{\sqrt{2}i} (K_n^* - K_n).
 \end{aligned}$$

$$J_c = \begin{vmatrix} \Sigma^+ \\ \Xi^0 \end{vmatrix}, \quad L_c = \begin{vmatrix} \mathbf{n} \\ \Sigma^- \end{vmatrix}, \quad S_c = \begin{vmatrix} S_{c_1} \\ S_{c_2} \\ -\Sigma^0 \end{vmatrix}, \quad S_{c_1} = \frac{1}{\sqrt{2}} (\mathbf{p} + \Xi),$$

$$S_{c_2} = \frac{1}{\sqrt{2}i} (\Xi^- - \mathbf{p}),$$

$$K_{c_1} = \begin{vmatrix} K_{c_1} \\ K_{c_2} \\ K_{c_3} \end{vmatrix}, \quad K_{c_1} = \frac{1}{\sqrt{2}} (K_c^* + K_c),$$

$$K_{c_2} = \frac{1}{\sqrt{2}i} (K_c^* - K_c),$$

where:

K_n destroys K^0 and creates \bar{K}^0 , K_n^* destroys \bar{K}^0 and creates K^0 ,

K_r destroys K^+ and creates \bar{K}^- , K_c^* destroys \bar{K}^- and creates K^+ .

In (6) the pion terms are charge independent, but not the K terms; the neutral K interactions are invariant for rotations in the 1, 2 plane of the ω spin space and ω_3 is conserved for them; the charged K interactions are invariant for rotations in the 1, 2 plane of the ζ spin and ζ_3 is conserved.

If now, in order to go further, we would postulate the possible existence of the neutral components K_{n_3} and K_{c_3} of the two K triplets, and add them to the other terms, we should obtain the following lagrangian (7)

$$(7) \quad \mathcal{L} = g_\pi (\bar{\mathbf{N}} i \gamma_5 \boldsymbol{\tau} \cdot \boldsymbol{\pi} \mathbf{N} + \bar{\Lambda}^0 i \gamma_5 \boldsymbol{\pi} \cdot \boldsymbol{\Sigma} + \text{h.c.} - i \bar{\boldsymbol{\Sigma}} i \gamma_5 \wedge \boldsymbol{\Sigma} \cdot \boldsymbol{\pi} + \Xi i \gamma_5 \boldsymbol{\tau} \cdot \boldsymbol{\pi} \Xi) +$$

$$+ g_{K_n} (J_n \Gamma_n \boldsymbol{\omega} \cdot \mathbf{K}_n J_n + \bar{\Lambda} \Gamma_n \mathbf{K}_n \cdot \mathbf{S}_n + \text{h.c.} - i S_n \Gamma_n \wedge \mathbf{S}_n \cdot \mathbf{K}_n + \bar{L}_n \Gamma_n \boldsymbol{\omega} \cdot \mathbf{K}_n L_n) +$$

$$+ g_{K_c} (\bar{J}_c \Gamma_c \boldsymbol{\zeta} \cdot \mathbf{K}_c J_c + \bar{\Lambda}^0 \Gamma_c \mathbf{K}_c \cdot \mathbf{S}_c + \text{h.c.} - i S_c \Gamma_c \wedge \mathbf{S}_c \cdot \mathbf{K}_c + \bar{L}_c \Gamma_c \boldsymbol{\zeta} \cdot \mathbf{K}_c L_c).$$

It then appears that in this situation, charge independence or conservation of total isospin T holds for pion interaction only: while for neutral K interactions we have a corresponding conservation of total ω , and for charged K 's interactions conservation of total ζ , which should be the laws substituting isospin conservation for the K -meson interactions. These conservation laws however should of course be only approximate owing to the baryon mass differences.

Thus both in (6) and (7) there is a kind of hexagonal symmetry evident from Fig. 2, by which the interaction terms related to the pions, the neutral K 's and the charged K 's, assume an exactly similar form and connect exactly similar groups of baryon states. The quantum numbers corresponding to the particles as designed in Fig. 2 are given in Table II (7).

The numbers written in brackets in Table II correspond only to the situation in which the interaction constants and the coupling type should be the same

(7) These numbers τ_3 and ω_3 for the labelling of baryon states were already proposed in C. CEOLIN and N. DALLAPORTA: *Nuovo Cimento*, **3**, 586 (1956).

TABLE II.

	C	$U = S + 1$	τ_3	ω_3	ζ_3
p	1	1	$+\frac{1}{2}$	$+\frac{1}{2}$	+1
n	0	1	$-\frac{1}{2}$	+1	$+\frac{1}{2}$
Λ^0	0	0	0	0	0
Σ^+	1	0	+1	$-\frac{1}{2}$	$+\frac{1}{2}$
Σ^0	0	0	0	0	0
Σ^-	-1	0	-1	$+\frac{1}{2}$	$-\frac{1}{2}$
Ξ^0	0	-1	$+\frac{1}{2}$	-1	$-\frac{1}{2}$
Ξ^-	-1	-1	$-\frac{1}{2}$	$-\frac{1}{2}$	-1

	$U = S$				
π^0	0	0	0	0	0
π^+	+1	0	+1	$0(-\frac{1}{2})$	$0(+\frac{1}{2})$
π^-	-1	0	-1	$0(+\frac{1}{2})$	$0(-\frac{1}{2})$
K^0	0	+1	$0(-\frac{1}{2})$	+1	$0(+\frac{1}{2})$
\bar{K}^0	0	-1	$0(+\frac{1}{2})$	-1	$0(-\frac{1}{2})$
K^+	+1	+1	$0(+\frac{1}{2})$	$0(+\frac{1}{2})$	+1
K^-	-1	-1	$0(-\frac{1}{2})$	$0(-\frac{1}{2})$	-1

and the grouping in isospin doublets of K^+ and K^0 and so on is still possible. Obviously, relations between charge C , hypercharge U and the different isospins which follow from this table when the full symmetry is allowed, are:

$$(8) \quad \begin{cases} C = \tau_3 + \frac{U}{2}, \\ U = \omega_3 + \frac{C}{2}, \\ C + U = 2\zeta_3. \end{cases}$$

When the interaction constants are different this grouping breaks up and only the numbers without brackets conserve their meaning and relations (8) for mesons are no longer valid.

Should we go still a step further and assume that, apart from the perturbations which according to a precedent suggestion⁽⁶⁾ are thought to be responsible for

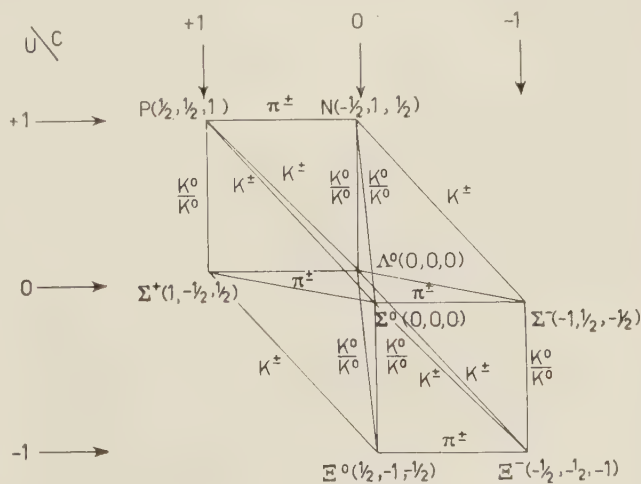


Fig. 2.

the mixing of Z^0 and Y^0 to give Λ^0 and Σ^0 and for the splitting of the masses of the baryons, there are also more fundamental reasons to disturb the original scheme of the baryons, as could be e.g. different intrinsic parities of the different baryons themselves, combined with different intrinsic parities of the three kinds of mesons, then the different terms of Lagrangians (5), (6) or (7) could be further distinguished by different kinds of coupling and of interaction strengths which could still provide a much wider choice of interaction possibilities in order to meet the experimental evidence without destroying the hexagonal symmetry if appropriate conditions between the couplings and strengths of the different terms should be respected. We shall not consider here the detailed aspects of these possibilities.

For what concerns the hypothetical K_s^0 and K_s^+ meson states, if they exist, it is unlikely that any of them should have a mass similar to that of the π^0 -meson, because in this case it should have been confused with it and its production should have apparently spoiled the experimental agreement with charge independence of π interaction. On the contrary, should anyone of them possess a mass high enough, it could, if scalar, decay into two π -mesons with a lifetime of the order of 10^{-23} and therefore easily escape detection and be confused with double pion production.

As a last remark one may observe that, should the parity of charged and neutral K's turn out to be effectively opposite, there would be no more objection to the assumption of direct $KK\pi$ interactions. Such an interaction could be from one side responsible for the splitting of the baryon masses; and it should be helpful also for correcting the predictions obtained by Pais according to the symmetry scheme for the cross section for strange particles production by pions in order to bring them closer to the experimental evidence.

* * *

I am thankful to Drs. C. CEOLIN and L. TAFFARA for discussion on some points of the subject.

Una particolare rappresentazione integrale della funzione $\Delta_1^{(+)}(\xi; a)$.

E. MONTALDI

Istituto di Scienze Fisiche dell'Università - Milano
Istituto Nazionale di Fisica Nucleare - Sezione di Milano

(ricevuto il 15 Dicembre 1958)

È ben noto che il valore di aspettazione di vuoto di un prodotto di $n+1$ campi scalari può scriversi come segue:

$$(1) \quad \langle 0 | A_1(x_1) \dots A_{n+1}(x_{n+1}) | 0 \rangle = i^n \int \prod_{k=1}^n da_{kl} G(-a_{kl}) \Delta_{n+1}^{(+)}(\xi_1, \dots, \xi_n; a_{kl}),$$

dove $G(-a_{kl})$ è una funzione peso — diversa da zero solo per valori positivi delle a_{kl} — e $\Delta_{n+1}^{(+)}(\xi; a)$ è una funzione singolare generalizzata, definita da:

$$(2) \quad \Delta_{n+1}^{(+)}(\xi; a) = \frac{(-i)^n}{(2\pi)^{3n}} \int \dots \int d^4p_1 \dots d^4p_n \exp \left[i \sum_{k=1}^n p_k \cdot \xi_k \right] \prod_{r \leq s=1}^n \delta(p_r \cdot p_s + a_{rs}) \prod_{l=1}^n \theta(p_{l,0});$$

$$\xi_k = x_k - x_{k+1}.$$

KÄLLÉN e WILHELMSSON ⁽¹⁾ hanno mostrato che, nella teoria di tali funzioni, il caso $n=4$ esplica un ruolo fondamentale; infatti, per $n > 4$, esistono formule di riduzione che permettono di esprimere la $\Delta_{n+1}^{(+)}$ in termini della $\Delta_5^{(+)}$, e, d'altra parte, basta eguagliare a zero le componenti di uno o più tetravettori ξ nella $\Delta_5^{(+)}$ per ottenere — a meno di un fattore di proporzionalità — i casi $n=1, 2$ e 3 ⁽²⁾.

Per questo motivo, i succitati Autori hanno studiato dettagliatamente la struttura della funzione $\Delta_5^{(+)}$, riuscendo a ricondurre le 16 integrazioni all'uopo necessarie ad una sola integrazione, coinvolgente funzioni di Hankel e funzioni elementari; essendo però il loro procedimento alquanto laborioso, ci è parso opportuno esaminare la possibilità di ottenere — per lo meno in qualche caso particolare — delle formule integrali semplificate. Nella presente nota faremo vedere che, sotto

⁽¹⁾ G. KÄLLÉN and H. WILHELMSSON: *Generalized singular functions* (Lecture notes, 1958).

⁽²⁾ Si noti, peraltro, che per $n=1$ e 2 è molto più agevole eseguire il calcolo diretto, senza passare attraverso la $\Delta_5^{(+)}$. Vedasi, ad esempio, D. HALL e A. S. WIGHTMAN: *Phys. Rev.*, **99**, 674 (1955).

l'ipotesi (*) che uno dei tetravettori ξ abbia lunghezza nulla, la funzione $\Delta_4^{(+)}$ ammette una semplice rappresentazione in termini della $\Delta_3^{(+)}$ (la cui espressione è conosciuta); la nostra deduzione poggia essenzialmente su una elementare proprietà delle funzioni di Bessel, ed evita in tal modo i lunghi sviluppi formali che sarebbero invece necessari se si passasse attraverso la funzione $\Delta_3^{(+)}$.

Consideriamo l'espressione di $\Delta_4^{(+)}(\xi; a)$:

$$(3) \quad \Delta_4^{(+)}(x, y, z; a_{11}, \dots, a_{23}) = \\ = \frac{i}{(2\pi)^9} \int d^4 p_1 d^4 p_2 d^4 p_3 \exp [i(p_1 \cdot x + p_2 \cdot y + p_3 \cdot z)] \prod_{r \leq s=1}^3 \delta(p_r \cdot p_s + a_{rs}) \prod_{k=1}^3 \theta(p_{k,0}).$$

Senza perdita di generalità, supporremo che siano verificate le condizioni:

$$(4) \quad a_{rs}^2 > a_{rr} \cdot a_{ss}, \quad r, s = 1, 2, 3,$$

per essere sicuri che la funzione $\Delta_4^{(+)}$ non sia identicamente nulla. Allora, procedendo come in K. e W. ⁽¹⁾, si ottiene senza difficoltà la formula:

$$(5) \quad \Delta_4^{(+)}(x, y, z; a_{11}, \dots, a_{23}) = \\ = \frac{i}{(2\pi)^9} \int d^4 p_1 d^4 p_2 d^4 p_3 \exp [i \sum_{k=1}^3 p_k \cdot u_k] \delta(p_1^2 + 1) \delta(p_2^2 - 1) \delta(p_3^2 - 1) \prod_{r \leq s=1}^3 \delta(p_r \cdot p_s) \theta(p_{1,0}),$$

in cui si è posto:

$$(6) \quad \begin{cases} u_1 = \sqrt{-a_{11}} \left(x + \frac{a_{12}}{a_{11}} y + \frac{a_{13}}{a_{11}} z \right), \\ u_2 = \sqrt{-\frac{A_{33}}{a_{11}}} \left(y - \frac{A_{23}}{A_{33}} z \right), \\ u_3 = \sqrt{-\frac{A}{A_{33}}} z, \end{cases}$$

e:

$$A = \det(a_{rs}), \quad A_{rs} = \text{cofattore di } a_{rs} \text{ in } A.$$

L'integrazione rispetto a p_3 può essere fatta esattamente, e dà:

$$(7) \quad \int d^4 p_3 \delta(p_3^2 - 1) \delta(p_3 \cdot p_1) \delta(p_3 \cdot p_2) \exp [i p_3 \cdot u_3] = \pi J_0 (\sqrt{u_3^2 + (p_1 \cdot u_3)^2 - (p_2 \cdot u_3)^2}).$$

dove J_0 è la funzione di Bessel di prima specie e d'ordine zero; infatti, osservando che p_1 deve giacere nel futuro del cono di luce (in virtù del fattore $\delta(p_1^2 + 1)\theta(p_{1,0})$),

(*) Questa ipotesi, che semplifica alquanto il nostro procedimento, non comporta alcuna restrizione. Infatti, se nessuno dei tetravettori ξ ha lunghezza nulla, basta considerare la funzione $\Delta_4^{(+)}(\xi'; a')$, dove le ξ' sono combinazioni lineari delle ξ (e analogamente per le a'); tale funzione risulta proporzionale alla $\Delta_4^{(+)}(\xi; a)$, ed è sempre possibile scegliere i coefficienti delle suddette combinazioni in modo tale che uno dei tetravettori ξ' abbia lunghezza nulla, rientrando così nel caso da noi trattato.

basta eseguire il calcolo nel particolare sistema in cui $p_1 = (1, 0, 0, 0)$, e quindi applicare la formula:

$$(8) \quad \int d^3 \mathbf{u} \delta(\mathbf{u}^2 - 1) \delta(\mathbf{u} \cdot \mathbf{x}) \exp [i \mathbf{u} \cdot \mathbf{y}] = \frac{\pi}{|\mathbf{x}|} J_0 \left(\sqrt{\mathbf{y}^2 - \frac{(\mathbf{x} \cdot \mathbf{y})^2}{\mathbf{x}^2}} \right),$$

che si può facilmente stabilire passando a coordinate polari.

Supponiamo ora che z (e quindi u_3) abbia lunghezza nulla; allora, sostituendo nella (5) la (7) — con $u_3^2 = 0$ — otteniamo:

$$(9) \quad \Delta_4^{(+)}(x, y, z; a_{11}, \dots, a_{23})|_{z^2=0} = \\ = \frac{\pi i}{(2\pi)^9} \int d^4 p d^4 q \exp [i(p \cdot u_1 + q \cdot u_2)] \delta(p^2 + 1) \delta(q^2 - 1) \delta(p \cdot q) \theta(p_0) J_0(\sqrt{(p \cdot u_3)^2 - (q \cdot u_3)^2}).$$

Osservando che ⁽³⁾:

$$(10) \quad J_0 \sqrt{a^2 - b^2} = \frac{1}{2\pi} \int_0^{2\pi} \exp [ia \cos \varphi + b \sin \varphi] d\varphi,$$

la (9) assume la forma:

$$(11) \quad \Delta_4^{(+)}(x, y, z; a_{11}, \dots, a_{23})|_{z^2=0} = \frac{i}{2(2\pi)^9} \int_0^{2\pi} d\varphi \cdot \\ \cdot \int d^4 p d^4 q \delta(p^2 + 1) \delta(q^2 - 1) \delta(p \cdot q) \theta(p_0) \exp [ip \cdot (u_1 + u_3 \cos \varphi) + iq \cdot (u_2 - iu_3 \sin \varphi)].$$

Ora, si può vedere che, se α , β e γ sono tre numeri positivi (con $\gamma > \sqrt{\alpha\beta}$), sussiste la relazione:

$$(12) \quad \int d^4 p d^4 q \delta(p^2 + 1) \delta(q^2 - 1) \delta(p \cdot q) \theta(p_0) \exp [i(p \cdot u + q \cdot v)] = \\ = - \frac{(2\pi)^6}{\sqrt{\gamma^2 - \alpha\beta}} \Delta_3^{(+)} \left(\frac{u}{\sqrt{\alpha}} - \frac{\gamma v}{\sqrt{\alpha(\gamma^2 - \alpha\beta)}}, v \sqrt{\frac{\alpha}{\gamma^2 - \alpha\beta}}; \alpha, \beta, \gamma \right).$$

Pertanto, otteniamo la formula di riduzione desiderata:

$$(13) \quad \Delta_4^{(+)}(x, y, z; a_{11}, \dots, a_{23})|_{z^2=0} = - \frac{i}{2(2\pi)^9 \sqrt{\gamma^2 - \alpha\beta}} \int_0^{2\pi} \Delta_3^{(+)}(\xi, \eta; \alpha, \beta, \gamma) d\varphi,$$

⁽³⁾ A. ERDELYI, W. MAGNUS, F. OBERHETTINGER and F. G. TRICOMI: *Higher transcendental functions*, 2, 82, formula (17).

con:

$$(14) \quad \xi = \frac{1}{\sqrt{\alpha}} \left\{ u_1 + u_3 \cos \varphi - \frac{\gamma}{\sqrt{\gamma^2 - \alpha\beta}} (u_2 - iu_3 \sin \varphi) \right\},$$

$$\eta = \sqrt{\frac{\alpha}{\gamma^2 - \alpha\beta}} (u_2 - iu_3 \sin \varphi).$$

Aggiungiamo che un ulteriore studio del problema — estendendo la definizione (2) al caso di vettori n -dimensionali — ha condotto a vari risultati (che riteniamo nuovi) riguardanti la teoria delle funzioni di Bessel; essi, da un punto di vista puramente matematico, potrebbero avere una certa importanza, e verranno riferiti in altra sede.

* * *

Ringrazio il prof. P. CALDIROLA per il suo cortese interessamento a questo lavoro.

PROPRIETÀ LETTERARIA RISERVATA

Direttore responsabile: G. POLVANI

Tipografia Compositori - Bologna

Questo Fascicolo è stato licenziato dai torchi il 1-I-1959